UNIVERSITY OF
KWAZULU-NATAL

MODIFICATION, RECONSTRUCTION AND COMMISSIONING OF A VAPOUR RECIRCULATION APPARATUS FOR HIGH-PRESSURE LOW-TEMPERATURE VAPOUR-LIQUID EQUILIBRIUM MEASUREMENTS

2010

JASON KNOCK

UNIVERSITY OF
KWAZULU-NATAL

MODIFICATION, RECONSTRUCTION AND COMMISSIONING OF A VAPOUR RECIRCULATION APPARATUS FOR HIGH-PRESSURE LOW-TEMPERATURE VAPOUR-LIQUID EQUILIBRIUM MEASUREMENTS

2010

JASON KNOCK

A dissertation submitted in fulfilment of the academic requirements for the degree of Master of Science in Engineering (Chemical) at the School of Chemical Engineering, University of KwaZulu-Natal (Durban)

PREFACE

The work described in this thesis was performed in the School of Chemical Engineering at the University of KwaZulu-Natal, from March 2004 to December 2006 under the supervision of Professor D. Ramjugernath.

I, Jason Knock, declare that

- The research reported in this dissertation, except where otherwise indicated is my original work.
- The dissertation has not been submitted for any degree or examination at any other university.
- This dissertation does not contain other persons' writing, unless specifically acknowledged as being source from other researchers. Where other written sources have been quoted, then a) their words have been re-written but the general information attributed to them has been referenced; b) where their exact words have been used, their writing has been placed inside quotation marks, and referenced.
- Where I have reproduced a publication of which I am an author, co-author or editor, I have indicated in detail which part of the publication was actually written by myself alone and have fully referenced such publications.
- This dissertation does not contain text, graphics or tables copied and pasted from the Internet, unless specifically acknowledged, and the source being detailed in the dissertation and in the reference sections.

_____

Jason Knock

As the candidate's supervisor, I, Professor D. Ramjugernath have approved this thesis for submission.

_____

Professor D. Ramjugernath

ABSTRACT

The vapour recirculation apparatus of Moodley [2002] was modified, reconstructed, and commissioned in order to be used in the acquisition of high-pressure vapour-liquid equilibrium (HPVLE) data at low temperatures. The original equipment of Moodley [2002] was modified with the aim of achieving the desired operating temperature range which the original equipment was unable to achieve. Major modifications were carried out on the cooling circuit allowing the equipment to reach temperatures as low as -30°C, a significant improvement to the original equipments minimum attainable temperature of -5°C. Modifications were also successfully carried out on the vapour recirculation pump of Moodley [2002], which failed when operated over extended periods at high pressures thus enabling the equipment to operate at pressures up to 10.0 bar, an improvement on the previous pressure operating limit of 6.9 bar.

The operating limits of the equipment were tested through measurement of pure-component vapour-pressures of isopentane at temperatures between -14 and +27.9°C and pressures up to 10.1 bar and on propane at temperatures between -30.1 and +26.0°C and pressures up to 9.7 bar. The isopentane vapour-pressure measurements had an average deviation of ±0.49% when compared to literature data while the propane vapour-measurements had a maximum average deviation of ±0.35% when compared to literature data indicating that the equipment was capable of measuring accurate vapour-pressure data at temperatures down to -30°C and pressures up to 10.0 bar.

The equipment was thereafter used in the acquisition of binary HPVLE data. Considerable time was spent developing and practicing the techniques used in the binary HPVLE measurements. Binary measurements were performed on the test system propane + 1-propanol at 19.9°C. To gain more confidence in the binary HPVLE measurements another test system, propane + isopentane was selected and binary HPVLE measurements were performed at 25°C and 0°C. The equipment was able to reproduce relatively accurate binary HPVLE results for the test systems at the selected isotherms. The equipment was thereafter used in the acquisition of a new set of binary HPVLE data for the propane + isopentane system at -10°C however owing to time constraints and chemical availability the acquisition of a complete set of data was not possible.

The binary HPVLE data was thereafter regressed via the direct method. The Peng-Robinson (PR) equation of state (EOS) and the Soave-Redlich-Kwong (SRK) EOS were each coupled

with the Mathias Copeman alpha function together with the Wong-Sandler mixing rule and the NRTL local composition model and applied to the binary systems at each of the isotherms investigated. Regressed data showed a relatively good agreement with measured experimental data for both binary systems investigated at all of the isotherms except the new -10°C isotherm of the propane + isopentane system.

ACKNOWLEDGEMENTS

Reaching a conclusion to this study seemed a far off possibility but thanks to the support and encouragement received from the numerous people in my life it has become a reality. Without the words of encouragement, technical support and assistance received from family, friends, colleagues, mentors and supervisors this milestone in my life would never have been accomplished. I would like to extend my sincerest gratitude to all who have played a part in assisting me in achieving this.

- I would first and foremost like to thank God for providing me with a means for undertaking such a study. All good things are bestowed upon us by His Almighty.
- My family who have supported and encouraged me every step of the way and without whom this would not be possible. My parents Ken & Beryl Knock, my late Grandmother Louise Knock, my brother Abner and sister Simone. Your love and guidance are much appreciated.
- My supervisor Professor Deresh Ramjugernath who played a pivotal role in affording me the opportunity to undertake this study. His guidance, patience and support has been invaluable to the success of this study.
- The mechanical workshop staff at the School of Chemical Engineering UKZN. Their willingness to always help and go the extra mile was always appreciated. A particular thanks goes to Mr Les Henwood and Mr Ken Jack.
- The computer and electronics staff at the School of Chemical Engineering UKZN for their assistance whenever needed. Mr Dhavaraj Naidoo, Mr Preyothen Nayager and Mr Colin Mandri.
- The rest of the staff at the School of Chemical Engineering UKZN who often supplied advice and assistance whenever it was sought.
- Colleagues and supervisors at Sappi Enstra Mill who often provided words of encouragement and support.
- The late Eugene Benade for his assistance with some of the drawings.
- A very special thanks goes out to all my friends and colleagues for the support and encouragement: Rochelle Parsons, Etienne Wilson, Seth Keshwar, Damir Turkovic, Keith Manning, David Johnson, Warren Bokwe, Rupert Candy, Brandon Catin ,Davide Magagna, Wesley Oaks, Ernest Ndzimandze, Sifiso Ntuli, Prashant Reddy, Viran Pillay, Dr. Tyrone Mcknight, Dr. Scott Clifford, Vivek Gadodia, Minal Soni, Caleb Narigasagu.
- The National Research Foundation for the funding received.

TABLE OF CONTENTS

PREFACE ..... *iii*

ABSTRACT ..... *iv*

ACKNOWLEDGEMENTS ..... *vi*

TABLE OF CONTENTS ..... *vii*

LIST OF FIGURES ..... *x*

NOMENCLATURE ..... *xiv*

1 INTRODUCTION *1*

2 LITERATURE REVIEW OF EXPERIMENTAL EQUIPMENT *3*

2.1 Classification of experimental variables **3**

2.2 Presentation of HPVLE data on phase diagrams **3**

2.3 Classification of experimental techniques **4**

2.4 Features of HPVLE equipment **6**

2.5 Difficulties associated with HPVLE experimentation **7**

2.5.1 Degassing of liquid components 7
2.5.2 Obtaining isothermal conditions 7
2.5.3 Attaining equilibrium 8
2.5.4 Temperature and pressure measurement 10
2.5.5 Sampling of the liquid and vapour phases 10
2.5.6 Preparation of withdrawn samples for analysis 12
2.5.7 Analysis of the equilibrium phases 13

2.6 The vapour recirculation method **14**

2.6.1 General description 14
2.6.2 The vapour recirculation pump 15
2.6.3 Difficulties encountered using the vapour recirculation method 16

2.7 Literature review of features of equipment used in the development of the vapour recirculation equipment used in this study **17**

2.7.1 Equilibrium cell design 17
2.7.2 Vapour recirculation pump design 18
2.7.3 Cooling system design 19
2.7.4 Sampling systems design 21
2.7.5 Sample preparation for analysis 22

3 THEORETICAL TECHNIQUES USED IN THE INTERPRETATION OF HIGH-PRESSURE VAPOUR-LIQUID EQUILIBRIUM DATA *23*

3.1 Thermodynamic equilibrium **23**

3.2 Methods used in the interpretation of HPVLE **25**

3.2.1 The direct method 25
3.2.2 The combined method 26

3.3 Equations of state **28**

3.3.1 Cubic equations of state 29

3.4 General considerations for treatment of the liquid-phase **42**

3.4.1 Activity coefficients 42
3.4.2 Models incorporating the excess Gibbs energy 43

4 EXPERIMENTAL APPARATUS *48*

4.1 Functional description of vapour recirculation apparatus 48

4.2 Equilibrium cell 51
4.2.1 Design 51
4.2.2 Temperature and pressure measurements 54

4.3 Heat exchange system 54

4.4 The thermostat 57

4.5 Vapour recirculation loop 61

4.6 The vapour recirculation pump 62

4.7 The cooling and temperature control system 63

4.8 Sampling and low-pressure analysis systems 66
4.8.1 Liquid sampling 66
4.8.2 Vapour sampling 68
4.8.3 Sample preparation for analysis 69

4.9 Measurement of system variables 72
4.9.1 Temperature 72
4.9.2 Pressure 72
4.9.3 Composition 72

4.10 Equipment safety 73

4.11 Summary of modifications made to the vapour recirculation apparatus of Moodley [2002]: 74

5 EXPERIMENTAL PROCEDURE 76

5.1 Gas chromatograph calibration 76

5.2 Vapour pressure & phase equilibrium measurements 78
5.2.1 Start-up of an experimental run 78
5.2.2 Charging of the equilibrium cell 80
5.2.3 Attainment of equilibrium 81
5.2.4 Sample withdrawal and analysis 82
5.2.5 Measuring a new HPVLE data point 86

6 SYSTEMS CHOSEN FOR EXPERIMENTATION 87

6.1 Pure-component vapour-pressure measurements 87

6.2 Binary system HPVLE measurements 88
6.2.1 Propane + 1-propanol 88
6.2.2 Propane + isopentane 89

7 EXPERIMENTAL RESULTS 90

7.1 Purity of chemicals 90

7.2 Accuracy of measurements 91
7.2.1 Temperature 91
7.2.2 Pressure 92
7.2.3 Composition 92

7.3 Vapour pressure measurements 93
7.3.1 Isopentane vapour pressure measurements 93
7.3.2 Propane vapour pressure measurements 95

7.4 Gas chromatograph calibrations 98

7.5 Binary system measurements 100
7.5.1 Propane (1) + 1-propanol (2) system 100
7.5.2 Propane (1) + Isopentane (2) system 102

8 DISCUSSION *106*

8.1 Theoretical treatment of the experimental data **106**
8.1.1 Application of the direct method 106
8.1.2 Regression of vapour pressures 107
8.1.3 Regression of binary system VLE data 108

8.2 Difficulties encountered during experimentation **119**
8.2.1 Obtaining low temperatures and isothermal conditions in the equilibrium cell 119
8.2.2 Reliability of the vapour recirculation pump 120
8.2.3 Leaks in the vapour recirculation loop 121
8.2.4 Setting the vapour recirculation rate 121
8.2.5 Sampling and analysis 122

9 CONCLUSION *123*

9.1 Equipment modifications **123**

9.2 Experimental measurements **124**

9.3 Data regression **124**

10 RECOMMENDATIONS *126*

BIBLIOGRAPHY *128*

APPENDICES *140*

A. CALIBRATIONS *140*

A.1 Calibration of temperature sensors **140**

A.2 Calibration of equilibrium cell pressure transducer **141**

B. PHYSICAL PROPERTIES OF COMPONENTS INVESTIGATED *143*

B.1 General pure component physical properties **143**

B.2 Vapour pressures **143**

C. Literature Data of Binary Systems Investigated *145*

C.1 Propane + 1-propanol system **145**

C.2 Propane + isopentane system **146**

LIST OF FIGURES

Figure 2-1: Classification of experimental methods used in HPVLE studies [Moodley, 2002]..... 5

Figure 2-2: Key features of a HPVLE experimental apparatus [Raal & Mühlbauer, 1994] 6

Figure 2-3: Features of a vapour recirculation apparatus [Malanowski, 1982]..... 14

Figure 2-4: Method of sealing used in the vapour recirculation pump of Moodley [2002] 19

Figure 2-5: Thermostat used by Moodley [2002] 20

Figure 4-1: Simplified flow diagram of Experimental Apparatus as modified from Moodley [2002] 49

Figure 4-2: Detailed flow diagram of the vapour recirculation Apparatus as modified from Moodley [2002] 50

Figure 4-3: Schematic diagram of the equilibrium cell [Moodley, 2002] 53

Figure 4-4: Schematic arrangement of heat exchange system and equilibrium cell as modified from Moodley [2002] 56

Figure 4-5: Modified thermostat with internal arrangement 58

Figure 4-6: Sealing arrangement of Thermostat viewing glass..... 60

Figure 4-7: Modified sealing arrangement of vapour recirculation pump 63

Figure 4-8 : Schematic diagram of the heating unit [Moodley, 2002] 65

Figure 4-9: Mounting of the liquid-sampling valve at the base of the equilibrium cell 67

Figure 4-10: Positions of the Valco six-port vapour-sampling valve [Moodley, 2002] 68

Figure 4-11: Schematic diagram of a jet-mixer [Moodley, 2002] 70

Figure 7-1: Comparison of experimental vapour-pressure data (♦) for isopentane with those predicted by the correlations of Reid et al. [1988] (–). 94

Figure 7-2: Deviations of experimental vapour-pressures for isopentane from the correlations of Reid et al. [1988]. 95

Figure 7-3: Comparison of experimental vapour-pressure data (♦) for propane with those predicted by the correlations of Reid et al. [1988] (–). 97

Figure 7-4: Comparison of experimental vapour-pressure data (o) for propane with those predicted by the correlations of Daubert & Danner [1993] (–). 97

Figure 7-5: Deviations of experimental vapour-pressures for propane from the correlations of Reid et al. [1988] (♦) and Daubert and Danner [1993] (o). 98

Figure 7-6: GC calibration with propane. 99

Figure 7-7: GC calibration with 1-propanol..... 99

Figure 7-8: GC calibration with isopentane. 100

Figure 7-9: Comparison of experimental VLE data (♦) for the propane + 1-propanol system at 19.9 °C with those of Nagahama et al. [1971] (o)..... 101

Figure 7-10: Comparison of experimental VLE data (♦) for the propane + 1-propanol system at 19.9 °C with those of Moodley [2002] (Δ). 102

Figure 7-11: Comparison of experimental VLE data (♦) for the binary propane + isopentane system at 25 °C with those of Vaughan & Collins [1942] (o)..... 103

Figure 7-12: Comparison of experimental VLE data (♦) for the binary propane + isopentane system at 0 °C with those of Vaughan & Collins [1942] (o)..... 104

Figure 7-13: Comparison of experimental VLE data (♦) for the binary propane + isopentane system at 0 °C with those of Moodley [2002] (Δ). 104

Figure 7-14: Experimental VLE data for the binary propane + isopentane system at -10 °C. .. 105

Figure 8-1: Comparison of experimental data (♦) for the Propane (1) + 1-Propanol (2) system at 19.9 °C to the P-x-y diagram generated via the PR-MC-WSMR(NRTL) model (–). 110

Figure 8-2: Comparison of experimental data (•) for the Propane (1) + 1-Propanol (2) system at 19.9 °C to the P-x-y diagram generated via the SRK-MC-WSMR(NRTL) model (–). 111

Figure 8-3: Comparison of experimental data (•) for the Propane (1) + Isopentane (2) system at 25 °C to the P-x-y diagram generated via the PR-MC-WSMR(NRTL) model (–). 115

Figure 8-4: Comparison of experimental data (•) for the Propane (1) + Isopentane (2) system at 25 °C to the P-x-y diagram generated via the SRK-MC-WSMR(NRTL) model (–). 116

Figure 8-5: Comparison of experimental data (•) for the Propane (1) + Isopentane (2) system at 0 °C to the P-x-y diagram generated via the PR-MC-WSMR(NRTL) model (–). 116

Figure 8-6: Comparison of experimental data (•) for the Propane (1) + Isopentane (2) system at 0 °C to the P-x-y diagram generated via the SRK-MC-WSMR(NRTL) model (–). 117

Figure 8-7: Comparison of experimental data (•) for the Propane (1) + Isopentane (2) system at -10 °C to the P-x-y diagram generated via the PR-MC-WSMR(NRTL) model (–). 117

Figure 8-8: Comparison of experimental data (•) for the Propane (1) + Isopentane (2) system at -10 °C to the P-x-y diagram generated via the SRK-MC-WSMR(NRTL) model (–). 118

Figure A-1: Pt-100 standard calibration chart..... 140

Figure A-2: Comparison of gauge vapour pressure measurements (♦) to values predicted by Reid *et al.* [1988] (○) for n-Pentane..... 141

Figure A-3: Calibration graph for equilibrium cell pressure transducer..... 142

LIST OF TABLES

Table 3-1: Temperature dependency models for the α(T) function in a CEOS 34

Table 3-2: Examples of modifications made to the attractive term for various EOS 35

Table 3-3: Examples of modifications made to the repulsive term of the generalized CEOS.....36

Table 4-1: Operating conditions for the Shimadzu Model GC-17A gas chromatograph.....73

Table 6-1: Literature HPVLE studies for the binary system propane + 1-propanol.....88

Table 6-2 :Literature HPVLE studies for the binary propane + isopentane system 89

Table 7-1: Vapour-pressure measurements for isopentane 94

Table 7-2: Vapour-pressure measurements for propane. 96

Table 7-3: GC Calibration Equations 98

Table 7-4: Experimental vapour-liquid equilibrium data for the binary propane(1) + 1-propanol(2) system at 19.9°C.....101

Table 7-5: Experimental vapour-liquid equilibrium data for the binary propane(1) + isopentane(2) system at 25, 0 and -10°C. 103

Table 8-1: Pure-component Mathias-Copeman coefficients together with percentage deviations for the PR-MC EOS 107

Table 8-2: Pure-component Mathias-Copeman coefficients together with percentage deviations for the SRK-MC EOS.....108

Table 8-3: Experimental VLE data for the Propane (1) + 1-Propanol (2) system at 19.9 ºC compared to regressed data obtained via the PR-MC-WSMR(NRTL) model.....109

Table 8-4: Experimental VLE data for the Propane (1) + 1-Propanol (2) system at 19.9 ºC compared to regressed data obtained via the SRK-MC-WSMR(NRTL) model.....110

Table 8-5: Model parameters regressed for Propane (1) + 1-Propanol (2) system at 19.9ºC through application of the PR-MC-WSMR(NRTL) model and the SRK-MC-WSMR(NRTL) model together with calculated deviations for the bubble point pressure and the propane vapour composition when comparing the calculated data to the experimental VLE data 111

Table 8-6: Model parameters regressed for the Propane (1) + Isopentane (2) system through application of the PR-MC-WSMR(NRTL) model and the SRK-MC-WSMR(NRTL) model.....112

Table 8-7: Experimental VLE data for the Propane (1) + Isopentane (2) system at 25 ºC compared to regressed data obtained via the PR-MC-WSMR(NRTL) model.....113

Table 8-8: Experimental VLE data for the Propane (1) + Isopentane (2) system at 25 ºC compared to regressed data obtained via the SRK-MC-WSMR(NRTL) model.....113

Table 8-9: Experimental VLE data for the Propane (1) + Isopentane (2) system at 0 ºC compared to regressed data obtained via the PR-MC-WSMR(NRTL) model.....114

Table 8-10: Experimental VLE data for the Propane (1) + Isopentane (2) system at 0 ºC compared to regressed data obtained via the SRK-MC-WSMR(NRTL) model.....114

Table 8-11: Experimental VLE data for the Propane (1) + Isopentane (2) system at -10 ºC compared to regressed data obtained via the PR-MC-WSMR(NRTL) model.....114

Table 8-12: Experimental VLE data for the Propane (1) + Isopentane (2) system at -10 ºC compared to regressed data obtained via the SRK-MC-WSMR(NRTL) model.....115

Table 8-13: Calculated deviations for the bubble point pressure and the propane vapour composition when comparing the calculated data derived via the PR-MC-WSMR(NRTL) and the SRK-MC-WSMR(NRTL) to the experimental VLE data for the Propane (1) + Isopentane (2) system at 25ºC. 118

Table 8-14: Calculated deviations for the bubble point pressure and the propane vapour composition when comparing the calculated data derived via the PR-MC-WSMR(NRTL) and the SRK-MC-WSMR(NRTL) to the experimental VLE data for the Propane (1) + Isopentane (2) system at 0 ºC 119

Table 8-15: Calculated deviations for the bubble point pressure and the propane vapour composition when comparing the calculated data derived via the PR-MC-WSMR(NRTL) and the SRK-MC-WSMR(NRTL) to the experimental VLE data for the Propane (1) + Isopentane (2) system at -10 ºC 119

Table B-1: Physical properties of components investigated in this study 143

Table B-2: Vapour pressure constants used in the equation of Reid et al. 144

Table B-3: Vapour pressure constants used in the equation of Daubert & Danner [1993].....144

Table C-1: Vapour-liquid equilibrium data for the propane (1) + 1-propanol (2) system at 19.9ºC [Nagahama et al., 1971].....145

Table C-2: Vapour-liquid equilibrium data for the propane (1) + 1-propanol (2) system at 19.9ºC [Moodley, 2002] 145

Table C-3: Vapour-liquid equilibrium data for the propane (1) + isopentane (2) system at 0ºC. [Vaughan & Collins, 1942].....146

Table C-4: Vapour-liquid equilibrium data for the propane (1) + isopentane (2) system at 25ºC. [Vaughan & Collins, 1942].....146

Table C-5: Vapour-liquid equilibrium data for the propane (1) + isopentane (2) system at 0ºC. [Moodley, 2002].....147

NOMENCLATURE

Abbreviations

1PCMR	1-parameter classical mixing rule
2PCMR	2-parameter classical mixing rule
AAD	Absolute average deviation
CEOS	Cubic equation/s of state
CMR	Classical mixing rule
EOS	Equation/s of state
FID	Flame ionization detectors
GC	Gas chromatograph
HPVLE	High-pressure vapour-liquid equilibrium
LN_2	Liquid Nitrogen
LPM	Liquid-phase model
MC	Mathias-Copeman
NECSA	Nuclear energy corporation of South Africa
NRTL	Non-random two-liquid activity coefficient model
OD	Outer diameter
PID	Proportional/Integral/Derivative
PR	Peng-Robinson
PTFE	Polytetrafluoroethylene (Teflon)
Pt	Platinum
PVT	Pressure-Volume-Temperature
RK	Redlich-Kwong
SRK	Soave-Redlich-Kwong
TCD	Thermal conductivity detectors
TCMR	Twu-Coon mixing rule
UNIQUAC	Universal Quasi-Chemical
VLE	Vapour-liquid equilibrium
WSMR	Wong-Sandler mixing rule

Symbols

A	Adjustable parameter in correlating equations, Helmholtz free energy, GC peak area, Constant used in vapour pressure prediction
A_{ij}	Adjustable parameter in excess Gibbs energy correlating equations
a	Adjustable attraction parameter in CEOS
B	Adjustable parameter in correlating equations, Second virial coefficient of a pure fluid in virial EOS, Constant used in vapour pressure prediction
B_{ij}	Cross second virial coefficient in virial EOS
b	Adjustable covolume parameter in CEOS
C	Constant used in vapour pressure prediction
D	Constant used in vapour pressure prediction
E	Constant used in vapour pressure prediction
$\hat{f}$	Fugacity
f°	Standard state fugacity
G	Excess Gibbs energy
g	Volume dependent parameter in the attractive term of a CEOS
g_{ji}	Energy parameter used in correlating equations for determination of excess Gibbs energy
H	Molar enthalpy
K	Equilibrium ratio
k_{ij}	Binary interaction parameter for mixing rules
l_{ij}	Binary interaction parameter for mixing rules
M	Mixture
N	Number of points in a data set
n	Number of moles of material
P	Pressure
P^{*}	Low pressure
R	Universal gas constant
R_D	Radius of gyration
S	Objective function in modified simplex algorithm
s_r	Percentage standard deviation
T	Temperature
V	Molar volume
V_T	Total volume

x	Liquid-phase mole fraction
y	Vapour-phase mole fraction
Z	Compressibility factor

Greek symbols

α	Adjustable attraction parameter in CEOS
α_{ij}	Non-randomness of mixture parameter used for NRTL equation
Λ	Numerical constant used in determination of Helmholtz free energy
Λ_{ij}	Adjustable interaction parameter used in determination of excess Gibbs energy
γ	Activity coefficient
τ_{ij}	Constant or function in NRTL equation, Adjustable interaction parameter
λ_{ij}	Molecular interaction parameters used in correlating equations for determination of excess Gibbs energy
$\hat{\gamma}$	Activity coefficient in mixture
$\hat{f}$	Fugacity
κ	Adjustable parameter in CEOS.
η	Adjustable parameter in the repulsive term of a CEOS
μ	Chemical potential, Dipole moment
ϕ	Fugacity coefficient
ω	Accentric factor
$\Gamma_i(T)$	Integration constant at constant Temperature

Subscripts

c	Critical state property
cal	Calculated
EOS	Equation of state
Experimental	Experimental quantity
exp	Experimental quantity
i	Component identity
j	Component identity
Literature	Literature quantity
nr	Non-random liquid theory
o	Zero pressure state

r	Reduced variable
vdW	van der Waals fluid
γ	Activity coefficient model

Superscripts

cal	Calculated
R	Reference
E	Excess quantity
exp	Experimental quantity
L	Liquid phase
V	Vapour phase

Overbars

-	Partial molar property

CHAPTER 1

INTRODUCTION

Separation processes account for a major portion of the capital outlay required in the design and construction of most modern chemical plants, as well as a large percentage of the energy costs during plant operation. As energy costs continue to escalate, optimal design of separation equipment is essential to ensure attractive returns from investment in new chemical plants. Vapour-liquid equilibrium (VLE) provides the framework on which the design of separation equipment is carried out. This importance has led to the development of a number of experimental and theoretical methods used in the determination of phase equilibrium data over the years.

Recently process simulators, which incorporate theoretical models to predict equilibrium phase behaviour, have been frequently used in the design of separation processes. Error in predicted data can however introduce significant error in the separation equipment design which can have major financial implications due to the likely inefficient operation of the new equipment. Accurate experimental data are thus essential for use in process equipment design as well as to validate the reliability of predictive models and improve accuracy of previously developed predictive models.

The Thermodynamic Research Unit of the School of Chemical Engineering at the University of KwaZulu-Natal (Durban) was previously approached by NECSA to perform a study on the phase behaviour of fluorinated compounds. Certain product streams at the NECSA plant situated in Pelindaba, Pretoria contained multicomponent mixtures of fluorinated hydrocarbons. These fluorinated compounds which have industrial use, are however not readily available at high purities, thus it was the aim of NECSA to invest in equipment capable of separating these compounds. As no existing theoretical predictive methods catered for the systems of interest new phase equilibrium experimental data were required. Initial laboratory studies performed at NECSA indicated that separation of the compounds would be possible via distillation at low-temperatures.

The acquisition of accurate experimental low-temperature high-pressure VLE (HPVLE) data, which involves the measurement of temperature, pressure and phase compositions, presents a challenging task and therefore availability of equipment capable of performing such measurements is scarce. Moodley [2002] in response to the requirements of NECSA, embarked on a study to develop a new piece of equipment to be used in the measurement of

isothermal VLE data over the temperature range -80 to +30°C, at pressures up to 10 bar. A new vapour recirculation apparatus was developed by Moodley [2002] but owing to limitations in the equipment design, the equipment was only able to reach temperatures down to -5°C and pressures up to 6.9 bar.

This study formed a continuation of the work of Moodley [2002]. The project aimed to rebuild and modify the vapour recirculation apparatus of Moodley [2002] to enable it to reach a wider range of operating conditions. The modified equipment was tested successfully at temperatures down to -30°C and pressures up to 10 bar showing a marked improvement when compared to the original design.

The modified equipment was used to perform vapour pressure measurements on isopentane between -14 and +27.9°C and on propane between -30.1 and +26.0°C. HPLVLE data was obtained for the binary system propane + 1-propanol at an isotherm of 19.9°C and compared to literature data. Further tests were done on the apparatus by measuring HPVLE data for the binary propane + isopentane system at isotherms of 25°C and 0°C and compared to literature data to verify equipment reliability. New phase equilibrium data for the propane + isopentane system was thereafter measured at -10°C.

The experimentally measured data was thereafter theoretically treated through regression via the direct method to obtain mathematical relationships to describe the binary systems investigated.

CHAPTER 2

LITERATURE REVIEW OF EXPERIMENTAL EQUIPMENT

The industrial importance of accurate VLE data has led to the development of a number of experimental methods used in acquisition of phase equilibrium data. This section outlines of the various classifications of the methods used in VLE data acquisition, which have been applied over the years. Difficulties associated with HPVLE data acquisition are also discussed with a larger focus on the vapour recirculation method used in this study. Literature used in the development of the equipment used in this study is discussed with an emphasis on the key features of the apparatus.

2.1 Classification of experimental variables

Deiters & Schneider [1986] classified the experimental variables in VLE experiments into two categories, namely, density and field variables. Density variables have different values in coexisting phases (e.g. mole fractions and densities), whereas field variables have the same values (e.g. pressure and temperature).

Measurement of field variables during experimentation is a relatively straightforward procedure as a number of methods for their accurate measurement have been developed. Accurate determination of the density variables presents a challenge during VLE measurement, especially when experimentation is being carried out at high pressures. Usually only one density variable is measured (e.g. component mole fractions in the equilibrium phases), during HPVLE studies.

2.2 Presentation of HPVLE data on phase diagrams

Phase diagrams provide a graphical record of the effect of temperature, pressure and composition on the kinds and numbers of phases that can exist in equilibrium with each other. Graphical representation of phase-equilibrium information provides an ease of interpretation of data by allowing the examination of interrelationships between variables and providing the ability to interpolate and extrapolate data.

There are a variety of different types of phase diagram types which can be used to represent data, with the simplest planar phase diagrams providing an illustration of the effects of a continuous variation of only two variables. To illustrate the effects of more than two variables a series of planar diagrams may be drawn, each at a constant value of one or more of those variables. More detail can be found on spatial three-dimensional diagrams, however these are difficult to construct and interpret.

Experimental data for two-component, vapour-liquid systems are usually presented as isobaric T-x-y, isothermal P-x-y, or isopleth P-T data depending on how the data were measured.

2.3 Classification of experimental techniques

High-pressure vapour-liquid equilibrium experimental methods were classified into two categories, the synthetic method and the direct method. This classification developed by Deiters & Schneider [1986] was based on the technique used to determine the equilibrium phase compositions.

The synthetic method involves preparing a mixture of known composition, then investigating its phase behaviour as a function of temperature and pressure. This method thus eliminates the need for analysis of the phase compositions, a challenging aspect of analytic methods, where samples are withdrawn from the equilibrium cell upon the attainment of phase equilibrium and analysed to determine the phase compositions. A third category involving equipment which combines the features of both the analytic and static methods, the combined method, has also emerged.

Experimental equipment is classified into two diverse classes based on the fluid dynamics in the equilibrium cell. Static methods involve charging a closed volume equilibrium cell with the components of the equilibrium system and efficient agitation of the vapour and liquid phases in the equilibrium cell. Equipment involving the flow or recirculation of at least one of the phases is classified into the dynamic method category. The static category is further subdivided into two categories, the static analytic method where sampling takes place and the static non-analytic method where there is no sampling. Sampling takes place in all dynamic methods and they are subdivided depending on whether its flow taking place and the type of flow or if recirculation is taking place and whether phase being circulated is either, liquid, vapour or both.

Moodley [2002] proposed the full classification of experimental methods illustrated in Figure 2-1. Both static and dynamic types of equipment have been applied successfully for HPVLE measurements. Although static type equipment is generally simpler than dynamic type equipment, the shorter equilibration time of the dynamic equipment provides an attractive alternative in certain instances. Dynamic equipment using the vapour recirculation method was used in this study and more detail of features of this class of equipment and the analytic methods employed during its use will be discussed subsequently.

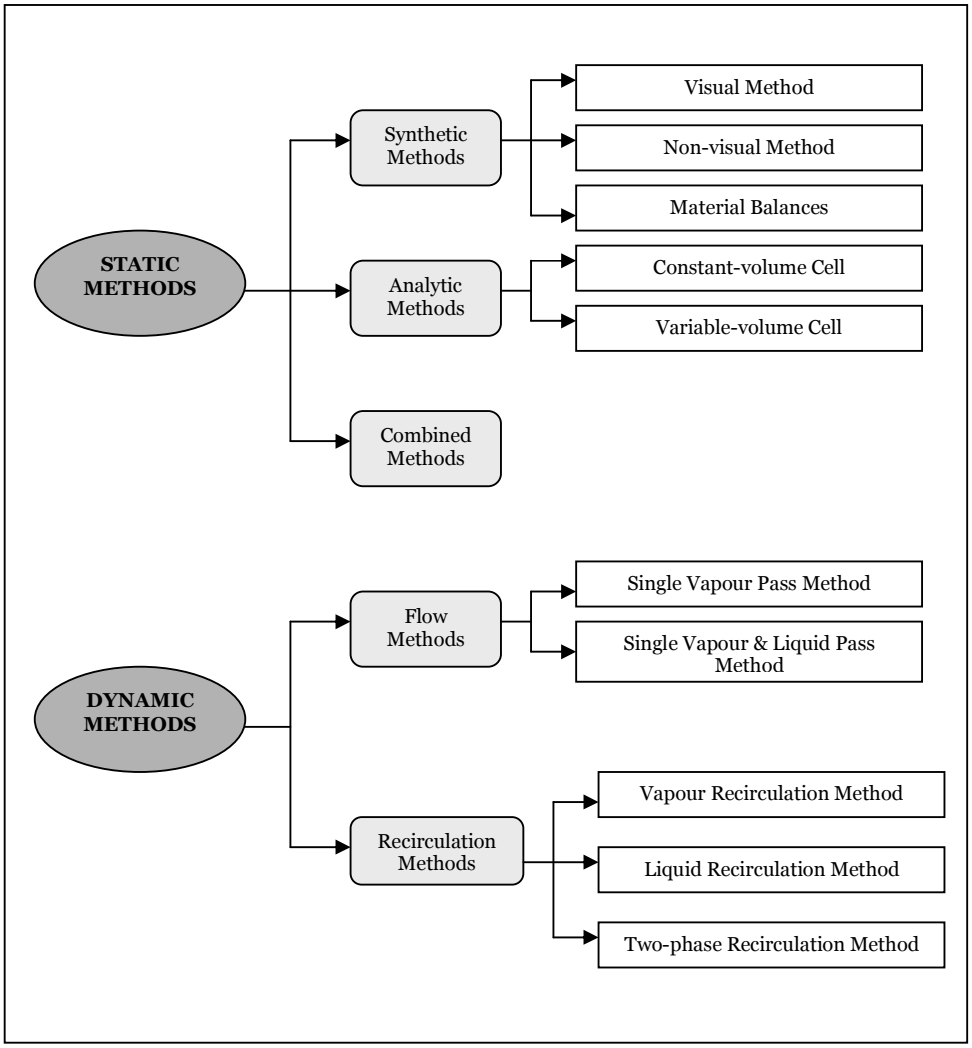

Figure 2-1: Classification of experimental methods used in HPVLE studies [Moodley, 2002]

2.4 Features of HPVLE equipment

Generally most HPVLE equipment employing the analytic method can be represented by Figure 2-2. Raal and Mühlbauer [1994] provided an excellent summary of the main features of equipment used for HPVLE studies:

- An equilibrium cell housing the vapour and liquid phases at equilibrium.
- A means of creating an environment which contains and controls the temperature of the equilibrium cell at a constant temperature for isothermal conditions. Examples from literature include, a nitrogen bath [Rogers & Prausnitz, 1970], water bath [Katayama *et al.*, 1989], oil bath [Legret *et al.*, 1980; Schotte, 1980] or a thermostatted air bath [Legret *et al.*, 1981; Mühlbauer & Raal, 1991].

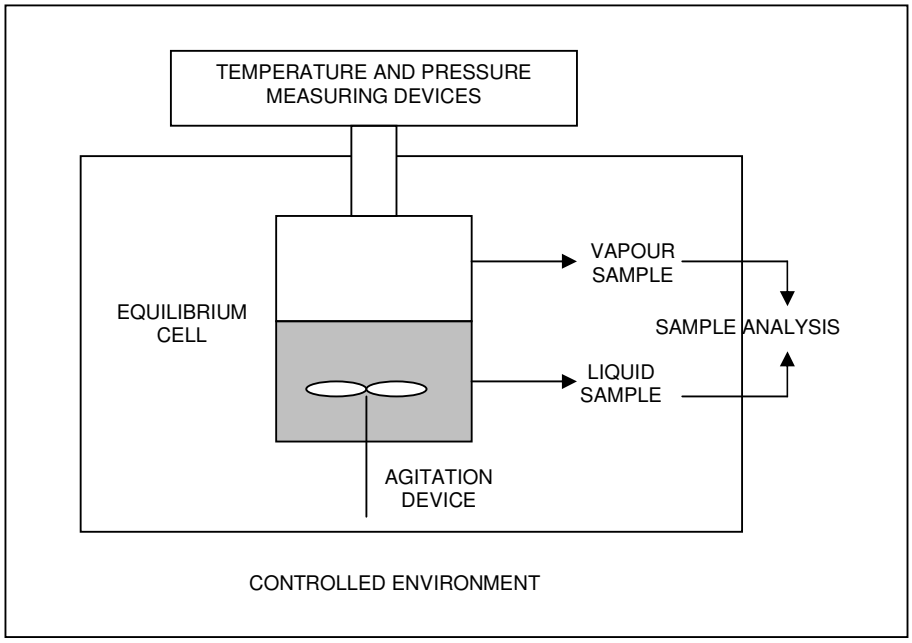

Figure 2-2: Key features of a HPVLE experimental apparatus [Raal & Mühlbauer, 1994]

- Agitation the contents of the equilibrium cell to speed up the attainment of equilibrium. Static cells usually use internal stirrers, while rocking of the equilibrium cell assembly has also been used as a method to attain equilibrium [Ashcroft *et al.*, 1983; Huang *et al.*, 1985]. The circulation of one or more phases provides the necessary agitation in the dynamic method as illustrated in the vapour recirculation equipment of Moodley [2002]. The use of internal stirrers has however been reported for some vapour recirculation methods [Freiteg & Robinson, 1986].
- Devices for the accurate measurement of the system temperature and pressure.

- A means of adjusting the equilibrium cell pressure and temperature when using a synthetic apparatus. This is necessary to produce phase separation. Adjustment of system pressure it is usually achieved by changing the internal volume of the equilibrium cell.
- When employing an analytic method a means of analyzing the vapour and liquid phases must be provided. The phases can either be analyzed in-situ using some type of optical device or they can be analyzed externally by removing a representative sample of each of the phases and analyzing the samples using an appropriate analytical device. The two-phase recirculation and the single vapour and liquid pass methods provide few difficulties when sampling is required, since a portion of the liquid and/or vapour flow is readily diverted through an external loop to remove a representative sample. The vapour recirculation method requires some sort of liquid sampling device while the static method has the difficulty of providing devices for both liquid and vapour sampling.

2.5 Difficulties associated with HPVLE experimentation

A number of challenges associated with obtaining accurate HPVLE data as reported in Raal & Mühlbauer [1994, 1998] are discussed in the following sections.

2.5.1 Degassing of liquid components

Prior to acquiring experimental data, it is necessary to remove dissolved gases from components that exist as liquids at room temperature when investigating volatile/non-volatile component systems, via a process referred to as degassing. This is necessary, especially at low pressures as these dissolved gases may compete with the volatile component in the liquid phase at low volatile component concentrations. Degassing can be conducted in situ. Legret *et al.* [1980] used a crystallizing process under vacuum. Battino *et al.* [1971], Van Ness & Abbot [1978] and Mühlbauer [1990] show different methods of degassing prior to sample introduction into the equilibrium cell.

2.5.2 Obtaining isothermal conditions

For true equilibrium conditions at a particular temperature under investigation there should be no thermal gradients in the equilibrium cell. Small thermal gradients in a static or dynamic apparatus can cause a noticeable error in the measured data.

Localized hot spots are a problem caused by direct radiative energy exchange between heaters and the equilibrium cell. To minimize the radiative heat transfer Herring & Barrick [1965] used stainless steel radiation and heat shields in their cryogenic apparatus, while chrome plating and copper sheeting was used by Eckert & Prausnitz [1965] in their experimental setup.

Attachments, fittings, and sampling devices provide temperature conductive paths to and from the equilibrium cell and the elimination of these paths are necessary. The equipment of Huang *et* al. [1985] and Wang *et al.* [1991] housed all lines, valves, and fittings associated with the equilibrium cell inside a constant temperature air bath with the equilibrium cell. This setup assisted in eliminating the effect of ambient temperature on the system temperature.

Effective insulation of the controlled environment housing the equilibrium cell from the surrounding environment at ambient conditions is necessary to ensure good control of the equilibrium cell temperature. A vacuum jacket provides a very effective insulation as seen in the cryostat of Eckert & Prausnitz [1965]. The more common insulation materials, fibrefrax, duraback, and polyurethane foam are also used to provide effective insulation. Moodley [2002] employed a thermostat with an evacuated annular space.

Installing temperature sensors in the walls of the equilibrium cell and in the constant-temperature bath assists in monitoring the temperature profile and testing for possible temperature gradients. Raal & Mühlbauer [1998] recommends this to be within 0.5 ºC, while Konrad *et al.* [1983] recommends that the axial temperature gradient in the equilibrium cell should not exceed 0.2 ºC.

2.5.3 Attaining equilibrium

Equilibrium is a static condition. In thermodynamics equilibrium is achieved when there is an absence of change with respect to time, as well as an absence of any tendency toward change on a macroscopic level. For this to be achieved all potentials that may cause change must be balanced.

When dealing with VLE measurements equilibrium is assumed to exist when there is no change in the properties of the vapour and liquid phases in the equilibrium cell. This is when

no changes in the pressure, temperature, composition, and sometimes refractive index of the coexisting phases can be detected with the available measuring devices.

High stirring rates or bubbling a vapour through a liquid volume improves contact between the phases and speeds up the attainment of equilibrium. Ramjugernath [2002] states that the rate at which equilibrium is reached decreases as the system approaches the state of equilibrium but due to continual variations in the surroundings and retarding resistances true equilibrium can probably never be attained.

A number of guidelines for determining whether equilibrium has been attained have been reported in literature Moodley [2002]:

- Aroyan and Katz [1951] used two methods to determine whether equilibrium had been achieved in their vapour recirculation apparatus. The first method involved determining the composition of the liquid phase as a function of the time of circulation. Once the composition levelled off with time it indicated that equilibrium had been closely approached in the system. As a second check the compositions of coexisting phases were compared upon reaching equilibrium by two different paths. Equilibrium compositions obtained by increasing the pressure to a definite value were compared with equilibrium compositions obtained by decreasing the pressure to the same value. Using these two methods, with agreement within experimental error, indicated that a state of equilibrium had been achieved.
- Another indication of equilibrium in binary systems as reported in literature is the stability of the vapour pressure of the mixture. Rigas *et al.* [1958] assumed a state of equilibrium when the system pressure remained constant for a period of 0.5 to 1 hour, while Klink *et al.* [1975] considered a constant cell pressure for at least 4 hours an indication of equilibrium. Fredenslund *et al.* [1973] considered a change in pressure of less than 0.05% in half an hour an indication of equilibrium.
- Moodley [2002] using a vapour recirculation apparatus reported the system to be at complete thermodynamic equilibrium if pressure, temperature and liquid level remained constant for at least 30 minutes after thermal equilibrium was achieved and the system pressure stabilised.
- Stability in refractive index was used by Besserer & Robinson [1971], Kalra & Robinson [1975], and Freitag & Robinson [1986] as an indication of equilibrium.

2.5.4 Temperature and pressure measurement

Thermocouples and platinum resistance thermometers (Pt-100Ω resistors or Pt-100 sensors) are usually used for temperature measurement in VLE equipment. Thermistors and quartz thermometers may also be used for temperature measurement, however their high sensitivities to temperature change are generally not required for a primary measuring device and they are rather used as a standard against which the measuring device is calibrated.

Pressure transducers and Bourdon pressure gauges are used as primary pressure measuring devices. Dead-weight piston gauges are extremely accurate pressure measuring devices and they are generally usually used as a standard against which the primary measuring device is calibrated.

2.5.5 Sampling of the liquid and vapour phases

Pressure drops associated with withdrawing a sample directly from a high pressure cell and thus changing the volume of the equilibrium cell can cause a significant disturbance to the equilibrium. Ramjugernath [2002], states that the disturbance to the equilibrium condition is directly proportional to the change in volume by sampling. The associated pressure drop gives an indication of the magnitude of the disturbance to the equilibrium.

There are two volume changes associated with sampling in analytic methods. The volume change associated with the size of the withdrawn sample, and the volume change associated with the sampling method. The capabilities of the analytical device used determine the size of the sample required while the method of sampling is generally chosen such that it produces a minimum disturbance during sampling by removing the smallest sample volume possible.

Numerous techniques have been developed which attempt to withdraw a sample without altering its overall composition and without adversely disturbing the equilibrium in the cell.

To avoid a pressure drop during sampling Aroyan & Katz [1951] injected mercury from a compression unit into a pressure control cylinder thus maintaining the pressure in the equilibrium cell during sampling, while Kobayashi & Katz [1953] injected mercury into the cell as the samples were drawn. A variable volume cell [Nasir *et al.,* 1980/1981; Nakayama *et al*.,1987; Staby & Mollerup, 1991] allowed adjustment of the internal volume of the cell

thus compensating for pressure changes associated with sampling. Adjustment of the overall volume of the system was achieved by installing a manually-operated volume regulator in the external loop of a recirculation-type apparatus [Stein *et al*., 1962a,b; Chang & Lu, 1967; Stein & Proust, 1971; Kubic & Stein, 1980/1981; Jennings & Teja, 1989; Wang *et al*., 1991]. This setup allowed compensation for pressure changes. Legret *et al*. [1981] used detachable sampling vessels to block off a sample from the equilibrium cell thus eliminating a reduction in pressure.

Providing a high ratio between the equilibrium cell volume and the volume of the withdrawn sample reduces the impact of volumetric disturbances to the systems equilibrium state. By using capillary tubing [Heintz & Street, 1983; Matos *et al*., 1989], micro-bores or special micro-sampling valves [Lagret *et al*., 1994] in order to withdraw a sample the pressure drop in the cell is minimized due to the small size of the sample withdrawn. There is however a limit to the size of the sample withdrawn depending on the sensitivity of the analytical device used. Using a large equilibrium cell volume [Sagara *et al*., 1972; Klink *et al*., 1975; Ashcroft *et al*., 1983; Reiff *et al*., 1987; Mühlbauer, 1990] minimized the effect of the volume changes associated with the sampling method and the quantity of the withdrawn sample. This solution however is not very attractive due to the increased use of chemicals which makes it very expensive. A simple method which employed the use of a second cell was proposed by Brunner *et al*. [1993].

A fast sampling method minimizes the time available for equilibrium changes. Fast-acting pneumatic or electromagnetic valves were used for the fast expansion of the sample directly into a gas flow line leading to a gas chromatograph [Figuiere *et al*., 1980; Danesh & Todd, 1990].

In two phase recirculation, liquid recirculation, vapour recirculation and liquid pass dynamic methods a portion of the liquid and/or vapour flow is continuously withdrawn from the equilibrium cell, passed through an external loop, where transfer to a GC is easily accomplished, and returned to the cell [Dorau *et al*., 1983; Weber *at al*., 1984; Morris & Donohue, 1985]. Thus for the circulating phase there is no volume change associated with the sampling method.

A novel sampling method involving the circulation of representative equilibrium samples through the sample loop of a GC six port valve was reported by Ramjugernath [2000].

Using an optical method for composition determination such as the spectroscopic method of Konrad *et al*. [1983] allows for the analysis of the coexisting equilibrium phases to be conducted in situ inside the equilibrium cell. This eliminates all the complexities associated with sampling resulting in no disturbance to the equilibrium cell.

2.5.6 Preparation of withdrawn samples for analysis

When measuring VLE data at high pressures it was observed by Deiters & Sneider [1986] that the main problem associated with analytic methods is the handling and preparation of the samples for analysis and not the actual determination of the composition of the samples. The main reason for this is that during HPVLE studies the equilibrium state is different to the required input state to an analytical device such as a GC or mass spectrometer, thus for analysis to take place the high-pressure sample must be converted to an appropriate low-pressure state. Care must be taken when handling the sample as any minor change in the temperature or pressure can lead to partial separation of components. When sampling the liquid phase, there is a tendency for the volatile component to flash preferentially, thus causing concentration gradients in the resulting vapour. These problems associated with the sample preparation result in an error in the quantitative analysis of the samples.

To counter these problems suitable methods of sample preparation which ensure homogenization of the withdrawn samples and prevent partial condensation of the withdrawn liquid samples have been reported in literature:

- To prevent partial condensation of samples during or after sampling Katayama *et al.* [1975] used separately-controlled temperature zones with the constant-temperature bath housing the liquid and vapour sampling flasks maintained at a temperature 10ºC higher than the bath housing the equilibrium cell. Sterner [1961] allowed the expansion of the liquid sample through a sampling valve into a large volume, evacuated glass reservoir system. Keeping the sample size small ensured complete evaporation of the liquid sample after the sampling valve was closed. Chang *et al.* [1966] used stainless-steel capillary tubing for the liquid-sampling lines. Once the sample left the equilibrium cell it was reduced to a pressure below atmospheric through a needle valve. To ensure complete vaporization of the sample the insulated sampling tube was heated to 150ºC using nichrome wire. These methods prevented condensation of samples but did not ensure the production of a homogeneous mixture.

- Some authors have reported the use of an agitated vessel in the sampling line to ensure homogenization of the liquid phase sample. A glass tube containing a loosely fitting soft iron core intermittently moved by a ring magnet was used by Wichterle & Kobayashi [1972] to ensure the formation of homogenous vaporized liquid sample.
- Nakayama *et al.* [1987] used a forced circulation system to homogenise the vaporised liquid sample.
- Kobayashi & Katz [1953] reported a method which involved a separate analysis of the volatile and non-volatile components in a sample.
- Jet-mixers were used by Mühlbauer & Raal [1991] to produce a homogenous sample. The swirling recirculating motion of the fluid in the device ensured homogeneity. These vessels were operated at a temperature about 50ºC higher than the equilibrium temperature to prevent condensation of the sample in them. Similar type jet-mixers were used by Moodley [2002].

2.5.7 Analysis of the equilibrium phases

When analyzing vapour and liquid phases the two most commonly used methods during HPVLE experimentation are gas chromatography (external) and spectroscopy (in-situ analysis).

Gas chromatography is the more frequently used method of external analysis, particularly when multi-component mixtures are being investigated. There are two main types of gas chromatography detectors which are used. Thermal conductivity detectors (TCD) which are able to detect hydrocarbons and non-hydrocarbons, and flame ionization detectors (FID) which are able to detect organics only. Problems encountered when using gas chromatography include the difficulty encountered due to the high-pressure, high-temperature equilibrium state being different to the required input into the chromatograph. Thus it is necessary to prepare the samples before input into the gas chromatograph. Another problem encountered is the difficulty of GC calibration when working with gas mixtures and gas-liquid mixtures. Raal [1992] developed a precise static volumetric calibration device for gas mixtures which was employed by Sancho [1998].

Street and Calado [1978] and Heintz & Streett [1983] reported using heat conductivity to determine compositions when investigating binary mixtures of volatile compounds, while mass spectrometry was used by Rigas *et al*. [1958], Street *et al*. [1964], and Yonker *et al*. [1984].

2.6 The vapour recirculation method

2.6.1 General description

Vapour recirculation was the first phase-recirculation method to be used in HPVLE studies. The vapour recirculation method was first attempted by Collie [1889] with further developments by Inglis [1906]. Figure 2-3 illustrates the main features of a vapour recirculation apparatus.

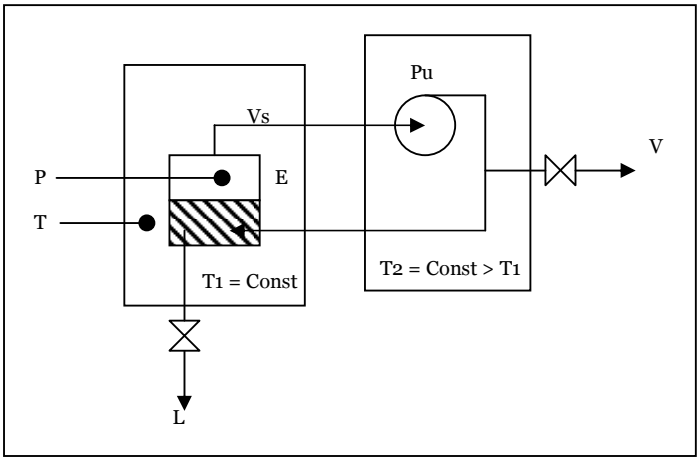

Figure 2-3: Features of a vapour recirculation apparatus [Malanowski, 1982]
E, Equilibrium cell; L, Liquid-phase sample; P, Pressure measuring device; Pu, Vapour recirculation pump; T, Temperature-measuring device; T1, T2, Constant-temperature environments; V, Vapour-phase sample; Vs, Recirculating vapour stream

Initially all the components are charged into the equilibrium cell until the desired initial liquid level in the cell is attained. The equilibrium cell is housed in a constant temperature environment. During experimentation the vapour phase is then continuously withdrawn from the top of the cell and circulated through an external loop with the aid of a pump. This external loop is usually housed in a different, higher, constant temperature environment to that of the cell. The vapour phase is then returned to the bottom of the equilibrium cell, where it is bubbled through the stationary liquid phase. This cycle is carried out until phase equilibrium is achieved. The good contact between the two phases, when using the vapour recirculation method, increases the speed at which equilibrium is attained especially in well designed equilibrium cells. Equilibration times of 5 to 10 minutes were reported by Calado *et al*. [1981] and Shah *et al*. [1990] when using their vapour recirculation apparatus. Once equilibrium has been attained the system temperature and pressure are measured, and samples of the liquid and vapour phases are withdrawn from the system and analyzed.

Sampling of the vapour phase is normally achieved by isolating a small portion of the recirculating vapour phase. Kaminishi *et al*. [1989] achieved this by installing a detachable sampling cell in the external vapour recirculation loop, while Nagahama *et al*. [1974] and Parrish & Steward [1975] isolated a sample between valves installed in the external recirculation loop. Fredenslund *et al*. [1973] used a method which involved temporarily diverting the recirculating vapour stream through the sampling loop of a multi-port GC valve. When applying these methods the disturbance of the equilibrium in the cell is almost totally eliminated.

Sampling of the liquid-phase in the vapour recirculation method requires a direct withdrawal of the liquid sample from the equilibrium cell. Sampling can be carried out using capillary tubing [Miller *et al*., 1977; Somait & Kidnay, 1978] or a sampling valve [Katayama *et al*., 1975; Mraw *et al.,* 1978] mounted on the body of the equilibrium cell. By incorporating a variable volume cell in the external vapour recirculation loop [Price & Kobayashi, 1959; Toyama *et al.,* 1962; Wang *et al.,* 1991; Jin *et al.,* 1993] compensation for pressure changes during the liquid-sampling process was provided. Fredenslund *et al*. [1973] used a piston-driven sampling rod.

2.6.2 The vapour recirculation pump

The design of a suitable pump for the circulation of the vapour phase presents a challenge when using the vapour recirculation method. The pump must be able to circulate the vapour phase through a closed system, against a low pressure drop, while fulfilling the following requirements as outlined by Moodley [2002]:

- Possess a small free volume that is readily purged at the normal pumping rate.
- Be capable of continuous start-stop operation for long periods of time.
- Deliver low flow rates of the order of 1 to 5 cm^3/s.
- Operate over a wide pressure range with a small rise in pressure across the device.
- Not contaminate the fluid by exposure to lubrication or stuffing-boxes.
- Must not allow stagnant regions of trapped material to develop.
- There must be minimal pulsations.
- There should be no system volume change during operation of the pump.
- The vapour flow rate should be able to be adjusted.
- The pump should be constructed of material which is compatible with the operating conditions i.e. temperatures and pressures, and the fluids which the pump is to handle.

There are a number of different types of vapour recirculation pumps which have been designed and successfully applied in practice including, magnetic recirculation pumps [Sterner, 1960], magnetic piston pumps [Elliot *et al.*, 1974], electromagnetic pumps [Stein *et al.*, 1962], positive-displacement pumps [Eckert & Prausnitz, 1965] and diaphragm pumps [Somait & Kidnay, 1978]. Moodley [2002] used a double acting pneumatic pump which essentially was a modification of the magnetically-driven double-acting pump of Behrens & Sandler [1983]. The main difference between the two pumps was that the pump of Behrens & Sandler [1983] was driven using magnetically-activated coils while the pump of Moodley [2002] was driven pneumatically.

2.6.3 Difficulties encountered using the vapour recirculation method

There are a number of difficulties associated with experimentation using the vapour recirculation method:

- It is necessary to maintain the temperature of the vapour phase in the recirculation loop at a temperature higher than the vapour dew-point to prevent condensation of the vapour. This is usually achieved by placing only the equilibrium cell in the thermostat, while maintaining the rest of the system at a higher temperature in an alternate environment. The vapour recirculation method is best suited for cryogenic work, due to the smaller possibility for partial condensation of the recirculating vapour phase than during high-temperature studies.
- An efficient heat exchange system is necessary to cool the superheated recirculating vapour in the external loop down to exactly the equilibrium temperature before it is returned to the equilibrium cell. This must be achieved because if vapour returns to the cell at the incorrect temperature it will cause vaporization of the liquid in the cell.
- Liquid entrainment in the recirculating vapour stream must be eliminated. This can be achieved by lowering the vapour recirculation rate or placing special separators/demisters in a portion of the vapour space of the equilibrium cell as demonstrated by Moodley [2002].
- The temperature, volume and pressure of the system must remain constant in order to attain a steady-state operation. Variations in these parameters will cause the quantities and compositions of the liquid and vapour phases to vary. The liquid-level in the equilibrium cell must be kept constant. This is constantly monitored by visual inspection. Pulsations introduced during operation of the vapour recirculation pump lead to pressure

fluctuations in the system. Pressure variations often lead to a change in vapour-phase composition which can result in a considerable error particularly in the critical region where the vapour is highly compressible. A well designed pump and a reduction in the flow rate of the recirculating phase can assist in minimizing or even eliminating these pulsations and the associated pressure variation problem.

2.7 Literature review of features of equipment used in the development of the vapour recirculation equipment used in this study

Literature reviewed here focuses on ideas that were used by Moodley [2002] in the development of the piece of equipment used in this study, as well as some interesting novel ideas incorporated into vapour recirculation equipment. The review highlights features and ideas used in the design of the equilibrium cell, the vapour recirculation pump, the cooling system to attain low temperatures, the sampling methods and the techniques used in the preparation of samples for analysis. A more in depth detailed review of vapour recirculation equipment reported in literature has been performed by Moodley [2002].

2.7.1 Equilibrium cell design

To permit viewing of contents, the equilibrium cell used in this study was constructed from heavy walled Pyrex tubing fitted with stainless steel end plates press fitted with Teflon to provide the necessary sealing between the main body and the end-plates together with Viton O-rings. The equilibrium cell with an internal volume of 17 cm^3 was fitted with demisters to prevent liquid entrainment in recirculting vapour. Vapour re-entering the cell passed through a distribution nozzle to assist in the formation of fine bubbles as the vapour passed through the liquid phase.

Eckert & Prausnitz [1965] employed heavy walled Pyrex tubing in the construction of their equilibrium cell to permit viewing of contents at low temperatures and high pressures. The apparatus of Price & Kobayashi [1951] which provides a good illustration of the basic components of a vapour recirculation apparatus makes use of a Jergusen transparent gauge with a stainless steel body to permit viewing of the cell contents with sealing between the metal and the glass being achieved with Teflon gaskets. Weber *et al.* [1984] reported using high-pressure glass windows in the design of the equilibrium cell to permit viewing of liquid level and the monitoring of the distribution of vapour re-entering the cell together with the detection of the formation of a second liquid phase. Weber *et al.* [1984] also made use of a

vapour distribution nozzle situated at the bottom of the cell together with a mist separator made of wire mesh situated at the top of the equilibrium cell.

2.7.2 Vapour recirculation pump design

A PCM Delasco DL Series Type DL12 peristaltic pump was initially used for vapour recirculation by Moodley [2002]. A number of problems were however experienced during the use of the pump when performing VLE measurements:

- Due to the inability to heat the internal rubber hose passing within the pump non-volatile components tended to condense inside the pump.
- The absorptive nature of the internal rubber hose resulted in the absorption of the components under investigation in varying amounts resulting in continuous fluctuations in compositions and equilibrium cell pressure making it impossible to achieve thermodynamic equilibrium. Surface fluorination of the hose only provided a temporary solution to this problem
- When operated at pressures above atmospheric leaks developed at the inlet and outlet connections of the pump. Upon further investigation it was found that the pump was not designed for use with gases but rather for the transfer of viscous liquids and slurries.

It was thus decided to discard the peristaltic pump and as no other suitable pump was available commercially a new pump was designed for use in the study by Moodley [2002]:

A pneumatic vapour recirculation pump was designed and constructed in the study by Moodley [2002]. The pump was made up of a double-acting pneumatic cylinder with a through-rod shaft. A floating piston housed inside a stainless steel head was fitted to each end of the shaft with sealing being achieved with two U shaped neoprene seals fitted back-to-back between each head. Usual operation of the pump driven by compressed air supplied at around 100 kPa saw the pump deliver flows at around 5.6 cm^3/s. The pump was tested successfully up to pressures of 650 kPa by Moodley [2002].

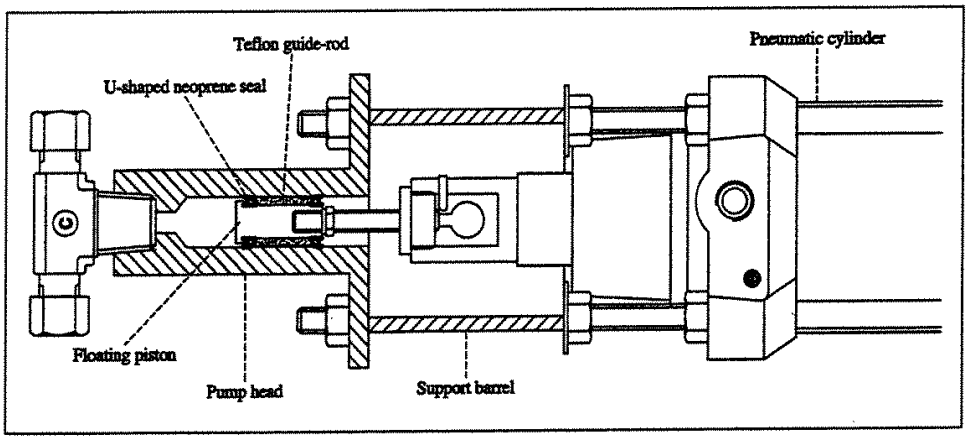

Figure 2-4: Method of sealing used in the vapour recirculation pump of Moodley [2002]

The design of the pneumatic pump of Moodley [2002] was based largely on the design by Behrens & Sandler [1983] with the main difference being that the earlier design by Behrens & Sandler [1983] was driven using magnetically activated coils while the pump of Moodley [2002] was pneumatically driven.

2.7.3 Cooling system design

In the equipment of Moodley [2002] cooling of the equilibrium cell and maintenance of isothermal conditions was achieved by housing the equilibrium cell in a thermostat through which nitrogen gas at a regulated temperature was blown entering at the bottom of the unit and exiting at the top. The cylindrically shaped thermostat was constructed from medium-walled Pyrex tubing with the wall constructed from two concentric Pyrex tubes with end-flanges constructed from aluminium. The double wall design resulted in an annular space of 18 mm between the inner and outer wall which was evacuated during experimentation using a high capacity vacuum pump to provide insulation with PTFE sleeves isolating the Pyrex from the aluminium end-flanges to provide for sealing and additional insulation. The heat exchanger used for heating recirculating vapour as it left the top of the equilibrium cell and the cooling unit which was responsible for cooling recirculating vapour before it re-entered the equilibrium cell were both also housed inside the thermostat. The nitrogen gas was cooled by passing it through a coil immersed in a low temperature bath containing liquid nitrogen or dry ice depending on the temperature at which the studies were being conducted. Prior to entry into the thermostat the nitrogen gas was passed through a heating unit which carefully adjusted the nitrogen gas temperature according to the desired equilibrium cell temperature.

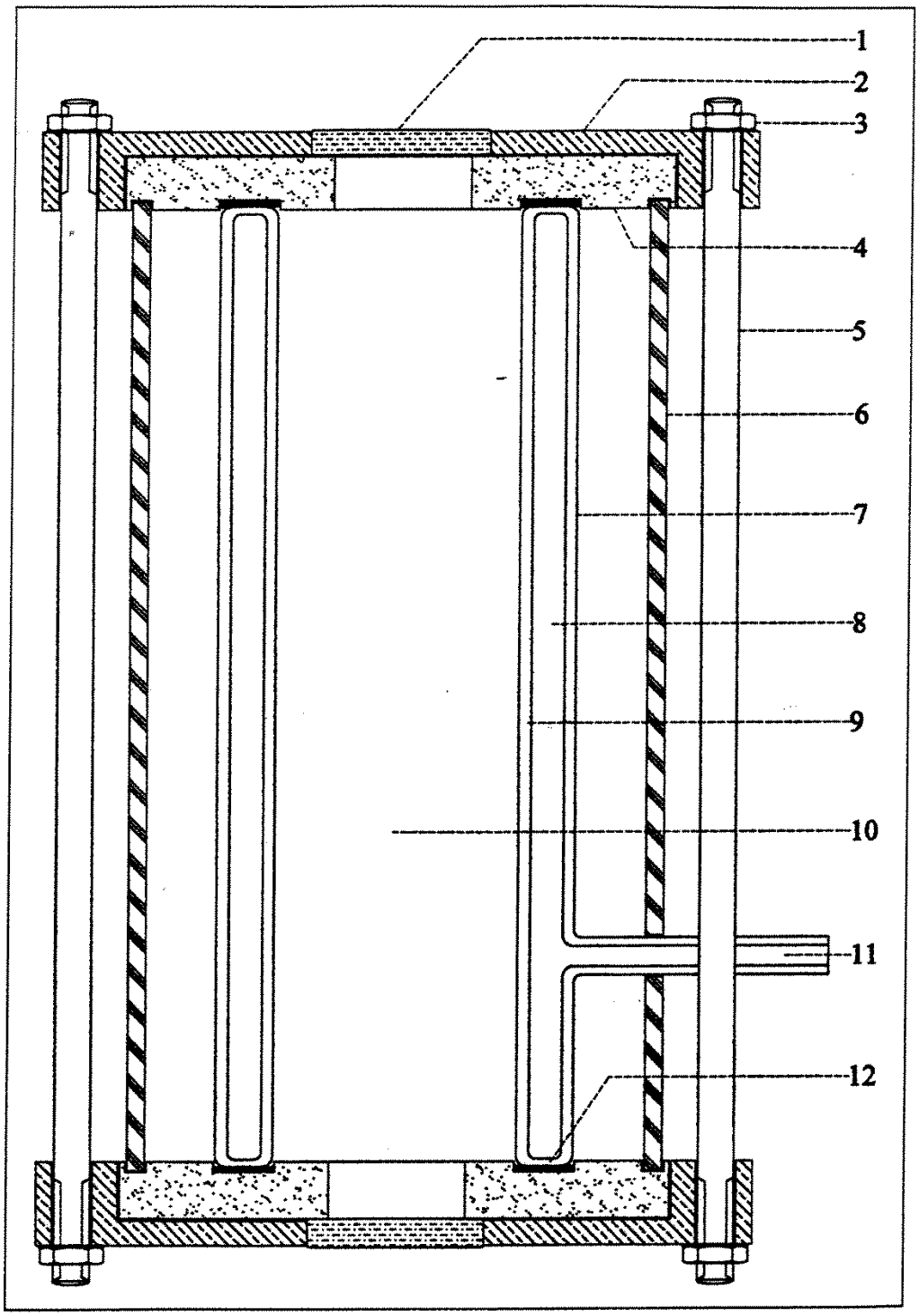

Figure 2-5: Thermostat used by Moodley [2002]
1, ELASTOSIL M4505 RTV-2 silicone rubber plug; 2, Aluminium end-plate; 3, Hexagonal nut; 4, Fluorosint PTFE end-plate; 5, Tie-rod; 6, Perspex shield; 7, Outer Pyrex tube; 8, Evacuated annular space; 9, Inner Pyrex tube; 10, Insulated central chamber of thermostat; 11, Connection to vacuum pump; 12, Expanded PTFE gasket

The equipment of Moodley [2002] was designed to perform measurements at temperatures down to -80°C, however the minimum attainable temperature in the equilibrium cell was only -5°C. The major factor contributing to this inability to achieve low-temperatures were problems experienced owing to the design of the thermostat. These problems included leakages of the thermostat and poor insulation of the thermostat which greatly limited the ability of the equipment to achieve low temperatures in the equilibrium cell as discussed in more detail in Section 4.4.

Eckert & Prausnitz [1965] made use of a vacuum cryostat with liquid nitrogen as the cooling medium to assist in achieving temperatures down to -203°C. Insulation of the system containing the equilibrium cell was achieved by evacuating the cryostat to pressures well below atmospheric pressure. The equipment of Fredenslund *et al.* [1973] made use of a cooling system involving the equilibrium cell housed inside thermostat, using liquid nitrogen as the cooling medium. Control of the temperature in the equilibrium cell was achieved by initially vaporizing the liquid nitrogen then blowing the vaporized nitrogen over an electric heater connected to a temperature controller before flowing over the equilibrium cell.

2.7.4 Sampling systems design

In the study by Moodley [2002] liquid phase sampling was carried out via a short, fine bore capillary of less than 1 mm in diameter machined in the bottom end-plate of the equilibrium cell. A 1/8-in. Whitey 31 series union-bonnet metering valve, mounted flush on the base of the equilibrium cell, was used to control the flow of liquid out of the cell. This arrangement ensured a small amount of stagnant, non-equilibrium material in the sampling system, with an estimated dead volume of less than 25 µl.

Sampling of the liquid phase by Price & Kobayashi [1959] was achieved via a capillary tube connected to the side of the equilibrium cell near its base with a snug fitting nichrome wire inserted into the line between the sampling valve and the equilibrium cell to minimize hold-up in the sample line. Eckert & Prausnitz [1965] made use of extended needle valves during liquid sampling. This method had the advantage in that it eliminated the need for flushing the sampling device thus allowing for a very small sample to be drawn. The liquid sampling device of Fredenslund *et al.* [1973] consisted of a 5 mm diameter rod protruding into the liquid phase in the cell with a 3.5 µl hole drilled vertically through the rod near the tip immersed in the liquid. Movement of the rod was achieved via a piston connected to it which

when activated caused the hole in the rod containing the liquid sample to be withdrawn into the cell wall from where it was flushed by helium for analysis.

A Valco six-port two-position valve was used by Moodley [2002] to isolate a portion of the recirculating vapour stream in the external vapour recirculation loop during vapour sampling. The manually operated valve was fitted with a 3.5 m long sample loop of fine bore 1/8 in. OD stainless steel tubing, to give a vapour sample of 5.4 cm^3. This sampling method ensured there was no change to the equilibrium cell volume during sampling.

Vapour sampling by Eckert & Prausnitz [1965] was achieved by isolating a section of the vapour recirculation loop then bleeding the isolated vapour into previously evacuated sample vessels. Tsang & Street [1981] employed a method where the vapour sample was drawn from the top of the vapour recirculation pump. Vapour was sampled by isolating a portion of vapour in a bypass line in the equipment of Weber *et al.* [1984].

2.7.5 Sample preparation for analysis

Moodley [2002] used jet-mixers for homogenisation of liquid samples as they were drawn from the equilibrium cell to obtain a sample of uniform composition representative of the equilibrium state. Two jet mixers were connected in series with the first jet-mixer directly connected to the sampling valve via a short length of 1/16 in. OD stainless steel tubing. The pressure difference between the high pressure equilibrium cell and the evacuated jet-mixer provided the driving force for the transfer of material to the first jet-mixer. A second jet mixer situated closer to the GC, ensured complete homogenization of the sample and eliminated the separation of volatile and non-volatile components as the sample was passed to the GC. A short, thin line of 1/16 in. OD stainless steel tubing was used to transfer the sample from the second jet-mixer to the GC.

A single jet-mixer was used for homogenization of the vapour samples in the equipment of Moodley [2002]. Switching the Valco six-port valve from the sampling position to the flushing position resulted in a transfer of the vapour sample into the evacuated jet-mixer with helium used to flush the sample loop and valve flow passages. Samples were then transferred to the GC for analysis.The preparation of both vapour and liquid samples for analysis using jet-mixers was also employed in earlier studies by Bradshaw [1985], Mühlbauer & Raal [1991, 1993] and Ramjugernath [2000].

CHAPTER 3

THEORETICAL TECHNIQUES USED IN THE INTERPRETATION OF HIGH-PRESSURE VAPOUR-LIQUID EQUILIBRIUM DATA

The acquisition of experimental VLE data presents a lengthily and skilled procedure with a significant amount of work going into the compilation of an accurate set of data. Based on this, together with the growing number of systems in industry for which VLE data is required for process design, it is realized that accurate experimental data available and the resources to generate this data, cannot cater for this vast demand. Additionally a basic set of experimental VLE data on its own is not sufficient for process design and optimization. These concerns have led to the development of techniques used in deriving numerical correlations which can be used to calculate the phase equilibrium for multi-component systems of interest.

These theoretically based techniques generally require a minimal amount of experimentation and once parameterised they enable interpolation and extrapolation of phase equilibrium data and can thus be used to predict phase behaviour at desired conditions.

This section discusses the methods used in the correlation of HPVLE data in particular, together with the various thermodynamic models used in phase equilibrium behaviour prediction.

3.1 Thermodynamic equilibrium

When there is no change in the macroscopic properties of a system with time, the system is considered to be in a state of equilibrium. In the case of vapour-liquid equilibrium, the system is considered to be in equilibrium when the temperature and pressures as well as the chemical potential of each species μ_i are the same in each of the phases. This is a static condition with no tendency for macroscopic change within the system with time. Smith *et al.* [1996] derived Equation (3-1) to describe the criterion for vapour-liquid equilibrium

$$\mu_i^V = \mu_i^L \tag{3-1}$$

where V is the vapour phase and L is the liquid phase and the chemical potential of species *i* is given by

$$\mu_i = \Gamma_i(T) + RT \ln \hat{f}_i \tag{3-2}$$

where R is the universal gas constant, $\hat{f}_i$ is the fugacity of species *i* and Γ_i(T) is the integration constant at constant T, as a function of temperature only.

Equation (3-2) cannot be used for the direct computation of the equilibrium relation and a relationship that can be expressed in terms of measurable variables is required. The isofugacity criterion to describe a state of vapour-liquid equilibrium thus follows:

$$\hat{f}_i^V = \hat{f}_i^L \tag{3-3}$$

The fugacity can be related to the measured variables temperature *T*, pressure *P*, liquid composition *x* and the vapour composition *y*, using auxiliary functions such as a fugacity coefficient ϕ or an activity coefficient γ thus allowing the use of Equation (3-3) in a practical context. The relationships can be expressed by the following definitions:

$$\hat{\phi}_i = \frac{\hat{f}_i}{x_i P} \tag{3-4}$$

which defines the components fugacity in the mixture or,

$$\hat{\gamma}_i = \frac{\hat{f}_i}{x_i f_i^\circ} \tag{3-5}$$

which defines the components activity coefficient in the mixture where f_i° is the arbitrarily defined standard-state fugacity of component *i*.

An important ratio used in VLE to relate the vapour and the liquid phase mole-fractions is the equilibrium ratio or the K-value which is defined as

$$K_i = \frac{y_i}{x_i} \tag{3-6}$$

where x_i and y_i are the liquid and vapour mole-fractions of species *i* respectively.

3.2 Methods used in the interpretation of HPVLE

The combined (gamma-phi) and direct (phi-phi) methods have been identified as the two main computational methods used in the interpretation of VLE. The two methods differ in that the combined method uses an activity coefficient to describe the liquid phase non-ideality and a separate fugacity coefficient to describe the vapour phase non-ideality, whereas fugacity coefficients are used to describe both the liquid and vapour phase non-idealities in the combined method. HPVLE data was initially interpreted using the combined method. However the computation of the hypothetical standard states of the supercritical components had many difficulties associated with it when employing the combined method and this led to the further development of the combined method to enable computation of such conditions which occur commonly during HPVLE.

3.2.1 The direct method

Fugacity coefficients are used to describe both the vapour and liquid phase non-idealities when using the direct method. A state of equilibrium in a system can therefore be described by

$$\hat{f}_i^V = \hat{\phi}_i^V y_i P = \hat{\phi}_i^L x_i P = \hat{f}_i^L \tag{3-7}$$

The equilibrium ratio is then given by

$$K_i = \frac{\hat{\phi}_i^L}{\hat{\phi}_i^V} \tag{3-8}$$

The vapour and liquid fugacity coefficients are functions of temperature, pressure, and phase compositions and are generally evaluated using an equation of state (EOS) explicit in pressure with the form $P = f(V,T)$, together with an appropriate mixing rule along with the following exact thermodynamic relationships:

$$\ln \hat{\phi}_i^V = \frac{1}{RT}.\int_{V_T^V}^{\infty}\left[\left(\frac{\partial P}{\partial n_i}\right)_{T,V_T,n_j} - \frac{RT}{V_T}\right]dV_T - \ln\left[\frac{PV^V}{RT}\right] \tag{3-9}$$

and

$$\ln \hat{\phi}_i^L = \frac{1}{RT}.\int_{V_T^L}^{\infty}\left[\left(\frac{\partial P}{\partial n_i}\right)_{T,V_T,n_j} - \frac{RT}{V_T}\right]dV_T - \ln\left[\frac{PV^L}{RT}\right] \tag{3-10}$$

where n is the number of moles of material, V_T is the total volume, V is the molar volume, and superscripts V and L represent the vapour and liquid phase properties respectively.

A number of difficulties associated with the application of the direct method as discussed by Raal & Mühlbauer [1998] and Ramjugernath & Raal [1999] are outlined as follows:

- A single EOS is used to describe the both the liquid and vapour phases over a range of conditions including the critical region. This requirement cannot be fully satisfied as there is currently no EOS which is able to perform this with the desired generality. Selection of a suitable EOS able to fully describe the *P-V-T* behaviour of the system over the entire phase composition and density range thus provides a challenge.
- The computational techniques used during dew point or bubble point calculations of multi-component mixtures often fail to converge in the critical region.
- The use of non-cubic EOS results in difficulties in assigning appropriate roots to the vapour and liquid phase densities.
- When mixtures are being studied, selection of an appropriate mixing rule may present problems as the empirical nature of the mixing rules make them suitable to describe only certain types of systems.

3.2.2 The combined method

The combined method makes use of an activity coefficient γ to describe the non-ideality of liquid phase while a fugacity coefficient ϕ is used to describe the non-ideality of the vapour phase. A state of equilibrium is therefore defined as follows:

$$\hat{f}_i^V = \hat{\phi}_i^V y_i P = \gamma_i x_i f_i^{\circ L} = \hat{f}_i^L \tag{3-11}$$

with the following equilibrium ratio

$$K_i = \frac{\gamma_i f_i^{\circ L}}{\hat{\phi}_i^V P} \tag{3-12}$$

Similarly to the direct method the fugacity coefficient is evaluated using Equation 3-11 together with a suitable EOS. The activity coefficient is a function of temperature *T*, pressure *P* and the liquid phase compositions of the components which make up the mixture and is evaluated separately using a liquid-phase model (LPM). The use of a separate fugacity coefficient to solely describe the vapour phase non-ideality is favourable in that it removes the problem of selecting a suitable EOS from the extensive range of available excess Gibbs functions for evaluation of the liquid phase fugacity, but introduces the difficulty in selecting suitable standard states for the evaluation of the temperature *T* and pressure *P* dependant standard-state fugacity of the liquid $f_i^{\circ L}$.

The activity coefficients of the components in the liquid phase are obtained via the Gibbs-Duhem equation, which relates the activity coefficient to the excess Gibbs energy:

$$\sum x_i d \ln \gamma_i = \sum x_i d\left(\frac{\overline{G}_i^E}{RT}\right) = \frac{V^E}{RT} dP - \frac{H^E}{RT^2} dT \tag{3-13}$$

or

$$\left[\frac{\partial(G)}{\partial P}\right]_{T,x} dP + \left[\frac{\partial(G)}{\partial T}\right]_{P,x} dT - \sum x_i d\overline{G}_i = 0 \tag{3-14}$$

Which at constant T and P simplifies to:

$$\sum x_i d\overline{G}_i = 0 \tag{3-15}$$

The activity coefficient represents the degree of non-ideality of component *i* in a mixture through the relationship between the liquid phase fugacity at the system temperature, pressure and liquid composition to an arbitrarily defined standard state fugacity $f_i^{\circ L}$ where the activity coefficient equals one. The standard state fugacity must be defined such that it equals the fugacity of the pure liquid component at the system temperature at a fixed composition and an arbitrary reference pressure. Selecting a compatible standard state provides a challenge when applying the combined method.

Difficulties associated with the application of the combined method have been discussed by Raal & Mühlbauer [1998] and Ramjugernath & Raal [1999] as follows:

- Often one of the components exists in a supercritical state at the system temperature, and a suitable liquid standard state fugacity needs to be defined for this non-condensable component.
- At high pressures vapour-phase non-idealities become more significant and thus require a suitable EOS and mixing rule to account for the non-idealities. Dependence of the vapour-phase fugacity coefficient on the vapour-phase composition results in lengthily calculation procedures.
- Derivation of the activity coefficients from the Gibbs-Duhem equation requires the use of a suitable liquid phase model (LPM).
- Suitable correlations are needed to determine liquid-phase pure-component molar volumes V_i^L and partial molar volumes $\overline{V}_i^L$.
- At high pressures the effect of pressure must be accounted for in the Gibbs-Duhem equation.
- This method introduces a large number of parameters to be regressed from the experimental data. This complexity results in the need to select a suitable regression procedure.

3.3 Equations of state

The physical properties pressure *P*, molar volume *V*, and temperature *T* which describe the mechanical state of a substance can be related by an equation of state (EOS) in the form $f(P,V,T) = 0$. EOS form the basis of high pressure phase equilibrium calculations and any equilibrium property can be determined using EOS together with suitable thermodynamic relations. Vapour-pressure, critical properties and densities of pure substances or mixtures

can also be calculated from EOS. EOS have thus been applied extensively during certain aspects of separation equipment design. The practicalities of EOS have resulted in the development of numerous different classes of EOS. This section discusses the more frequently used EOS in phase equilibrium studies.

3.3.1 Cubic equations of state

Cubic equations of state (CEOS) are defined as equations which are cubic in volume. CEOS are able to represent both liquid and vapour phases over a wide range of conditions and have thus been applied quite considerably to vapour-liquid equilibrium calculations. CEOS are generally represented explicitly with respect to pressure which is defined as the sum of a repulsive term $P_{repulsive}$ and an attractive term $P_{attractive}$. Generally CEOS only contain two parameters, the attraction parameter a which is a measure of the attractive forces between the molecules and the covolume parameter b which is the excluded volume or the part of the molar volume which is not available to a molecule due to the presence of other molecules.

3.3.1.1 Development of cubic equations of state

The most basic CEOS the van der Waals EOS gives a good representation of the structure of a CEOS:

$$P = \frac{RT}{V-b} - \frac{a}{V^2} \tag{3-16}$$

or more generally according to the definition of a CEOS:

$$P = P_{repulsive} + P_{attractive} \tag{3-17}$$

Where,

$$P_{repulsive} = \frac{RT}{V-b} \quad \text{(van der Waals hard-sphere equation)} \tag{3-18}$$

$$P_{attractive} = \frac{a}{V^2} \tag{3-19}$$

The van der Waal EOS was the first CEOS to give a qualitative description of the vapour and liquid phases and represent the vapour-liquid coexistence. The simplicity of this two parameter EOS was found to be sufficient for use with non-polar spherical and non-spherical molecules [Sadus, 1992], however representation was poor when applied to mixtures containing strongly polar molecules which tend to be strongly self associating. This is largely due to the inadequate consideration given to intermolecular forces in the two parameter van der Waal EOS.

The inability of the van der Waal equation to accurately represent a wide array of molecules has led to the modification of the equation and the subsequent development of a large number of other more accurate CEOS often referred to as modern CEOS. Most subsequent CEOS generally retain the van der Waals separation of the repulsive and attractive terms. The repulsive term of van der Waal was generally left unchanged while the attractive term was usually modified such that it has temperature dependence.

The generalized CEOS form originating from the van der Waal CEOS, is represented by Equation

$$P = \frac{RT}{V-b} - \frac{a(T)}{g(V)} \tag{3-20}$$

where *g(V)* is a function of molar volume. The modern CEOS developed can be grouped into four categories depending on the modification made to the van der Waal CEOS:

1. Modifications of the attractive term
2. Improved repulsive models
3. Modifications to both terms
4. Equations for non-spherical models

The first cubic EOS to be widely accepted for fugacity calculations and the most noted modification of the van der Waal CEOS is the Redlich-Kwong (RK) EOS developed by Redlich & Kwong [1949]. This equation which has a modified temperature dependent attractive term generally has success only when applied to nearly ideal systems or simple fluids.

$$P = \frac{RT}{V-b} - \frac{a/T^{0.5}}{V(V+b)} \tag{3-21}$$

The limited accuracy of the Redlich-Kwong EOS saw the emergence of numerous proposals to try improve the accuracy of the equation. Modifications either focused on providing a better temperature dependence of the parameters *a* and *b*, or changing the function *g(V).* Of the numerous modifications, the modification of Soave [1972] the Soave-Redlich-Kwong (SRK) EOS and the modification by Peng & Robinson [1976] the Peng-Robinson (PR) EOS have achieved widespread acceptance and have been successfully applied to VLE calculations for conventional as well as non-conventional fluid mixtures.

The modification by Soave [1972] saw a modification to the attractive term in the RK EOS by introducing a temperature dependent attraction parameter *a.*

$$P = \frac{RT}{V-b} - \frac{a(T)}{V(V+b)} \tag{3-22}$$

where,

$$a(T) = a_c.\alpha(T_r, \omega) \tag{3-23}$$

$$a_c = 0.42747\frac{R^2T_c^2}{P_c} \tag{3-24}$$

$$b = 0.08664\frac{RT_c}{P_c} \tag{3-25}$$

$$\sqrt{\alpha} = 1 + \kappa(1 - \sqrt{T_r}) \tag{3-26}$$

where κ is a constant characteristic of each substance which can be correlated against the accentric factors of the components investigated according to the following:

$$\kappa = 0.480 + 1.57\omega - 0.176\omega^2 \tag{3-27}$$

The SRK EOS can be rewritten as a cubic polynomial with respect to the compressibility factor *Z*:

$$Z^3 - Z^2 + Z(A - B - B^2) - AB = 0 \tag{3-28}$$

where,

$$Z = \frac{PV}{RT} \tag{3-29}$$

$$A = \frac{a(T)P}{(RT)^2} \tag{3-30}$$

$$B = \frac{bP}{RT} \tag{3-31}$$

When solving Equation (3-28) to obtain the compressibility factor the maximum and minimum real positive roots are assigned to vapour and liquid phase roots respectively. This results in the following expressions for determination of the vapour and liquid phase fugacity coefficients using the SRK EOS:

$$\ln \phi_i = Z_i^V - 1 - \ln(Z_i^V - B) - \frac{A}{B} \ln\left(\frac{Z_i^V + B}{Z_i^V}\right) \tag{3-32}$$

$$\ln \phi_i = Z_i^L - 1 - \ln(Z_i^L - B) - \frac{A}{B} \ln\left(\frac{Z_i^L + B}{Z_i^L}\right) \tag{3-33}$$

The SRK EOS saw success when applied to the computation of vapour pressures of a number of hydrocarbons as well as in the prediction of phase behaviour of multicomponent systems containing polar and non-polar components.

Studies by Peng & Robinson [1976] revealed a poor correlation of liquid-phase specific volumes between data predicted using the RK EOS and literature data. This error was found to increase by around 20% from reduced temperatures to near the critical point. Peng & Robinson [1976] proposed a modification to the attractive term of the SRK EOS to improve the prediction of volumetric properties. The modification of the attractive term saw the over estimation of the compressibility factor as estimated by the RK EOS (Z_c = *1/3)* reduced to 0.307. The Peng & Robinson (PR) EOS is written as follows:

$$P = \frac{RT}{V-b} - \frac{a(T)}{V(V+b)+b(V-b)} \tag{3-34}$$

where,

$$a(T) = a_c.\alpha(T) \tag{3-35}$$

$$a_c = 0.457235\frac{(RT_c)^2}{P_c} \tag{3-36}$$

$$b = 0.077796\frac{RT_c}{P_c} \tag{3-37}$$

$$\alpha(T) = \left[1+\kappa\left(1-\sqrt{\frac{T}{T_c}}\right)^2\right] \tag{3-38}$$

$$\kappa = 0.37464 + 1.5422\omega - 0.26992\omega^2 \tag{3-39}$$

The PR EOS can also be represented in the form of the compressibility factor and reduces to the following for a pure component:

$$Z^3 - (1-B)Z^2 + Z(A-3B-2B^2) - (AB-B^2-B^3) = 0 \tag{3-40}$$

With the fugacity coefficients of the vapour and liquid phases given by the following respectively:

$$\ln\phi_i = Z_i^V - 1 - \ln(Z_i^V - B) - \frac{A}{2\sqrt{2}B}\ln\left(\frac{Z_i^V + (1+\sqrt{2})B}{Z_i^V + (1-\sqrt{2})B}\right) \tag{3-41}$$

$$\ln\phi_i = Z_i^L - 1 - \ln(Z_i^L - B) - \frac{A}{2\sqrt{2}B}\ln\left(\frac{Z_i^L + (1+\sqrt{2})B}{Z_i^L + (1-\sqrt{2})B}\right) \tag{3-42}$$

It was concluded by Peng & Robinson that their EOS was as good as, if not better than the SRK EOS particularly in the prediction of liquid-phase densities. The successes of the SRK and PR EOS have seen them as the more widely used EOS in industrial applications. Disadvantages in the application of the EOS described above see poor prediction of liquid phase densities, the use of inaccurate generalised parameters for non-hydrocarbons (polar

and associating fluids) and the unreliable phase behaviour prediction of long chain molecules.

Table 3-1: Temperature dependency models for the $\alpha(T)$ function in a CEOS [Moodley, 2002]

Redlich & Kwong [1972]	$\alpha = \frac{1}{\sqrt{T}}$	(3-43)
Soave [1972]	$\alpha = \left[1 + \kappa\left(1 - \sqrt{T_r}\right)\right]^2$	(3-44)
	$\kappa = 0.480 + 1.574\omega - 0.176\omega^2$	(3-45)
Peng & Robinson [1976]	$\alpha = \left[1 + \kappa\left(1 - \sqrt{T_r}\right)\right]^2$	(3-46)
	$\kappa = 0.480 + 1.574\omega - 0.176\omega^2$	(3-47)
Mathias [1983]	$\alpha = \left[1 + \kappa_0\left(1 - \sqrt{T_r}\right) - \kappa_1\left(1 - T_r\right)\left(0.7 - T_r\right)\right]^2$	(3-48)
	$\kappa_0 = 0.48508 + 1.55191\omega - 0.15613\omega^2$	(3-49)
Mathias & Copeman [1983]	$\alpha = \left[1 + \kappa_1\left(1 - \sqrt{T_r}\right) + \kappa_2\left(1 - \sqrt{T_r}\right)^2 + \kappa_3\left(1 - \sqrt{T_r}\right)^3\right]^2$	(3-50)
Soave [1984]	$\alpha = 1 + \kappa_1\left(1 - T_r\right) + \kappa_2\left(\frac{1}{T_r} - 1\right)$	(3-51)
Stryjek & Vera [1986a,c,d]	$\alpha = \left[1 + \kappa\left(1 - \sqrt{T_r}\right)\right]^2$	(3-52)
1. SV	$\kappa = \kappa_0 + \kappa_1\left(1 + \sqrt{T_r}\right)\left(0.7 - T_r\right)$	(3-53)
2. SV2	$\kappa = \kappa_0 + \left[\kappa_1 + \kappa_2\left(\kappa_3 - T_r\right)\left(1 - \sqrt{T_r}\right)\right]\left(1 + \sqrt{T_r}\right)\left(0.7 - T_r\right)$	(3-54)
	$\kappa_0 = 0.378893 + 1.4897153\omega - 0.17131848\omega^2 + 0.0196554\omega^3$	(3-55)
Melhem et al. [1989]	$\alpha = \exp\left[\kappa_1\left(1 - T_r\right) + \kappa_2\left(1 - \sqrt{T_r}\right)\right]$	(3-56)
Twu et al. [1991]	$\alpha = T_r^{\kappa_1(\kappa_2 - 1)} \exp\left[\kappa_3\left(1 - T_r^{\kappa_2\kappa_3}\right)\right]$	(3-57)
Zabaloy & Vera [1998]	$\alpha = 1 + \kappa_1 T_r \ln T_r + \kappa_2\left(T_r - 1\right) + \kappa_3\left(T_r^2 - 1\right)$	(3-58)

Table 3-2: Modifications made to the attractive term for various EOS [Moodley , 2002]

Redlich & Kwong [1949]	$\frac{a}{\sqrt{T}V(V-b)}$	(3-59)
Soave [1972]	$\frac{a(T)}{V(V-b)}$	(3-60)
Peng & Robinson [1976]	$\frac{a(T)}{V(V+b)+b(V-b)}$	(3-61)
Fuller [1976]	$\frac{a(T)}{V(V+cb)}$	(3-62)
Schmidt & Wenzel [1980]	$\frac{a(T)}{V^2+ubV+wb^2}$	(3-63)
Harmens & Knapp [1980]	$\frac{a(T)}{V^2+cbV+(c-1)b^2}$	(3-64)
Patel & Teja [1982]	$\frac{a(T)}{V(V+b)+c(V-b)}$	(3-65)
Stryjek & Vera [1986a]	$\frac{a(T)}{V(V+b)+b(V-b)}$	(3-66)
Trebble & Bishnoi [1987]	$\frac{a(T)}{V^2+(b+c)V+(bc+d^2)}$	(3-67)
Yu & Lu [1987]	$\frac{a(T)}{V(V+c)+b(3V+c)}$	(3-68)
Twu, Coon & Cunningham [1992b]	$\frac{a(T)}{V(V+4b)+c(V+b)}$	(3-69)
Twu, Sim & Tassone [2000]	$\frac{a(T)}{(V+3b)+(V-0.5b)}$	(3-70)

A number of modifications to the generalized form of the thermodynamic CEOS have been proposed over the years, as researchers attempted to improve the prediction of phase behaviour over a broader range of components and mixtures. Modifications were carried out on the temperature dependence of the function $\alpha(T)$ with examples of developed correlations displayed in Table 3-1 compiled by Moodley [2002]. Modifications were also carried out to the function g(V) of the attractive term of the generalized CEOS with examples of the more popular modifications contained in Table 3-2 [Moodley, 2002].

Modifications have also been carried out on the repulsive term of the generalized CEOS to better represent asymmetric fluids which are generally not well represented in the equations discussed thus far. Table 3-3 compiled by Moodley [2002] displays some reported modifications to the repulsive term of the generalized CEOS.

Table 3-3: Examples of modifications made to the repulsive term of the generalized CEOS [Moodley, 2002]

Reiss, Frisch & Lebowitz [1959]	$\frac{1+\eta+\eta^2}{(1-\eta)^3}$	(3-71)
Thiele [1963]	$\frac{1+\eta+\eta^2}{(1-\eta)^3}$	(3-72)
Guggenheim [1965]	$\frac{1}{(1-\eta)^4}$	(3-73)
Carnahan & Starling [1969]	$\frac{1+\eta+\eta^2-\eta^3}{(1-\eta)^3}$	(3-74)
Boublik [1981]	$\frac{1+(3\alpha-2)\eta+(3\alpha^2-3\alpha+1)\eta^2-\vartheta^2\eta^3}{(1-\eta)^3}$	(3-75)

Where,

$$\eta = \frac{b}{4V} \tag{3-76}$$

It has been noted by Naidoo [2004] that modifications generally made to existing CEOS and development of new CEOS are largely carried out with specific applicability to fluids under investigation and can thus not be assumed to be suitable for other fluids not discussed. Wei & Sadus [2000] discuss of modifications carried out to the generalized CEOS in more specific detail. Raal & Mühlbauer [1998] provide an outline on the application of CEOS in the computation of vapour-liquid equilibrium.

3.3.1.2 Extension of cubic equations of state to mixtures

The application of CEOS to mixtures requires methods to assist in determining the parameters *a* and *b* for the mixture under investigation. The method applied generally makes use of appropriate mixing and combining rules which are applied to determine accurate parameters for the mixture.

The van der Waals one-fluid-theory or the classical mixing rule (CMR), proposed by van der Waal has been identified as the simplest mixing rule available. The CMR was initially derived from the Virial EOS as in Smith *et al.* [2001] and basically defines the particular EOS mixture parameter as the sum of the corresponding pure component parameters a_M and b_M.

$$a_M = \sum_j \sum_i x_i x_j a_{ij} \tag{3-77}$$

$$b_M = \sum_j \sum_i x_i x_j b_{ij} \tag{3-78}$$

This model carries the assumption that the radical distribution function of the molecules which make up the component are all identical and thus performs relatively accurately when there is a small size difference between the molecules. The cross parameters a_{ij} and b_{ij} are determined via combining rules making use of the pure component parameters a_i and b_i.

$$a_{ij} = \left(1 - k_{ij}\right)\sqrt{a_i a_j} \tag{3-79}$$

$$b_{ij} = \left(1 - l_{ij}\right)\frac{b_i + b_j}{2} \tag{3-80}$$

Where k_{ij} and l_{ij} are binary interaction parameters for the compounds, obtained via regression of experimental VLE data for each pair of compounds making up the system. l_{ij} is often set to zero for simple mixtures however in certain instances a better representation of VLE data is achieved by the inclusion of l_{ij} as a second interaction parameter. When $l_{ij}=0$ the model is referred to the 1-parameter classical mixing rule (1PCMR), and when $l_{ij}\neq 0$ it is referred to as the 2-parameter classical mixing rule (2PCMR). The general expression of the second virial coefficient of a pure fluid is a function of temperature only and is represented as follows:

$$B_M = \sum_i \sum_j x_i x_j B_{ij}(T) \tag{3-81}$$

The fugacity coefficient of a component i in a mixture when evaluated via the SRK or PR EOS's can be represented by the following general expression [Smith *et al.* 1996]:

$$\begin{aligned} \ln \hat{\phi}_i = {} & \frac{\bar{b}_i}{b_M}\left(Z_M - 1\right) - \ln\frac{\left(V_M - b_M\right)Z_M}{V_M} + \frac{a_M / b_M RT}{c_1 - c_2} \\ & \times\left(1 + \frac{\bar{a}_i}{a_M} - \frac{\bar{b}_i}{b_M}\right)\ln\frac{V_M + c_2 b_M}{V_M + c_1 b_M} \end{aligned} \tag{3-82}$$

Where $\bar{a}_i$ and $\bar{b}_i$ are partial parameters for species i defined as follows:

$$\bar{a}_i = \left[\frac{\partial\left(n a_M\right)}{\partial n_i}\right]_{T, n_{j\neq 1}} \tag{3-83}$$

$$\bar{b}_i = \left[\frac{\partial\left(n b_M\right)}{\partial n_i}\right]_{T, n_{j\neq 1}} \tag{3-84}$$

These generalized expressions used to extend the SRK and PR EOS's to mixtures are not dependent on the mixing rule used to determine the mixture parameters a_M and b_M.

Shortcoming in the prediction of liquid-phase non-idealities sees the CMR being limited in its application to mixtures that exhibit moderate solution non-ideality. This shortcoming saw the development of activity coefficient models to describe highly non-ideal systems through the incorporation of the excess Gibbs energy G^E to describe the liquid-phase non-ideality.

Mixing rules have been divided into five main groups by Raal & Mühlbauer [1995]: the classical, density-dependent, composition-dependent, density-independent and local composition mixing rules. Certain boundary conditions must be satisfied by the mixing and combining rules. Criteria that must be satisfied, states that the mixing rule must not result in the second virial coefficient being non-quadratic in composition. The mixing rules will be discussed according to those that do not incorporate the excess Gibbs energy models and those which incorporate the excess Gibbs energy models discussed in Section 3.4.2.

Mixing rules not incorporating the excess Gibbs energy G^E

Wong & Sandler [1992] developed the Wong & Sandler mixing rule (WSMR) which made use of the excess Helmholtz free energy A^E at infinite pressure instead of the excess Gibbs energy G^E at infinite pressure which satisfied the boundary conditions for mixing rules. The choice of excess Helmholtz free energy over excess Gibss free energy is due to the weaker dependence of A^E on pressure resulting in the elimination of the necessity to assume $V^E = 0$ for a liquid. The excess Helmholtz free energy at infinite pressure can be described as follows for a van der Waals type CEOS:

$$A^E_{EOS}\left(T, P \to \infty, x_i\right) = \Lambda\left[\frac{a_M}{b_M} - \sum_i x_i \frac{a_i}{b_i}\right] \tag{3-85}$$

Where Λ is the numerical constant that is dependent on the EOS state used:

$$\Lambda = -\ln(2) \quad \text{for the SRK EOS}$$

$$\Lambda = \frac{1}{\sqrt{2}}\ln\left(\sqrt{2}-1\right) \text{ for the PR EOS}$$

Due to the weaker dependence of A^E on pressure the following approximations can be applied:

$$\begin{aligned} A^E_{EOS}(T, P \to \infty, x_i) &= A^E_\gamma(T, P \to \infty, x_i) \\ &= A^E_\gamma(T, P^*, x_i) \\ &= G^E_\gamma(T, P^*, x_i) - P^* V^E(T, P^*, x_i) \\ &= G^E_\gamma(T, P^*, x_i) \end{aligned} \tag{3-86}$$

Where A^E_λ is the excess Helmholtz energy given by an activity coefficient model and P^* is a low pressure. By combining the above relationships Wong & Sandler obtained the following relationship between the parameters a_M and b_M:

$$a_M = b_M \cdot \left[\sum_i x_i \frac{a_i}{b_i} + \frac{G^E_\gamma(T, P^*, x_i)}{\Lambda} \right] \tag{3-87}$$

Wong & Sandler [1992] observed that although the CMR for the parameters a_M and b_M is sufficient to ensure the proper compositional dependence of the second virial coefficient, it is not a necessary condition. The CMR in fact only provides one solution to the following relation obtained from statistical mechanics:

$$B_M = \sum_i \sum_j x_i x_j B_{ij}(T) = \sum_i \sum_j x_i x_j \left(b - \frac{a}{RT} \right)_{ij} = b_M - \frac{a_M}{RT} \tag{3-88}$$

The second virial coefficient boundary condition can be satisfied by the following relation which is obtained from Equation 3-87 and the last equality of Equation 3-88:

$$b_M = \frac{\sum_i \sum_j x_i x_j \left(b - \frac{a}{RT} \right)_{ij}}{1 - \sum_i x_i \frac{a_i}{b_i RT} - \frac{1}{\Lambda} \cdot \frac{G^E_\gamma(T, P^*, x_i)}{RT}} \tag{3-89}$$

Wong & Sandler [1992] thus proposed the following model referred to as the WSMR written in terms of the binary interaction parameter k_{ij}, resulting from the relationships for the virial coefficients in Equations 3-87 and 3-89:

$$\left(b - \frac{a}{RT} \right)_{ij} = (1 - k_{ij}) \frac{\left[\left(b_i - \frac{a_i}{RT} \right) + \left(b_j - \frac{a_j}{RT} \right) \right]}{2} \tag{3-90}$$

The WSMR has been extensively studied over the years owing to its successes in phase equilibrium predictions of a wide range of non-ideal mixtures over a large range of temperature and pressure when combined with a suitable CEOS. Wong & Sandler [1992] discuss the capabilities of the WSMR in more detail while limitations of the WSMR and modifications to the mixing rules are discussed by Orbey & Sandler [1995], Coutsikos *et al.* [1995] and Twu & Coon [1996] together with a number of other authors.

Orbey & Sandler [1995] found that a single mixing rule can be used to describe the behaviour of non-ideal binary pairs as well as binary pairs of the same mixture that could be described by the CMR through a modification to the WSMR. The modified mixing rule which is highlighted by the new cross virial term is represented as follows together with the proposed new expression for A^E which is valid only for a special case where the fluid satisfies the 1PCMR and combining rules:

$$\left(b-\frac{a}{RT}\right)_{ij}=\frac{1}{2}\left(b_i+b_j\right)-\frac{\sqrt{a_i a_j}}{RT}\left(1-k_{ij}\right) \tag{3-91}$$

$$A^E=\frac{\delta x_1 x_2}{x_1 b_1+x_2 b_2} \tag{3-92}$$

The mixing rule as modified by Orbey & Sandler [1995] is only applicable when used directly with certain free-energy models such as the modified NRTL.

Twu & Coon [1996] proposed a new a new mixing rule the Twu-Coon mixing rule (TCMR) which differed from the WSMR in that it had two second virial coefficient binary interaction parameters, k_{ij} and l_{ij}. The introduction of an additional parameter results in great flexibility of the TCMR when used during VLE data treatment.

The TCMR can be derived from the following relationship:

$$A_{nr}^E=\Delta A-\Delta A_{vdW} \tag{3-93}$$

Where A_{nr}^E is the excess Helmholtz free energy obtained using non-random liquid theory based on the local-composition concept and ΔA is the difference between the molar Helmholtz free energy of a mixture and that of the same mixture of an ideal gas at the same

temperature, pressure and composition. ΔA_{vdW} is the Helmholtz free-energy departure function evaluated for a van der Waals fluid.

The TCMR is represented in Equations 3-94 and 3-95

$$a_M^* = \frac{a_M P}{R^2 T^2} = b_M^* \cdot \left(\frac{a_{M,vdW}^*}{b_{M,vdW}^*} + \frac{1}{\Lambda} . \frac{A_{nr}^E}{RT} \right) \tag{3-94}$$

$$b_M^* = \frac{b_M P}{RT} = \frac{b_{M,vdW}^* - a_{M,vdW}^*}{1 - \left(\frac{a_{M,vdW}^*}{b_{M,vdW}^*} + \frac{1}{\Lambda} . \frac{A_{nr}^E}{RT} \right)} \tag{3-95}$$

where the reduced properties a^* and b^* are defined as follows:

$$a^* = \frac{aP}{R^2 T^2} \tag{3-96}$$

$$b^* = \frac{bP}{RT} \tag{3-97}$$

The parameters $a_{M,vdW}^*$ and $b_{M,vdW}^*$ are evaluated after prior evaluation of the mixture attraction and covolume parameters $a_{M,vdW}$ and $b_{M,vdW}$ given by the van der Waals 2PCMR.

3.4 General considerations for treatment of the liquid-phase

3.4.1 Activity coefficients

As discussed in Section 3.2.2 the activity coefficient γ functions to correct for the non-ideality of the liquid phase. The liquid phase activity coefficient can be calculated from the following relationship for G^E [Smith *et al.*, 1991]:

$$\ln \gamma_i = \left[\frac{\partial \left(G^E / RT \right)}{\partial n_i} \right]_{T,P,n_{j\neq 1}} = \frac{G^E}{RT} - \sum_{k \neq i} x_k \left[\frac{\partial \left(G^E \right) / RT}{\partial x_k} \right]_{T,P,x_{j\neq i,k}} \tag{3-98}$$

The summability relation is generally applied to allow evaluation of G^E with respect to the known activity coefficients.

$$\frac{G^E}{RT} = \sum_i x_i \ln \gamma_i \tag{3-99}$$

with

$$\sum_i x_i d \ln \gamma_i = 0 \tag{3-100}$$

Equation 3-100 when represented in the integrated form can be used to relate the activity coefficients of the components of a particular mixture. A number of widely used semi-empirical liquid-phase models (LPM) which relate the activity coefficients of a system to G^E are available. Isothermal studies result in a pressure change to achieve equilibrium as the composition of the liquid changes. Accurate VLE data correlation requires the activity coefficients be evaluated at the same reference pressure P^R. This is necessary as the experimentally obtained isothermal activity coefficients are at different pressures and thus need to be corrected from the experimental pressure P to the reference pressure.

3.4.2 Models incorporating the excess Gibbs energy

Raal & Mühlbauer [1998] noted that models used in the determination of G^E differ in complexity depending on how the components of the system differ with respect to molecular size and chemical nature. Due to the weak dependence of $\frac{G^E}{RT}$ on pressure, the pressure dependence is often neglected in most models and thus most empirical models express the excess Gibbs energy as a function of mole fraction, volume fraction and molecular surface fractions. Mole fractions are generally excluded where there is a significant difference in the size or chemical nature of the components in the system.

The three-suffix (two-parameter) Margules equation (3-101) is one of the simplest models proposed. Despite this being one of the oldest models it still provides a useful tool in the correlation of activity coefficient data for binary mixtures.

$$\frac{G^E}{RT} = x_1 x_2 \left[A_{21} x_1 + A_{12} x_2 \right] \tag{3-101}$$

where A_{12} and A_{21} are the adjustable interaction parameters. The activity coefficients of the components of a binary mixture are defined as follows:

$$\ln \gamma_1 = x_2^2 \left[A_{12} + 2\left(A_{21} - A_{12} \right) x_1 \right] \tag{3-102}$$

$$\ln \gamma_2 = x_1^2 \left[A_{21} + 2\left(A_{12} - A_{21} \right) x_2 \right] \tag{3-103}$$

Subsequent developments of the three-suffix Margules equation has seen the introduction of an additional interaction parameter. The four-suffix (three-parameter) Margules equation developed to allow the treatment of different systems. The Margules equations were found to sufficiently represent certain non-ideal systems however in instances where the molecule sizes differ significantly the models generally yield poor results.

The van Laar equation (3-104) was the simplest model developed to deal with the occurrence of different size molecules in a system, by incorporating the size difference of the molecules in the model.

$$\frac{G^E}{RT} = x_1 x_2 \left[\frac{A_{12} A_{21}}{A_{12} x_1 + A_{21} x_2} \right] \tag{3-104}$$

where the activity coefficients are calculated as follows:

$$\ln \gamma_1 = A_{12} \left[\frac{A_{21} x_2}{A_{12} x_1 + A_{21} x_2} \right]^2 \tag{3-105}$$

$$\ln \gamma_2 = A_{21} \left[\frac{A_{12} x_1}{A_{12} x_1 + A_{21} x_2} \right]^2 \tag{3-106}$$

The Margules and van Laar equations find great use in their ability to represent experimentally determined activity coefficients with only a few interaction parameters.

These equations are often used to smooth out data and as a tool for interpolation and extrapolation with respect to composition when experimental data is scarce. Malanowski & Anderko [1992] and Walas [1985] discuss the van Laar and Margules equations applicability's and shortcomings in more detail.

Empirical models described thus far are based on the principle that the ratio between the molecules of the species present in the vicinity of any molecule is the same as the ratio of the component mole fractions in the mixture. Most modern theoretical developments are now based on the concept of local composition which states that within a solution, local compositions, different from overall mixture composition, are presumed to account for the short range order and non-random molecular orientations resulting from differences in molecular size and intermolecular forces.

Wilson [1964] introduced the first local-composition model for the determination of excess Gibbs energy:

$$\frac{G^E}{RT} = -x_1 \ln\left(x_1 + \Lambda_{12} x_2\right) - x_2 \ln\left(\Lambda_{21} x_1 + x_2\right) \tag{3-107}$$

with the following relationships derived for the activity coefficients:

$$\ln \gamma_1 = -\ln(x_1 + \Lambda_{12} x_2) + x_2 \left[\frac{\Lambda_{12}}{x_1 + \Lambda_{12} x_2} - \frac{\Lambda_{21}}{x_1 \Lambda_{21} + x_2} \right] \tag{3-108}$$

$$\ln \gamma_2 = -\ln\left(x_2 + \Lambda_{21} x_1\right) - x_1 \left[\frac{\Lambda_{12}}{x_1 + \Lambda_{12} x_2} - \frac{\Lambda_{21}}{\Lambda_{21} x_1 + x_2} \right] \tag{3-109}$$

The adjustable interaction parameters Λ_{12} and Λ_{21} are related to the pure-component molar volumes V_i and the characteristic energy differences $\Delta\lambda_{ji}$ as follows:

$$\Lambda_{ji} = \frac{V_i}{V_j} \exp\left(-\frac{\lambda_{ji} - \lambda_{jj}}{RT} \right) = \frac{V_i}{V_j} \exp\left(-\frac{\Delta\lambda_{ji}}{RT} \right) \tag{3-110}$$

where

$$\Delta_{ji} = \lambda_{ji} - \lambda_{jj} \tag{3-111}$$

and

λ_{ij} = Molecular interactions between molecules *i* and *j*.

λ_{ji} = Molecular interactions between molecules *j* and *i*.

The characteristic energy difference $\Delta\lambda_{ji}$ is considered to be temperature dependent, however studies have shown that often the temperature dependence can be ignored without introducing significant error. The explicit temperature dependence of the adjustable interaction parameters in the Wilson equation allows activity coefficients to be computed from isothermal data as well as isobaric data.

The ability of the Wilson equation to address the case of different size molecules as well as accounting for the energy of interaction between molecules has seen it produce good representation of systems exhibiting severe deviations from ideality. Solutions of polar or associating compounds in non-polar solvents have been well represented by the Wilson equation.

Despite the flexibility of the equation disadvantages of the Wilson equation have been noted. These include inaccuracies in the prediction of liquid-liquid equilibria due to the inability in predicting miscibility gaps, non-suitability with systems exhibiting maxima or minima of activity coefficients and the requirement that the adjustable parameters Λ_{12} and Λ_{21} be positive to allow accurate representation over the entire data range.

A number of local-composition models have been derived from the Wilson equation following its successes. Renon & Prausnitz [1968] proposed the NRTL (Non-Random-Two-Liquid) equation (3-112) which can be successfully applied to miscible as well as completely miscible systems thus addressing one of the key disadvantages of the Wilson equation.

$$\frac{G^E}{RT} = x_1 x_2 \left[\frac{\tau_{21} G_{21}}{x_1 + G_{21} x_2} + \frac{\tau_{12} G_{12}}{G_{12} x_1 + x_2} \right] \tag{3-112}$$

where:

$$\tau_{ji} = \frac{g_{ji} - g_{ii}}{RT} = \frac{\Delta g_{ji}}{RT} \tag{3-113}$$

$$G_{ji} = \exp(-\alpha_{ji} \tau_{ji}) \tag{3-114}$$

with the activity coefficients given by:

$$\ln \gamma_1 = x_2^2 \left[\tau_{21} \left(\frac{G_{21}}{x_1 + G_{21} x_2} \right)^2 + \frac{\tau_{12} G_{12}}{(G_{12} x_1 + x_2)^2} \right] \tag{3-115}$$

$$\ln \gamma_2 = x_1^2 \left[\tau_{12} \left(\frac{G_{12}}{G_{12} x_1 + x_2} \right)^2 + \frac{\tau_{21} G_{21}}{(x_1 + G_{21} x_2)^2} \right] \tag{3-116}$$

where g_{ji} is defined as the energy parameter between molecules of components i and j respectively and α_{ij} is referred to as the non-randomness of the mixture which is usually derived directly from experimental data. Renon & Prausnitz [1968] have reported values ranging from 0.2 to 0.7 while Malanowski & Anderko [1992] report the use of values between -1 to 0.5. When there is a limited availability of experimental data Walas [1985] recommends using a value of 0.3 for non-aqueous mixtures and 0.4 for aqueous organic mixtures. The adjustable interaction parameters Δg_{ji} when used in the NRTL equation can be taken as independent of temperature over narrow temperature ranges, and over wider ranges they take the form of a linear function of temperature. It has however been noted that the temperature dependency does not improve VLE data representation but rather allows the simultaneous description of vapour-liquid equilibria and heats-of-mixing [Malanowski & Anderlko, 1992].

The NRTL equation provides a good alternative to the Wilson equation when dealing with strongly non-ideal mixtures, in particular partially miscible systems where the Wilson equation fails, however inaccuracies and inferiority to the Wilson equation have been found in the dilute region and when representing strongly asymmetric systems that are highly non-ideal. Modifications to the NRTL equation to address its shortcomings have been carried out over the years with the UNIQUAC (Universal Quasi-Chemical) equation developed by Abrams & Prausnitz [1975] being one of the more widely applied models in industry.

CHAPTER 4

EXPERIMENTAL APPARATUS

The HPVLE measurements were carried out on an apparatus based on the dynamic method of vapour recirculation. The apparatus of Moodley [2002] was rebuilt and had modifications carried out on its original construction design, in order to eliminate past problems encountered with the equipment, thus enabling it to reach a wider range of operating conditions. The equipment of Moodley [2002] although designed to obtain data at temperatures as low -80°C, was only able to reach temperatures down to -5°C due to problems encountered owing to the construction design of the equipment. Major modifications were carried out on the nitrogen recirculation loop (the cooling system), with the re-design of the thermostat construction and the addition of a pre-cooler into the loop, thus enabling the equipment to successfully reach temperatures as low as -30°C and obtain data at these temperatures in this study. The addition of the pre-cooler into the system greatly reduced the consumption of dry-ice during operation thus resulting in much lower operating costs and allowing a more stable temperature control over long periods, across all temperatures within the design range. The vapour recirculation pump designed in the study by Moodley [2002] was modified in order for it to accommodate higher pressures. The modified equipment was tested successfully up to pressures of 1000 kPa which exceeded the capabilities of the old equipment which could only reach pressures up to 650 kPa due to failures of the vapour recirculation pump when used at high pressures over extended periods as deduced during tests done during this study.

This section provides a detailed description of equipment used in this study including the modifications carried out to certain components of the equipment used in the study by Moodley [2002] to enable the equipment to reach a much wider range of operating conditions.

4.1 Functional description of vapour recirculation apparatus

Vapour and liquid phases were present in the isothermal equilibrium cell as the experiment was being carried out. The vapour phase was continuously drawn from the top of the equilibrium cell and then passed through a heated external vapour recirculation loop before being returned to the bottom of the cell. A double-acting pneumatic pump was used to circulate the vapour phase. The external loop was heated to prevent condensation of the vapour stream. Before entering the cell, the vapour was passed through a heat exchange

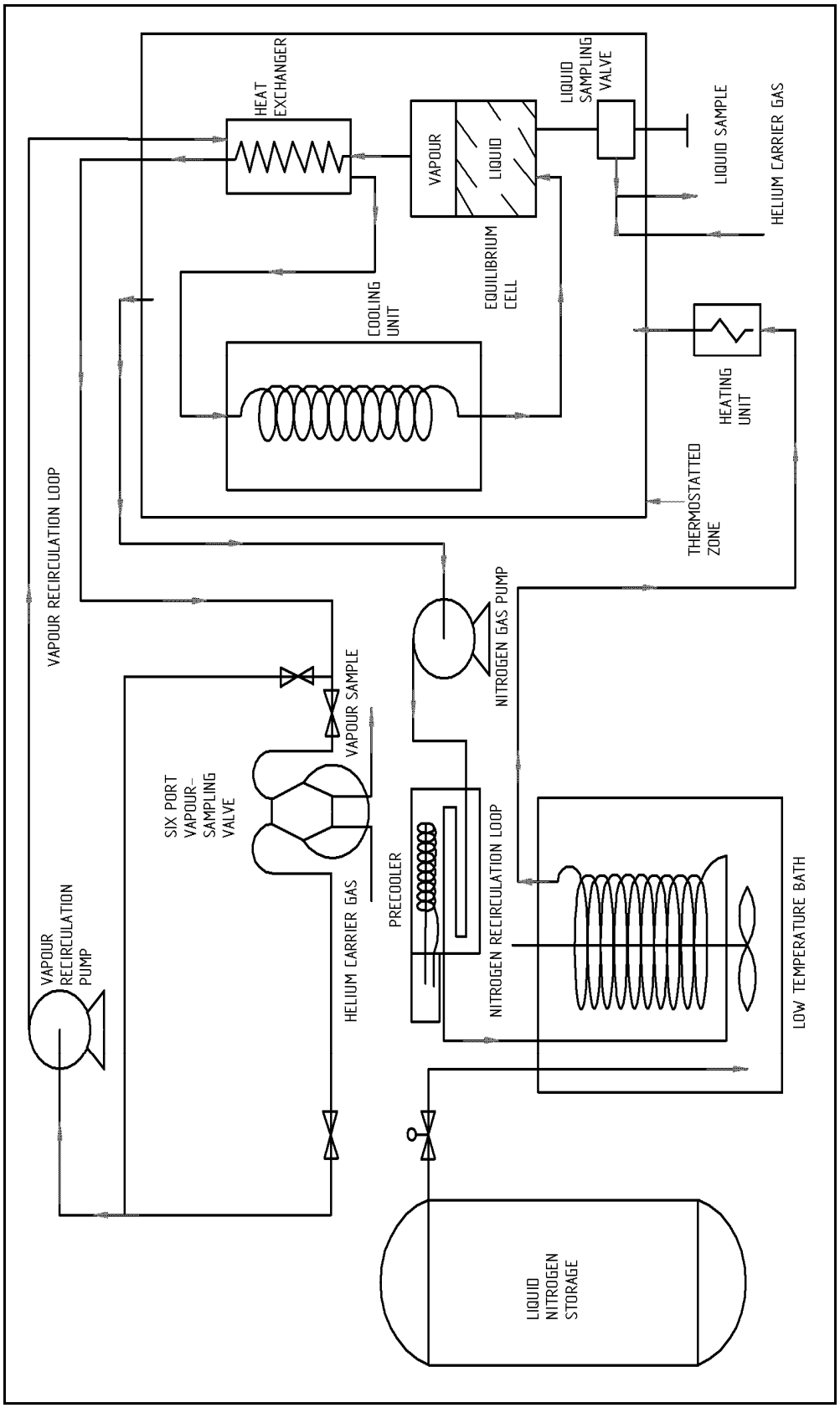

Figure 4-1: Simplified flow diagram of Experimental Apparatus as modified from Moodley [2002]

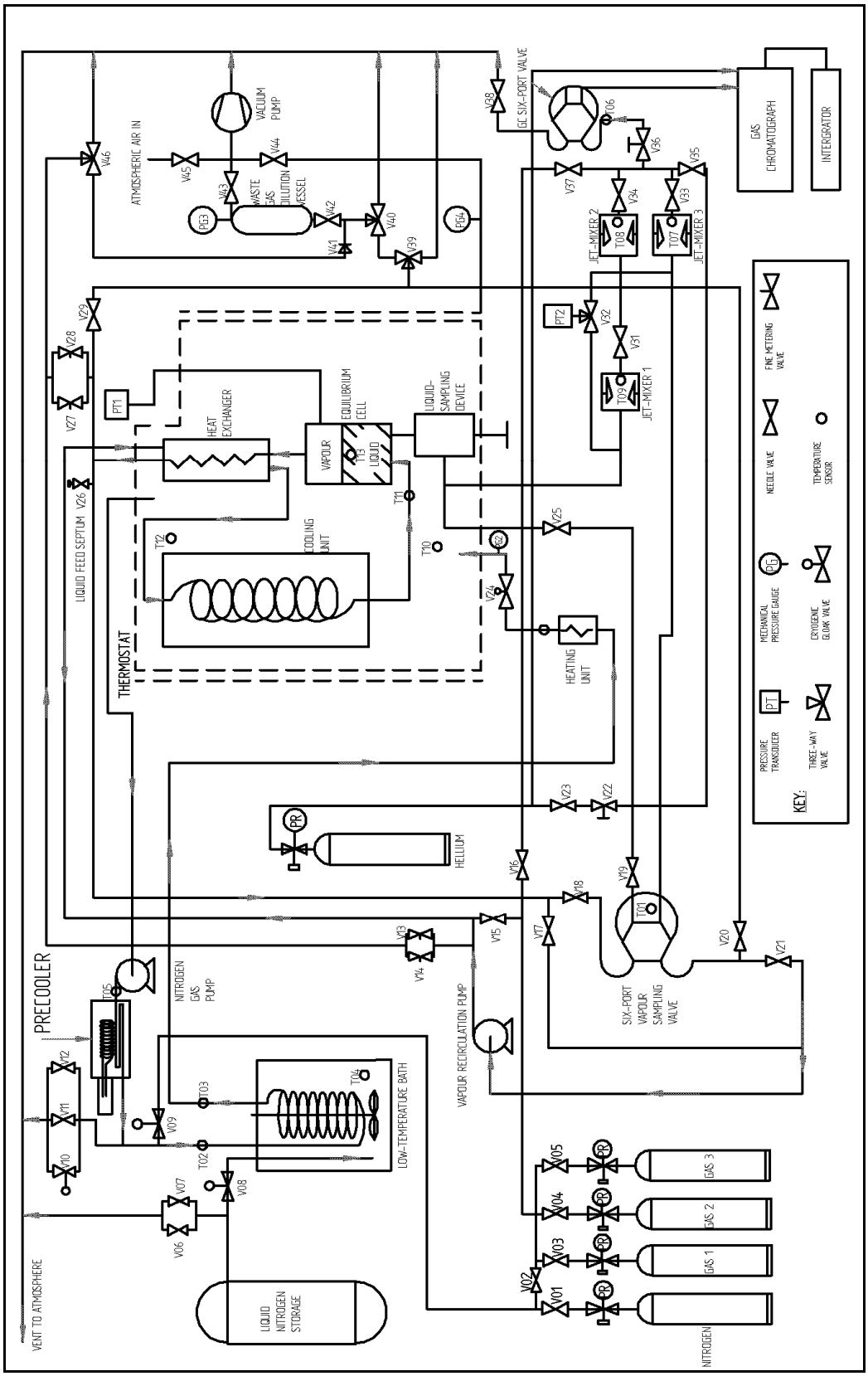

Figure 4-2: Detailed flow diagram of the vapour recirculation Apparatus as modified from Moodley [2002]

system consisting of a heat exchanger and a cooling unit in order to adjust the temperature of the returning vapour to the equilibrium temperature. The vapour returning to the cell was bubbled through the liquid phase to provide agitation and speed up the attainment of equilibrium. This cycle was repeated until equilibrium was assumed to be achieved, at which time the vapour recirculation was stopped and the system was left to stand. If the temperature and more importantly the pressure remained constant over a period of approximately 60 minutes, and there was no change to the liquid level in the equilibrium cell, the system was deemed to be at equilibrium. Once equilibrium was attained in the cell the system variables were noted and samples of the liquid and vapour phases were drawn, homogenized and analyzed via gas chromatography.

The equilibrium cell was maintained under isothermal conditions by housing it inside a constant-temperature environment, the thermostat. Nitrogen gas was circulated at a controlled temperature through the thermostat, thus maintaining isothermal conditions inside the equilibrium cell. The nitrogen gas was circulated with a Metall bellows pump. The nitrogen gas was cooled first by passing it through the pre-cooler which was composed of a section of the line immersed in a low temperature bath. The bath was cooled with an industrial refrigeration unit fitted with cooling coils which were immersed in the bath containing a mixture of water and ethylene glycol. Further cooling of the re-circulating nitrogen was achieved via a coil immersed in a second bath which was cooled either by a cold finger or by an acetone-dry-ice mixture depending on the desired equilibrium cell temperatures. An acetone-dry-ice mixture was used when working at temperatures below 5ºC other than that operation of the pre-cooler together with the cold finger immersed in the acetone bath provided sufficient cooling to achieve temperatures down to 5 ºC. The cooled nitrogen gas was then passed through a heating unit, which controlled the temperature in the equilibrium cell, by adjusting the temperature of the re-circulating nitrogen gas before it entered the thermostat based on feedback from the temperature sensor situated in the equilibrium cell.

4.2 Equilibrium cell

4.2.1 Design

The equilibrium cell identical to the one used by Moodley [2002], was a vertical cylindrical Pyrex tube fitted with stainless steel end plates. This design was based on the design of Stein *et al.* [1962].

The tube constructed from annealed, heavy-walled, Pyrex borosilicate glass made up the cell wall. The ends of the tubing had square ends which were bevelled and fire polished. The tubing had a length of 100 mm and an outer diameter of 20 mm with a wall thickness of 2.5 mm to give an equilibrium cell with an internal volume of 17 cm^3.

The use of heavy walled Pyrex tubing for the cell wall permitted viewing of the cell contents while still achieving the desired mechanical strength of the apparatus. Viewing of the cell contents was necessary for a number of reasons the primary reason being to monitor the liquid level during experimentation. For equilibrium to be achieved the liquid level was to remain constant, thus fluctuation of the liquid-level had to be avoided during experimentation. It was also necessary to view the cell contents, when charging the apparatus during start-up, when sampling the liquid phase for analysis and also to detect liquid entrainment in the re-circulating vapour phase and observe the bubbling of the vapour through the liquid phase.

The tensile strength of Pyrex tubing increases at low temperatures thus this material was considered safe for use at cryogenic temperatures and high pressures. The equilibrium cell was designed for a minimum operating temperature of -80ºC and a maximum operating pressure of 17 bar(a).

The equilibrium cell had end-plates constructed from 316 stainless-steel, with a sleeve constructed from Fluorosint PTFE press fitted into each of the plates. The end-plates were fitted to the ends of the cell and bolted together with four external tie rods. The nuts to these tie rods were finger-tightened to minimize strain on the tubing while still ensuring the cell remained leak tight.

The Pyrex tubing was shielded from the stainless-steel by the PTFE sleeves thus minimizing friction between the metal and glass. There was a low coefficient of friction between the PTFE and the glass. Other desirable properties of the PTFE included its good dimensional stability, in that it retained its size and shape and was not distorted easily, and also it has an excellent chemical resistance which is important as it was exposed directly to the chemicals in the equilibrium cell.

Viton o-rings were used for sealing between the Pyrex wall and the end-plates of the equilibrium cell. Two Viton o-rings were inserted between the glass wall and PTFE sleeve and another between the sleeve and metal end-plate at each end of the cell. The o-rings were

able to withstand the vacuum while the cell was being evacuated as well as the pressure under operating conditions.

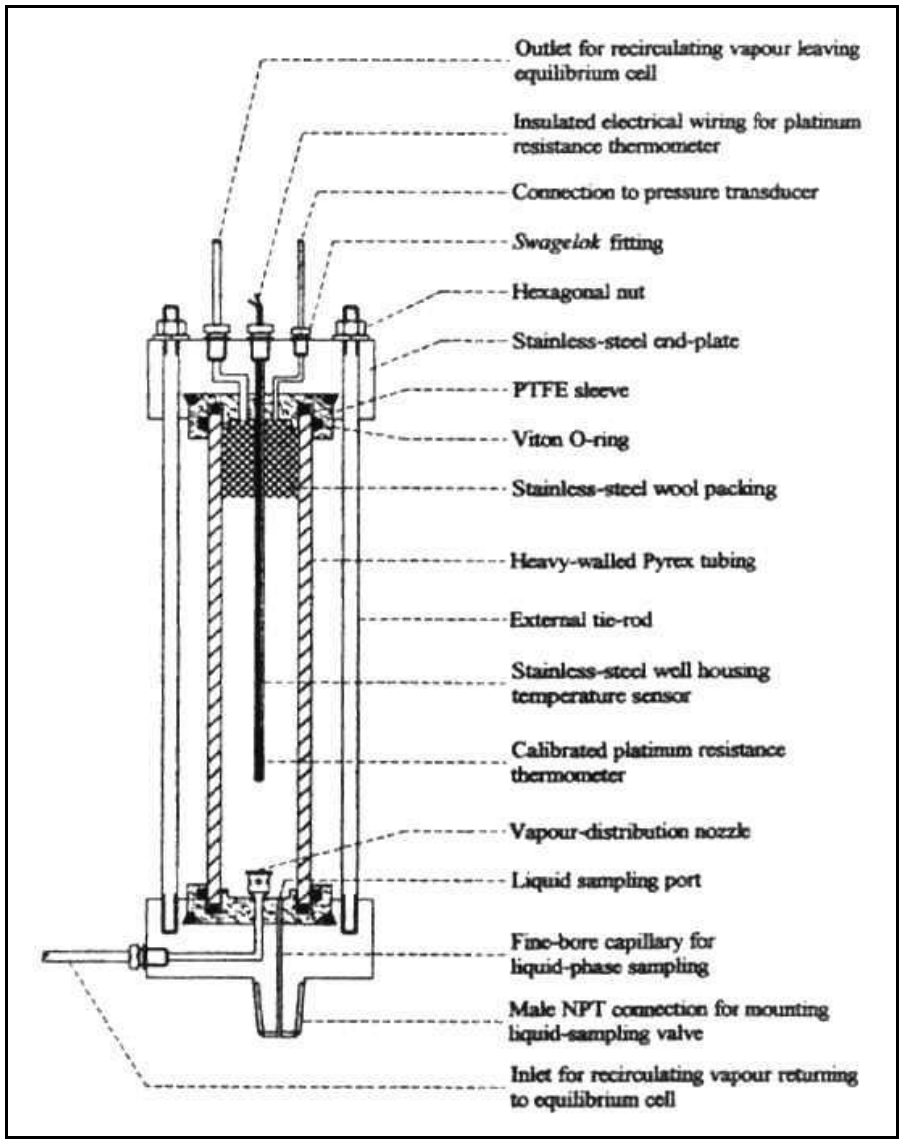

Figure 4-3: Schematic diagram of the equilibrium cell [Moodley, 2002]

The bottom of the cell was fitted with a vapour distribution nozzle with holes of approximately 1 mm drilled into it. This ensured the fine bubbling of the vapour through the liquid phase as the re-circulating vapour stream entered the equilibrium cell. This provided the necessary agitation of the liquid phase and ensured intimate contact between the vapour and liquid phases, thus speeding up the attainment of thermodynamic equilibrium. A small piece of flexible stainless-steel wool was packed in the vapour space at the top of the equilibrium cell. This served as a demister minimizing liquid entrainment in the re-circulating vapour.

The equilibrium cell was considered to be angularly symmetric. Thus there was no preferred radial direction for concentration and temperature gradients to develop in the cylindrical equilibrium cell.

4.2.2 Temperature and pressure measurements

4.2.2.1 Temperature

A 100Ω 1/10-DIN 2-wire platinum resistance thermometer (Pt-100 sensor) conforming to BS 1904 [1984] was used to measure the temperature in the equilibrium cell. The sensor housed in a stainless-steel well constructed from thin-walled 1/8-in. tubing was mounted centrally in the equilibrium cell and fixed to the top end-plate using a Swagelok fitting. The sensor was positioned about 25 mm above the vapour distribution nozzle in the cell ensuring the sensor remained submerged in the liquid phase during experimentation.

The sensor provided input into a Eurotherm 2204 controller which provided a 3-digit display of the cell temperature in units of degrees Celcius (ºC).

4.2.2.2 Pressure

Measurement of the equilibrium cell pressure was accomplished with a 0 to 300 psia (0 to 20.68 bar(a) Sensotec Model Super TJE transducer. A Sensotec model GM display unit was used to process the transducer signal and provide a visual indication of the system pressure in units of Pounds per square inch absolute (psia). The transducer was connected to the top of the equilibrium cell via a short length of fine-bore 1/16-in. OD stainless-steel tubing. The transducer was mounted outside the controlled environment just above the thermostat. Armourflex was used to insulate the line external to the thermostat leading to the transducer as well as the transducer. Insulation of the transducer was necessary to minimize the impact of external temperature influences on the accuracy of the pressure measurement.

4.3 Heat exchange system

It was necessary to cool the vapour returning to the equilibrium cell to precisely the equilibrium temperature during the vapour recirculation process. Superheated vapour returning to the cell would cause undesirable vaporization of the liquid present in the cell,

while an over-efficient cooling system would result in the vapour condensing before it reached the equilibrium cell. The vapour stream leaving the equilibrium cell also needed to be heated to prevent its condensation before it entered the external vapour recirculation loop. Cooling of this vapour stream was achieved via an efficient heat exchange system similar to the system employed by Moodley [2002], comprising of the heat exchanger and the cooling unit arranged as displayed in Figure 4-4.

The heat exchanger of Moodley [2002] used in this study was constructed of a 1.25-in. OD stainless-steel pipe with stainless-steel plates welded to its ends. The pipe housed a 1.15-m long coil of 1/8-in OD stainless-steel tubing. The coil made up a heat transfer area of about 115 cm^3. All lines into and out of the heat exchanger were connected to the end plates using Swagelok fittings.

The cooling unit was made up of a 2.75-m long coil, constructed of 1/8-in. OD stainless-steel tubing housed in a ¾-in OD stainless-steel pipe. A modification to the cooling unit employed by Moodley [2002]. Unlike the heat exchanger, the cooling unit did not have any end plates thus effectively it was a coil surrounded by a pipe.

Both the heat exchanger and the cooling unit used counter-current flow of hot and cold media to promote heat transfer. The re-circulating vapour leaving the equilibrium cell flowed upward through the heat exchanger coil before entering the external recirculation loop, while superheated vapour returning to the equilibrium cell from the external recirculation loop flowed downward directly over the coil of the heat exchanger. This heating of the vapour entering the external vapour recirculation loop was necessary in order to keep its temperature above its dew-point and prevent condensation during recirculation. After passing through the heat exchanger the vapour returning to the equilibrium cell was cooled further by passing it downward through the coil of the cooling unit before entering the equilibrium cell. Nitrogen gas provided the cooling as it passed upward over the cooling unit coil. It was necessary to cool this returning vapour stream to precisely the equilibrium temperature before returning it to the equilibrium cell to prevent disturbances to the equilibrium.

A Class-A Pt-100 sensor was installed on the vapour recirculation line before it entered the equilibrium cell to give an indication of the efficiency of the heat exchange system in cooling the returning vapour to the equilibrium cell temperature.

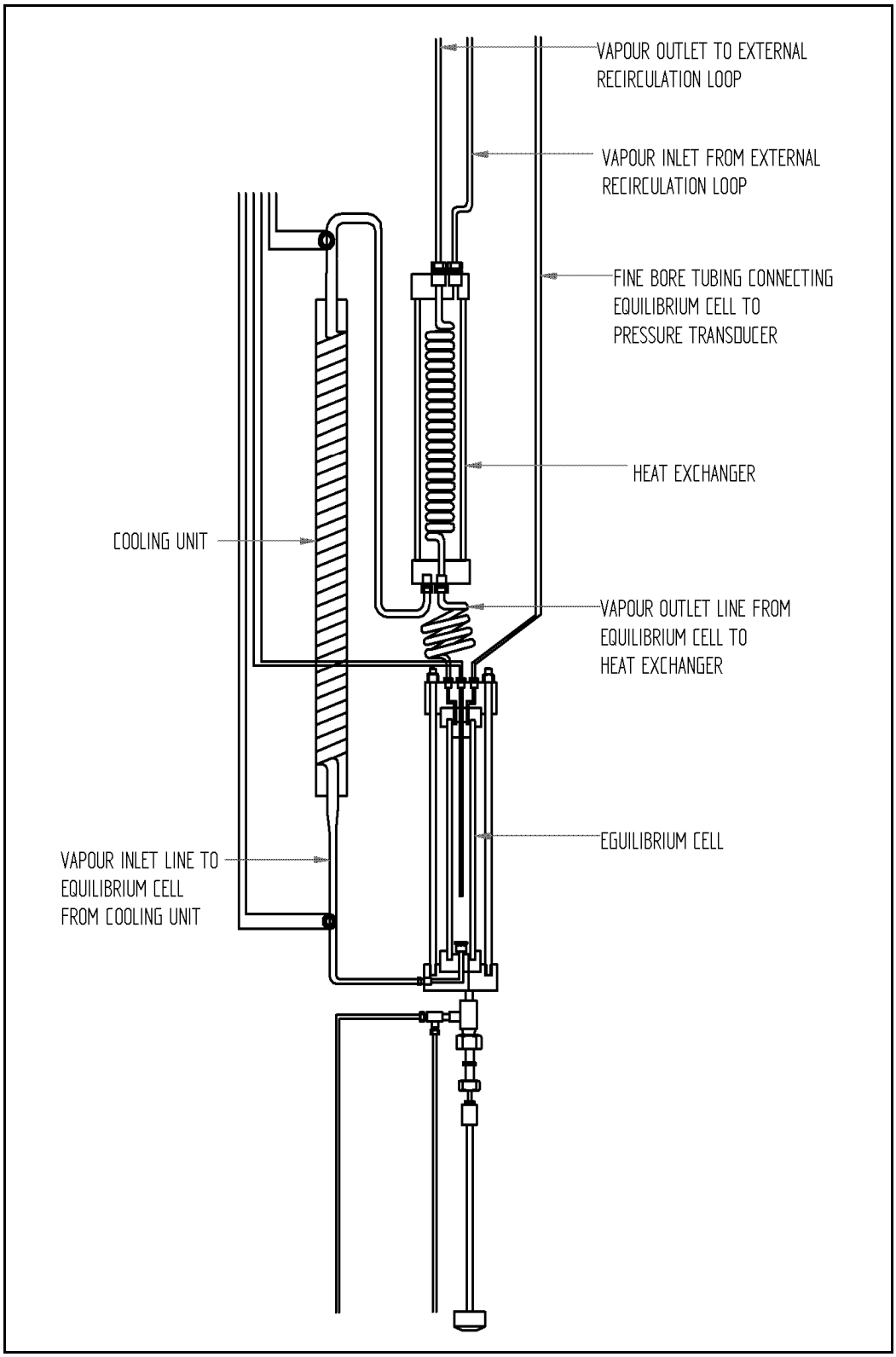

Figure 4-4: Schematic arrangement of heat exchange system and equilibrium cell as modified from Moodley [2002]

4.4 The thermostat

Isothermal conditions were maintained in the equilibrium cell by housing it inside a constant temperature environment, the thermostat. Nitrogen gas at a controlled temperature was blown through the thermostat, entering at the bottom and flowing upward over the equilibrium cell before exiting at the top. The heat exchanger and cooling unit were also housed inside the thermostat. A major limiting factor in the ability to achieve the low temperatures for which the equipment was designed for in the study by Moodley [2002] were problems associated with the design of the thermostat.

The thermostat of Moodley [2002] had a number of problems associated with it:

- High leakage of nitrogen gas from the thermostat, resulting from poor sealing between the thermostat body and the end-plates, as well as poor sealing methods used for piping and wiring passing through the end-plates. This meant that the desired low temperatures could not be achieved. It also resulted in a high consumption of nitrogen gas, as the nitrogen gas lost from the system had to be continuously replaced in order to maintain the desired operating pressure in the thermostat.
- The insulation achieved by the thermostat wall was poor and was insufficient for work at very low temperatures. A major factor contributing to this was that the evacuated space in the thermostat wall was only 9 mm wide as opposed to the recommended 1 in. wide evacuated space. Another factor contributing to poor insulation was that a high vacuum could not be attained in the annular space as the vacuum pump had to be used in other sections of the apparatus resulting in a loss of the strength of the vacuum in the wall with time while the pump was being used in other sections. The use of Swagelok compression fittings instead of proper vacuum fittings in the line between the vacuum pump and the thermostat also limited the intensity and stability of the vacuum achieved in the annular space of the thermostat wall.
- The materials of construction of the thermostat and the problems associated with sealing limited the operating pressure of the thermostat. A higher operating pressure in the thermostat would improve the heat transfer between the equilibrium cell and the nitrogen gas in the thermostat allowing much lower temperatures to be achieved in the equilibrium cell.

In order to eliminate these problems, the original thermostat was discarded and a new thermostat was designed and constructed as illustrated in Figure 4-5.

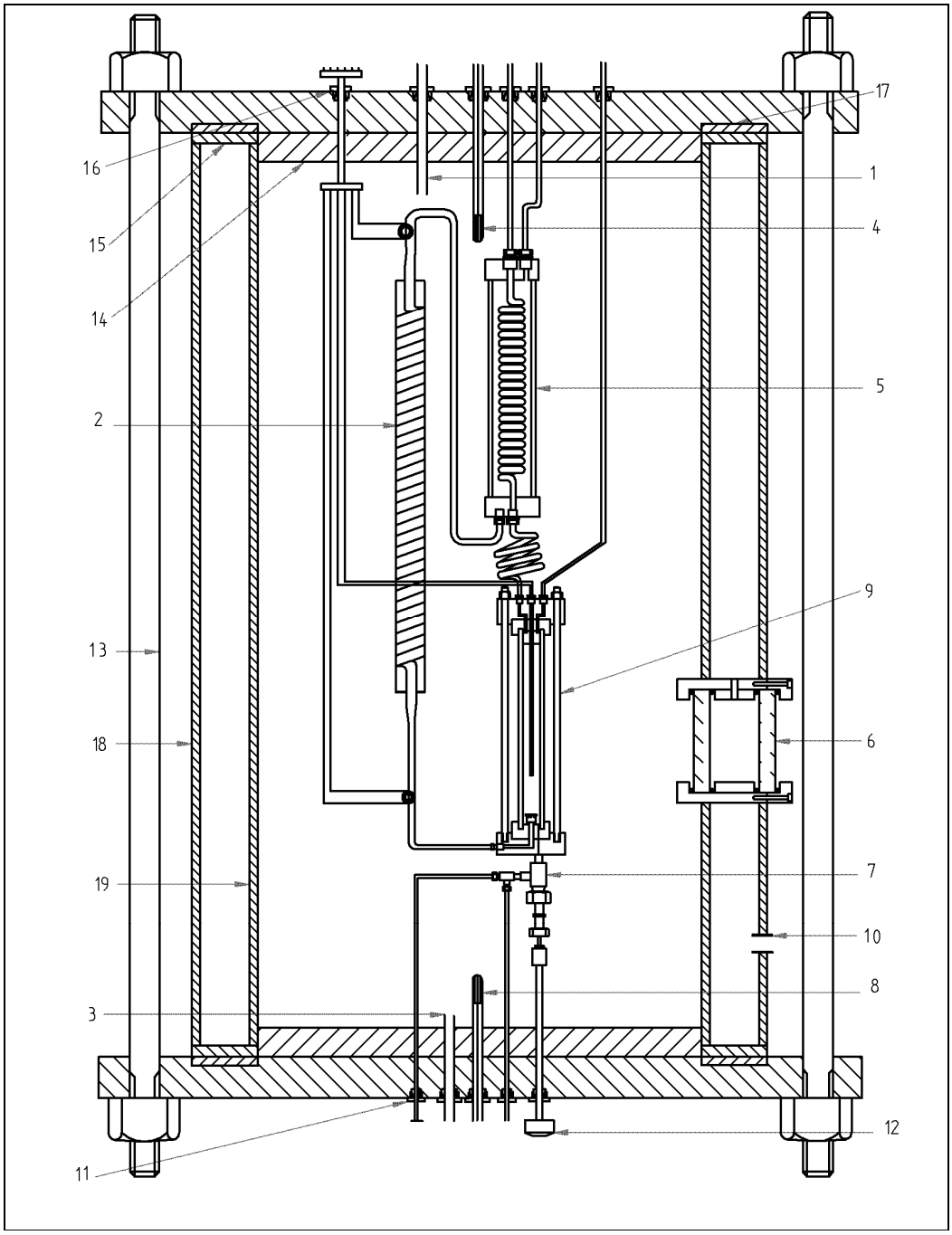

Figure 4-5: Modified thermostat with internal arrangement

1, Nitrogen gas outlet; 2, Cooling unit; 3, Nitrogen gas inlet; 4, Temperature sensor for top of thermostat; 5, Heat exchanger; 6, Viewing window; 7, Liquid sampling valve; 8, Temperature sensor for bottom of thermostat; 9, Equilibrium cell; 10, Vacuum pump suction; 11, Teflon ferrule used for sealing; 12,Liquid sampling valve handle; 13, External tie-rod; 14, PTFE Sleeve for insulation; 15, Flat plate; 16, Temperature sensor connector piece; 17, Teadit TF 1510 Gasket; 18, Thermostat outer pipe; 19, Thermostat inner pipe

To eliminate leaks and to accommodate higher pressures during operation it was decided to construct the new thermostat using 316 stainless-steel instead of glass. The main body of the

cylindrically shaped thermostat with a height of 800 mm, consisted of an inner pipe of 100 mm inner diameter with 10 mm walls and an outer pipe of 150 mm diameter with 10 mm wall thickness, joined at their ends with a 10 mm thick stainless steel ring constructed from flat plate. The ring had an outer diameter of 150 mm and an inner diameter of 110 mm. This configuration resulted in an annular space of 40 mm between the inner and outer walls of the thermostat, which greatly improved the insulation of the equipment. The annular space had a ¼" outlet fitting with a ball valve which would permit the annular space to be evacuated, then closed off via the valve to allow the vacuum pump to be used elsewhere in the equipment. Once evacuated and closed off the vacuum in the annular space was maintained as long as desired.

To permit viewing of the cell contents, a viewing window illustrated in Figure 4-6 was installed along the length of the thermostat. The viewing window had a viewing diameter of 20 mm which was sufficient to view the liquid level and the bubbling of the vapour through the liquid phase. It was constructed from a 12 mm thick 2.5" Pyrex sight glass and a 12.5 mm thick 2.5" diameter piece of Perspex on the outside exposed to the atmosphere, with a 22 mm gap between the two provide an annular space for insulation. The annular space between them was evacuated during operation via a small hole drilled in the space which led to the annular space of the thermostat. The sight glass and the fibreglass were housed in machined stainless steel housing and sealing was achieved using Viton o-rings.

End plates of the thermostat were constructed from 15 mm thick 316 stainless steel. Major problems were experienced with sealing at the end-plates of the previous design and switching to 316 stainless steel provided a major improvement to the sealing. The end plates were bolted together with four external tie-rods. Sealing between the end-plates and the main thermostat body was achieved using a highly compressible PTFE gasket, Teadit TF 1510. All piping passing through the end plates passed through Swagelok fittings screwed into the end plates, with sealing being achieved by tightening the pipes up against the Swagelok fittings using Teflon ferrules. Teflon ferrules were used as opposed to stainless steel to allow the thermostat to be opened up for inspection and maintenance without having to cut the piping passing through the end plates which would have been necessary had stainless steel ferrules been used. This arrangement of the piping passing through the end-plates saw a total elimination of leaks in this area. Wires from the Pt-100 sensors situated inside the thermostat needed to also pass through the end plates of the thermostat so that they could be connected to their display units. This provided a challenge as this had to be achieved without allowing a source of leaks to develop where the wires passed through the end plates. An unconventional

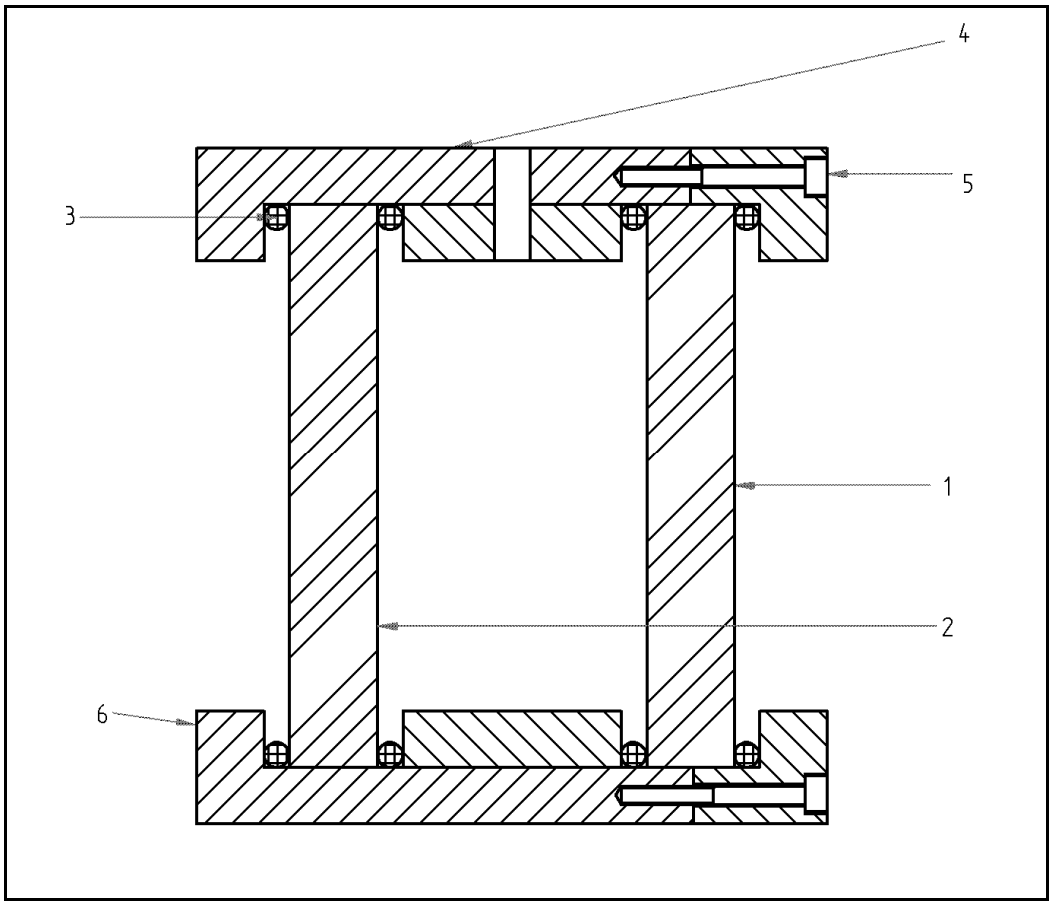

Figure 4-6: Sealing arrangement of Thermostat viewing glass
1, Perspex window; 2, Pyrex sight-glass; 3, Viton 0-ring; 4, Vacuum connector segment; 5, Bolt; 6, Stainless-steel billet

approach was employed here to achieve this. Individual wires from each Pt-100 sensor were stripped of the plastic insulation and individually set in a 1/4" piece of stainless steel tubing with epoxy ensuring no contact between the different wires. This tubing with individual wires was then passed through a Swagelok fitting, fitted to the top end-plate of the thermostat. Each individual wire was soldered to a point on a common multi-connector piece, one situated inside the thermostat and the second externally located. These connecters together with the epoxy embedded wires provided the connection between the Pt-100 sensors and the corresponding temperature display units. Short circuits were checked for and tests were done to ensure correct displays were allocated to the Pt-100 sensors. Calibration of the equilibrium cell Pt-100 sensor was undertaken with this connection in place to ensure no error was introduced with this unconventional setup. The new thermostat was successfully leak tested up to 600 kPa with no leaks apparent in any part of the thermostat. This leak free thermostat would assist greatly in achieving the desired low temperatures at which VLE measurements were to be carried out.

Two Class-A Pt-100 temperature sensors each inserted into a stainless well were mounted in the end-plates of the thermostat, one at the bottom and one at the top. Although the sensors were not of very high accuracy, they were still able to provide an indication of the temperature gradient across the thermostat.

4.5 Vapour recirculation loop

The vapour recirculation loop functioned to remove the vapour phase from the equilibrium cell for sampling, and as a means of agitating of the cell contents upon the return of the re-circulating vapour to the cell. The vapour recirculation loop employed in this study was identical to the vapour recirculation loop of Moodley [2002] with the exception of the modified vapour recirculation pump and the system volume regulator employed by Moodley [2002] which was discarded.

The loop was constructed of 1/8-in. OD stainless steel tubing and had two sections, the section located in the thermostat, and the external recirculation loop, i.e. the section of the loop located outside the thermostat,

The external recirculation loop consisted of a vapour recirculation pump and a vapour sampling valve. In the thermostat the vapour recirculation loop passed through the heat exchanger and cooling unit before re-entering the equilibrium cell.

It was necessary to maintain the re-circulating vapour at a temperature high enough to prevent condensation. This was achieved in the external recirculation loop by the use of nichrome wire wound around the tubing. The wire with a resistance of approximately 10 Ω/m was wrapped in 0.18-mm thick 3M Class-B glass cloth electrical tape. Two Variac voltage regulators controlled the power supply to the nichrome wire which was wound in two separate sections to minimize the total resistance of the system. These separate sections were each connected to a voltage regulator. It was necessary to use two separate voltage regulators to reduce the total resistance to the voltage regulators and thus allow each voltage regulator to operate at a much lower and safer voltage.

The vapour phase was re-circulated using a double acting pneumatic pump designed and built in the study by Moodley [2002]. Modifications were however carried out on the original pump of Moodley [2002] as discussed in Section 4.6. A sampling loop was attached to the vapour-sampling valve which was located externally. The vapour-sampling valve with

the sampling loop was isolated from the rest of the vapour recirculation loop when a vapour sample was required during experimentation.

4.6 The vapour recirculation pump

The vapour recirculation pump used to re-circulate the vapour phase was similar to the one used by Moodley [2002]. The vapour recirculation pump of Moodley [2002] was only tested at pressures up to 6.5 bar(a). Upon testing it at higher pressures for extended periods the pump failed due to leaks developing along the pump heads. These leaks were due to the failure of the neoprene seals which provided the sealing against the stainless steel chamber walls. Failure of the seals at high pressures was due to their shape and more especially wear caused by friction between the walls of the pump head and the seals when operated for extended periods, due to a lack of lubrication.

It was therefore decided to modify the vapour recirculation pump in order for it to accommodate higher pressures and to ensure reliable operation over extended periods. Modifications were only carried out on the sealing along the pump head illustrated in Figure 4-7 as the rest of the pump was operating reliably.

The pneumatic pump consisted of a double-acting pneumatic cylinder with a through-rod shaft. Each end of the shaft was fitted with a floating piston housed inside a stainless-steel head. The entire piston in the pump head was modified. The neoprene seals along with the Teflon guide rods were discarded and replaced with new pistons consisting of cylindrical solid steel billets each with three Viton o-rings spaced evenly along the length of the piston. The o-rings provided the sealing along the chamber walls of the pump. Upon testing this setup, it was found that the seals failed when used over extended periods under high pressures. Lack of lubrication was found to be the problem due to the fact that the pump was used for gases. To solve this problem a lubricant was placed in the space between the 1st and 3rd o-rings thus providing the necessary lubrication. Care was taken not to contaminate the area of the piston exposed to the contents of the vapour recirculation loop with the silicon based lubricant. Any exposure of the lubricant could lead to the entrainment of chemical components of the lubricant into the re-circulating vapour stream thus contaminating the system under investigation, resulting in inaccurate experimental data. Successful tests were run on the pump to observe the performance of the pump over extended periods of time.

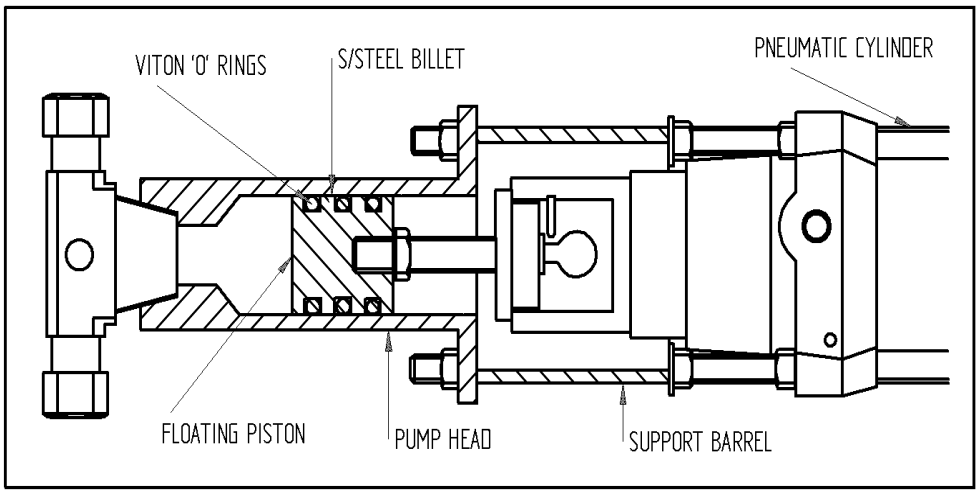

Figure 4-7: Modified sealing arrangement of vapour recirculation pump

Compressed air supplied at around 1 bar(g) was used to drive the pump. Air was supplied to either end of the pneumatic cylinder to drive the shaft in the opposite direction, with a double acting control valve used to regulate the flow of air. Back-pressure sensors located at the air inlet/outlet ports were used to detect when the end of the pumping stroke was reached, these sent signals to the control valve which in turn switched the air supply between the ends of the cylinder to ensure a smooth pumping action. Four gravity-operated check valves ensured one-directional flow of fluid through the pump.

The flow rate and hence vapour recirculation rate could be varied by adjusting the flow rate of exhaust air from the pneumatic cylinder as required during different stages of experimentation.

4.7 The cooling and temperature control system

The nitrogen recirculation loop served to provide nitrogen at a precisely controlled temperature to the thermostat to maintain a constant temperature environment for the equilibrium cell.

The loop consisted of a nitrogen gas pump, a section immersed in a bath cooled by a refrigeration unit (the pre-cooler), a cooling coil immersed in a low temperature bath and a heating unit. The loop was constructed from ¼-in. OD stainless steel tubing. Since the nitrogen gas was at very low temperatures proper insulation was essential. The stainless steel tubing was insulated with a layer of Armourflex.

The nitrogen gas was circulated using a Metall Bellows Pump MB602. The pump was rated for operation as low as -100 °C and was capable of delivering flow rates up to 50 litres per minute. The effect of nitrogen gas on the pump was minimal as only the stainless-steel, Teflon and Viton surfaces of the pump were exposed to the nitrogen gas.

Prior to final cooling the nitrogen gas was passed through the pre-cooler, a piece of line immersed in a bath containing an ethylene glycol/water mixture cooled using a refrigeration unit manufactured by A.C.S Air Conditioning & Refrigeration. The refrigeration unit had a power rating of 12,000 BTU/hr and consisted of a 4.0 m long ¼ in OD copper tubing which was immersed in the bath. The pre-cooler was incorporated into the system to eliminate the large amount heat which was generated by the nitrogen recirculation pump and transferred to the re-circulating nitrogen gas. This cooling of the nitrogen cooling gas reduced the load on the low temperature bath allowing lower and more stable temperatures to be achieved and also minimizing the consumption of dry ice when used.

After the pre-cooler, the nitrogen gas in the loop was cooled by passing it through a coil immersed in a low temperature bath. The coil was 5.5m long constructed from ¼-in. OD stainless-steel tubing. The stainless steel cryogenic bath was cylindrically shaped with an internal volume of 42 litres and a lid constructed from PTFE. The bath was fitted with an overhead mechanical stirrer to provide agitation of the bath contents thus promoting heat transfer. The stirrer could be operated at a rotational speed varying from 40 to 2000 rpm, and could handle suspensions with viscosities up to 60 Pa.s.

Either dry ice together with a solvent or liquid nitrogen (LN_2) could be used as the cooling medium in the low-temperature bath depending on the range of temperatures required for a particular study. During this study dry ice together with acetone was used as the cooling medium when working at temperatures below 5°C. When working at temperatures above 5°C a cold finger immersed in acetone in the low temperature bath provided sufficient cooling for the experiments to be carried out.

Before the nitrogen gas entered the thermostat it was necessary to adjust its temperature so that isothermal conditions could be maintained in the thermostat and the desired equilibrium temperature could be attained in the equilibrium cell. The heating unit as designed by

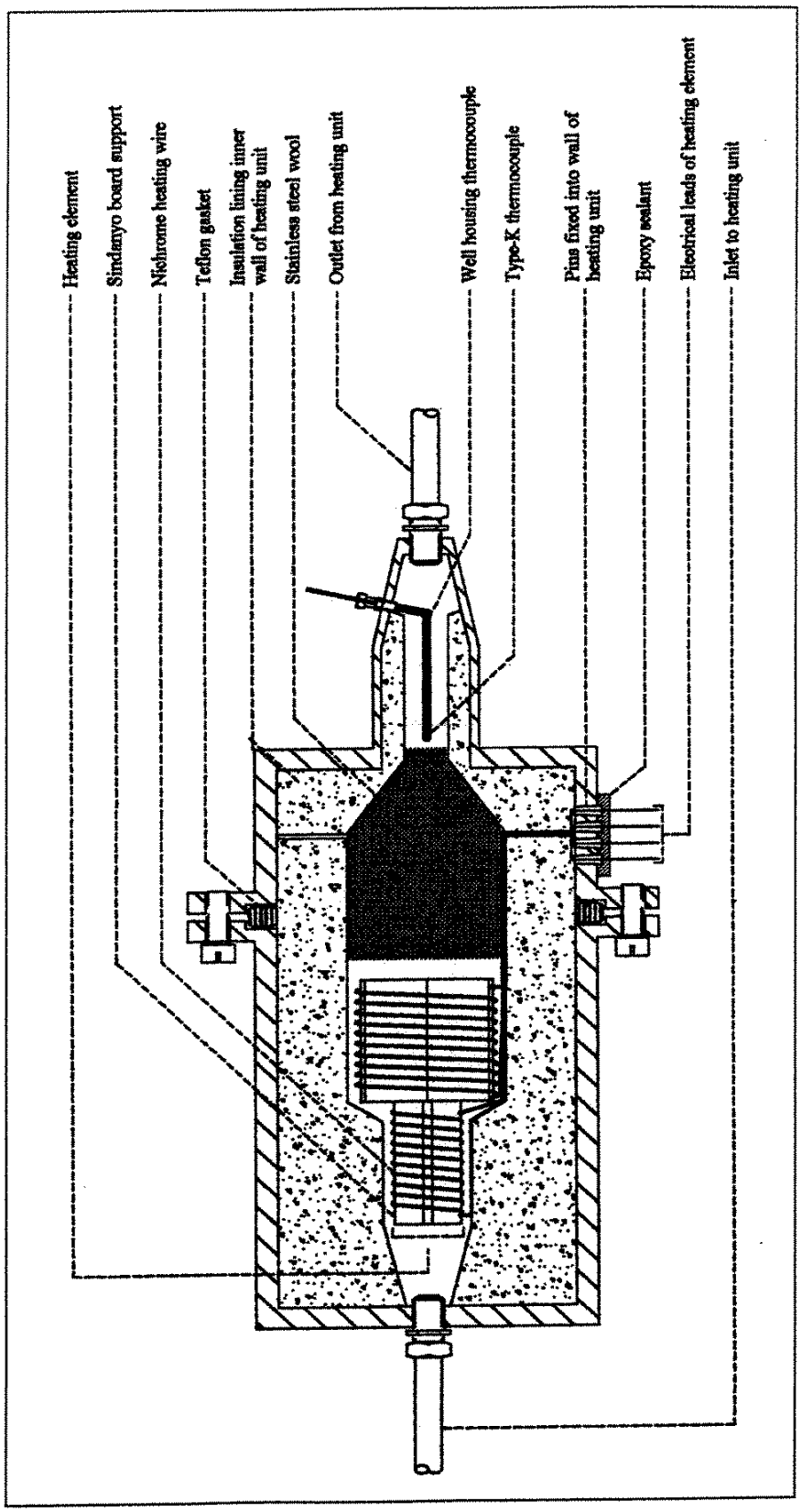

Figure 4-8 : Schematic diagram of the heating unit [Moodley, 2002]

Moodley [2002], Figure 4-8, consisted of a heating element housed inside a stainless-steel shell with an internal surface lined with insulation provided the necessary temperature adjustment. The heating element had a total resistance of 15.3 Ω and consisted of nichrome wire wound around a cross shaped support constructed from Sindayo board which was mounted in the heating unit such that the cross-shaped structure of the support lay normal to the flow of gas. This arrangement created the necessary turbulence in the re-circulating nitrogen to promote mixing and thus an even temperature distribution in the nitrogen gas. A Pt-100 sensor was housed inside a stainless-steel well at the outlet of the heating unit to provide a temperature indication of the gas leaving the heating unit.

Temperature in the equilibrium cell was controlled using a Eurotherm Model 2204 temperature controller which regulated the heating of nitrogen gas blown over the equilibrium cell. A Pt-100 sensor located inside the equilibrium cell provided the input to the controller which in turn provided the input to a Eurotherm solid-state relay which controlled the switching of an AC circuit containing the heating element in the heating unit. Protection of the heating element, rated for a maximum current of 5 A, was achieved by controlling the voltage across the heating element using a Variac voltage regulator. An ammeter was installed to allow the current to be monitored together with a 4.5 A fuse to provide further protection. Control parameters for the PID Eurotherm 2204 controller were determined via automatic tuning.

All stainless-steel tubing carrying the nitrogen gas was insulated with a thick layer of Armourflex, an insulating material designed for the purpose.

4.8 Sampling and low-pressure analysis systems

4.8.1 Liquid sampling

In the method of vapour recirculation the liquid sample has to be drawn directly from the equilibrium cell. A sample withdrawal method which caused a minimal disturbance to the system during sampling as devised by Moodley [2002] was employed in this study. In this study the method also had to be effective at low temperatures.

The liquid was sampled via a short, fine-bore capillary of less than 1 mm in diameter machined in the bottom-end plate of the equilibrium cell. Figure 4-9 illustrates the mounting of the liquid sampling valve on the equilibrium cell. The flow of liquid out of the cell was

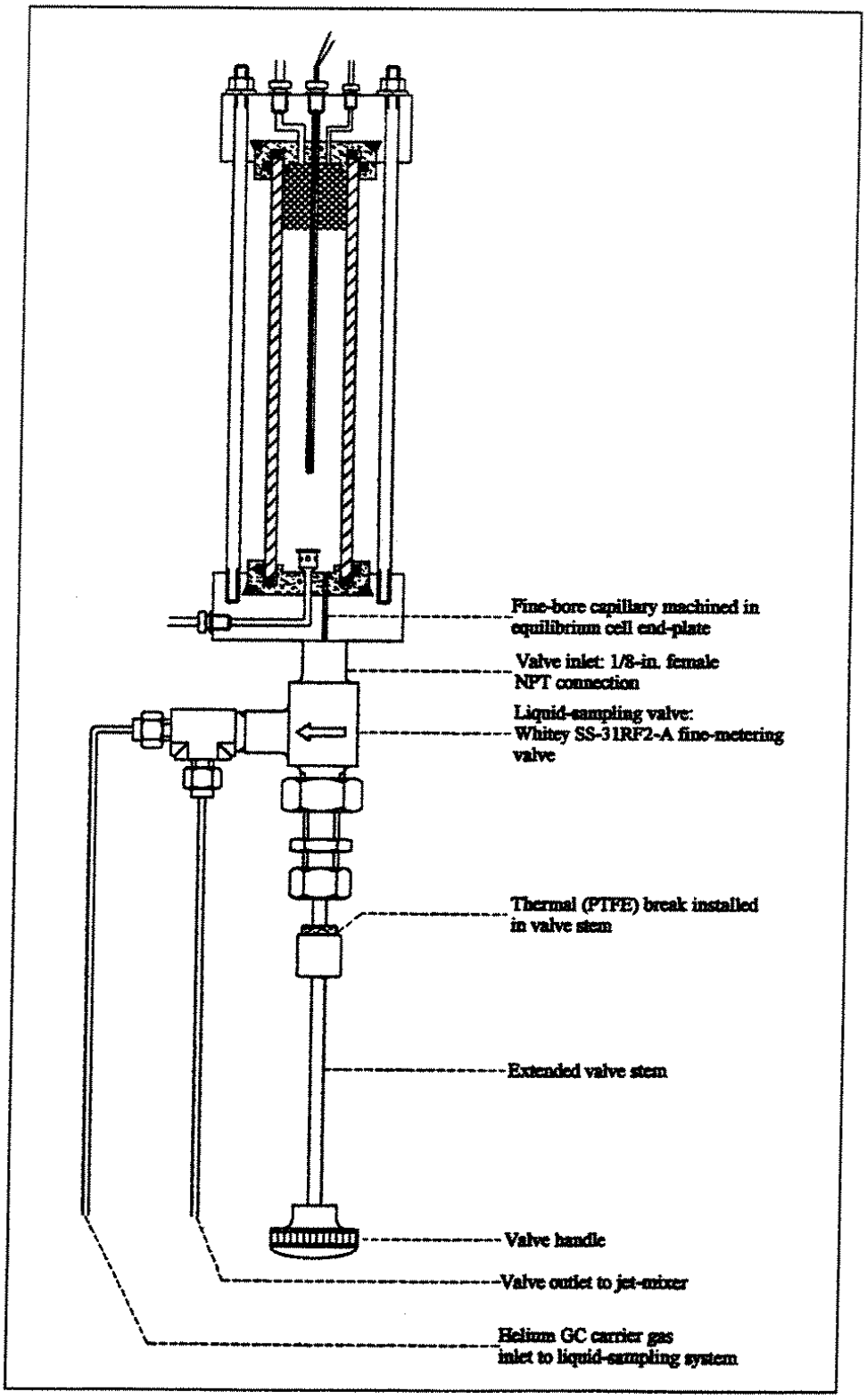

Figure 4-9: Mounting of the liquid-sampling valve at the base of the equilibrium cell [Moodley, 2002]

controlled using a 1/8-in Whitey 31 series union-bonnet metering valve. The valve was mounted flush on the base of the equilibrium cell via a 1/8-in. male NPT connection machined at the outlet of the capillary. This setup resulted in a dead volume estimated to be less than 25 µl between the sampling port in the equilibrium cell and the valve seat. Thus there was a very small accumulation of stagnant, non-equilibrium material in the sampling system.

The sampling valve was housed in the thermostat but was manually operated from outside via an extended valve stem. The conduction of heat from the external environment to the equilibrium cell was minimized by installing a thermal break constructed from fluorosint PTFE in the valve stem.

The length of time for which the valve was opened and the pressure difference between the cell and Jet-mixer 1 determined the quantity of liquid drawn from the cell during sampling.

4.8.2 Vapour sampling

The vapour recirculation method allows for the vapour sample to be obtained without disturbing the equilibrium of the cell. Most times the vapour sample is obtained by isolating or diverting a portion of the re-circulating vapour stream.

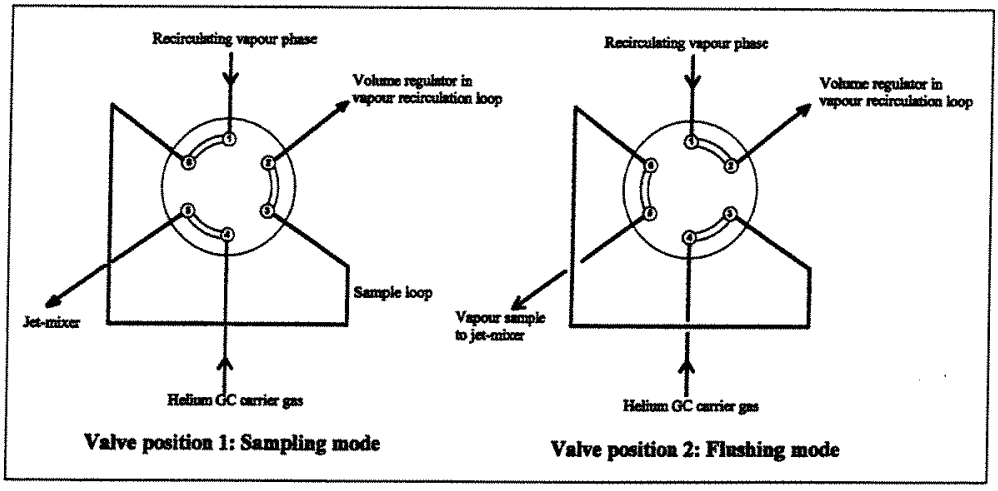

Figure 4-10: Positions of the Valco six-port vapour-sampling valve [Moodley, 2002]

The vapour sampling was achieved in the same method as Moodley [2002] via a Valco six-port two-position valve with 1/8 in. ports. The valve was rated for use at temperatures up to

225 °C and pressures up to 400 psi (27,600 kPa). The manually operated valve was mounted in the external recirculation loop and thus was not exposed to the low temperatures inside the thermostat. A 3.5 m sample loop of fine-bore 1/8 in. OD stainless-steel tubing was fitted to the valve yielding a 5.4 cm^3 vapour sample. This provided an adequate quantity of sample for multiple analyses via gas chromatography.

The valve was initially maintained in its sampling position during experimentation, resulting in the vapour phase flowing through the sample loop of the valve. Once equilibrium was achieved in the equilibrium cell the loop was charged with vapour of equilibrium composition. The valve was then switched to its flushing position and the sample trapped in the loop was then transferred to the low-pressure analysis system. Figure 4-10 depicts the different valve positions for either the sampling mode or flushing mode. This method of sampling ensured no change in the equilibrium cell volume thus causing no disturbance to the equilibrium during sampling.

4.8.3 Sample preparation for analysis

For accurate HPVLE measurements to be conducted it is critical that the sample to be analysed is completely homogenised. Raal & Mühlbauer [1998] reported obtaining a homogeneous sample, particularly when sampling the liquid phase of volatile/non-volatile component systems, to be one of the major challenges during experimentation. The problem arises during the throttling of the sample across a sampling valve, from the high pressure equilibrium cell to an evacuated region. During this process, preferential flashing of the volatile component results in a higher concentration of the volatile component further upstream, resulting in a non-homogeneous gas mixture with an incorrect representation of the sample composition, which ultimately leads to error during compositional analysis. Jet-mixers were used to homogenise samples before compositional analysis in this study. Figure 4-11 by Moodley [2002] illustrates the general structure of the jet-mixers used in this study.

During sampling, liquid or vapour samples were flushed directly into an evacuated jet-mixer. Owing to the pressure difference samples entering the jet-mixer did so at a high velocity and this together with the internal shape of the jet-mixer resulted in a re-circulating motion until a uniform and stable pressure was achieved in the jet mixer. Helium gas at a controlled pressure was thereafter flushed into the jet-mixer to induce further mixing of the sample ensure complete homogenisation of the sample.

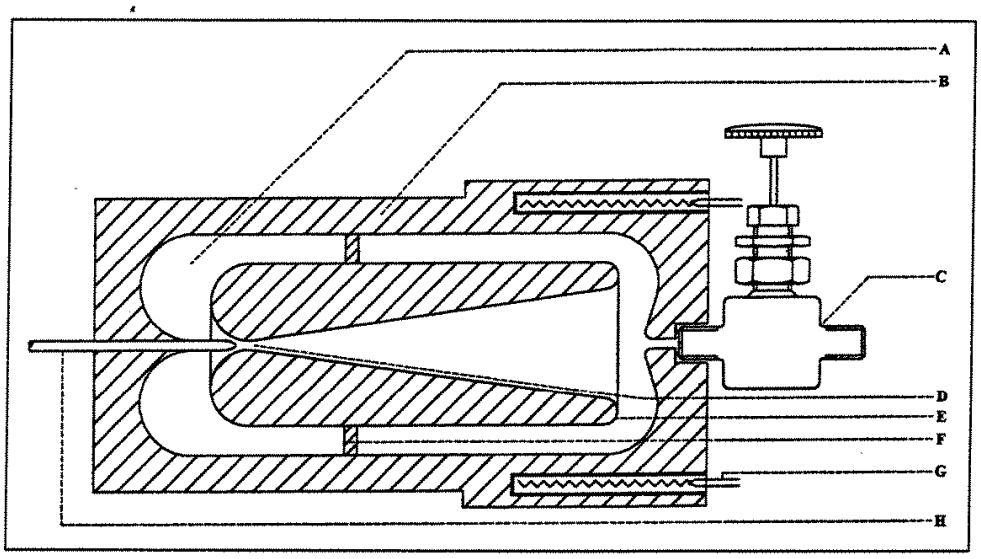

Figure 4-11: Schematic diagram of a jet-mixer [Moodley, 2002]
A, Mixing chamber; B, Jet-mixer wall; C, jet-mixer outlet valve; D, Nozzle orifice; E, Internal nozzle; F, Nozzle support; G, Cartridge heating element; H, Inlet to jet-mixer

The jet–mixers were manufactured from machined 316 stainless-steel and contained a mixing chamber cylindrical in shape with cardioid-shaped end pieces to induce a circulatory flow pattern. A cylindrical nozzle with rounded ends, centrally mounted in the mixing chamber, had a Venturi throat with an orifice diameter of less than 2 mm to produce the acceleration and hence induce the vaporization of the liquid sample as it entered the jet-mixer. A 1/8 in OD stainless steel tube with a tapered end, which protruded into the jet-mixer and discharged directly into the internal nozzle orifice, provided the inlet to the jet-mixers. The tapered end assisted in increasing the velocity of the sample as it entered the jet-mixer. A 1/8 in Whitey needle valve, screwed directly into the body of the jet-mixer was used to control the flow of material exiting the jet-mixer.

To prevent condensation of material in the jet-mixer, the jet-mixer was heated using cartridge heating elements evenly spaced along the circumference of the jet-mixer at its rear end. Each jet-mixer was fitted with three heating cartridges. To prevent heat loss and the formation of thermal gradients the jet-mixer was insulated using fibrefrax and duraback. Condensation of material in lines from the jet-mixer to the analytical device was prevented by heating the lines using nichrome wire similarly to the vapour recirculation loop.

4.8.3.1 Liquid sample preparation for analysis

Two jet-mixers connected in series were used in the liquid sampling system [Moodley, 2002]. Jet-mixer 1 had a total internal volume of 300 cm^3 while the second smaller jet-mixer 2 had an internal volume of 65 cm^3. A short length of 1/16 in OD stainless-steel tubing was used to connect jet-mixer 1 directly to the liquid sampling valve. To prevent the separation of volatile and non-volatile components in the line between the jet-mixer and the GC, which tends to occur if the distance of the line is too long a second smaller jet-mixer, jet-mixer 2, was installed closer to the GC. This was required as the distance of the line would have been too long if jet-mixer 1 was directly connected to the GC. The homogenised sample was then transferred from jet-mixer 2 to the GC via a thin line of 1/16 in OD stainless steel tubing.

4.8.3.2 Vapour sample preparation for analysis

By switching the six-port vapour sampling valve from the sampling position to the flushing position the pressure gradient between the sample loop and the evacuated jet-mixer resulted in the transfer of the vapour sample to jet-mixer 3 used in the homogenisation of the vapour sample. Helium was thereafter used to flush any material remaining in the sample loop and the valve flow passages into the jet-mixer diluting the sample and producing a mixture of uniform composition for analysis. Transfer of the homogenised vapour sample to the GC was achieved similarly to the liquid sampling system with a line of 1/16” OD stainless-steel tubing directly connected from jet-mixer 3 to the GC.

4.8.3.3 Jet-mixer Temperature Control

Temperatures were measured in jet-mixer 1 and jet-mixer 2 using two Class-A Pt-100 sensors inserted into the bodies of each of the jet-mixers. The temperature sensors each provided an input into a two separate Shinka temperature controllers which controlled the switching of two OMRON MK2P-S contact relays connected to the heating cartridges of the jet-mixers. The temperatures of jet-mixer 2 and jet-mixer 3 were controlled using a common controller which provided an output signal to both sets of heating elements. The temperatures in the jet-mixers were controlled at a minimum temperature at which the partial pressure of the least volatile component in the system under investigation was only 10 % of its saturation pressure.

4.8.3.4 Jet-mixer pressure measurement

Jet-mixer pressures were measured using a Sensotec Model TJE pressure transducer with pressure displayed using a Sensotec Model GM display. The transducer was rated for 0 to 75 psia (0 to 517 kPa) was connected to a three-way ball valve, via 1/16 in OD stainless-steel tubing, which was used to connect the transducer to either the liquid or the vapour sampling system by switching the valve position. The three-way valve was connected to the inlet of jet-mixer 1 via 1/16 in OD stainless-steel tubing and measured the pressure in the jet-mixer only when its outlet was closed. Opening the outlet of jet-mixer 1 allowed the pressure in both liquid sampling jet-mixers to be measured. The inlet of jet-mixer 3 of the vapour sampling system was also linked to the three-way valve via 1/16 in OD stainless steel tubing.

4.9 Measurement of system variables

4.9.1 Temperature

Temperature measurements were carried out at various locations in the apparatus. Class-A Pt-100 sensors were used at all locations except for the equilibrium cell which had a 1/10-DIN Pt-100 sensor which provided a higher accuracy. The equilibrium cell sensor and the sensors in the jet mixers provided inputs to temperature controllers which gave a visual display of the temperatures at these corresponding locations while controlling them. The remaining Pt-100 sensors were connected to a multichannel TCL Model RTS 16 selector box which provided an input to a Model 4003 digital display unit. This setup allowed for the temperatures at the various locations to be scrolled through and displayed on the display unit.

4.9.2 Pressure

Pressure measurement was carried out in the equilibrium cell as described in Section 4.2.2.2 and pressure measurement in the jet-mixers were carried out as described in Section 4.8.3.4.

4.9.3 Composition

Gas chromatography was considered to be the best method of compositional analysis for this application. A Shimadzu Model GC-17A chromatographic unit equipped with both a thermal conductivity detector (TCD) and flame ionization detector (FID) was used.

The GC was equipped with a manually operated six-port valve. The valve was fitted with a 3.0-m long sample loop of 1/8-in.OD stainless-steel tubing having an internal volume of about 4.6 cm^3. A homogenized sample flowed from a jet-mixer through the loop of the GC six-port valve at a controlled rate during sample analysis. The GC was automatically activated when the valve was switched from its sampling position to its flushing position and helium carrier gas then flushed the sample from the sample loop into the GC for analysis.

All binary sample analysis was carried using the following column:

- 30 m × 0.53 mm, J & W Scientific GS-Q column

The GC operating conditions were set up according to the binary system investigated as displayed in Table 4-1.

Table 4-1: Operating conditions for the Shimadzu Model GC-17A gas chromatograph

Operating Condition	Propane + 1-Propanol	Propane + Isopentane
Column Pressure [kPa]	50	50
Column Flow [cm^3/min]	6.2	6.2
Total Flow [cm^3/min]	272	272
Control mode	Split	Split
Split ratio (1:X)	28	28
Injector temperature [°C]	200	200
Oven temperature [°C]	70	175
FID temperature [°C]	250	250

The GC was connected to a PC on which the CLASS-GC10 computer software package was installed to allow control and operation of the GC. The software enabled the chromatographic peaks to be plotted on the PC screen and also calculated the areas under the peaks generated during analysis.

4.10 Equipment safety

The following safety features were incorporated into the equipment:

- The cabinet, in which the equipment was enclosed, had ducting fitted from its roof to the laboratory exhaust fan ducting. During experimentation the exhaust fans were switched

on to ensure elimination of any gases present. The exhaust fan ducting was vented to the atmosphere outside the laboratory. The Perspex cabinet doors were kept closed during experimentation.

- Two Swagelok pressure relief valves, V13 and V14, were installed at the outlet of the vapour recirculation pump. A further two similar relief valves, V27 and V28, were installed in the vapour recirculation line close to the Pyrex equilibrium cell. The valves were installed in pairs to provide backup in the event of valve failure.
- A pressure relief valve, V07 was installed on the LN_2 feed line from the PCC to the low temperature bath to permit venting in the event of the accumulation and vaporization of the LN_2 in the line. LN_2 was not used during this study.
- Two cryogenic pressure relief valves, V11 and V12 were installed in the nitrogen recirculation loop at the nitrogen recirculation pump discharge.
- The heavy-walled Pyrex tubing used in the construction of the equilibrium cell was rated for pressures of 17 bar at 23 °C. This was well above the maximum pressure of 10 bar at which the equipment was used. Strength of the material also increased at low temperatures which further enhanced the pressure capabilities of the equipment.

4.11 Summary of modifications made to the vapour recirculation apparatus of Moodley [2002]:

- New pressure transducer with a wider range was installed for the measurement of equilibrium pressures.
- The cooling unit was modified by removing the end-plates and leaving it effectively as a coil surrounded by a pipe.
- The thermostat material of construction was changed from Pyrex to 316 stainless-steel.
- The dimensions of the thermostat were changed with the size of the annular space between the inner and outer wall increasing from 25 mm to 40 mm thus improving insulation.
- A viewing window was installed on the thermostat with a novel sealing arrangement to permit viewing of the equilibrium cell contents.
- The end plates of the thermostat were modified to improve sealing.
- Sealing arrangements of piping entering and leaving the thermostat was changed to eliminate leaks.
- New valves were installed to improve the sealing arrangement for the annular space vacuum pump connection point.

- Wires entering and leaving the thermostat were embedded in epoxy within a pipe passing through the thermostat end plates and connected to multi connector pieces on the interior and exterior of the thermostat to eliminate leaks occurring where the wires were passed through the end plates of the thermostat.
- Vapour recirculation pump piston sealing arrangement was modified. The neoprene seals along with the Teflon guide rods were discarded and replaced with new pistons consisting of cylindrical solid steel billets each with three Viton o-rings spaced evenly along the length of the piston.
- The system volume regulator was discarded.
- A pre-cooler consisting of a piece of line immersed in a bath containing an ethylene glycol/water mixture cooled using a refrigeration unit was installed in the cooling circuit to assist in cooling and minimize the consumption of dry ice.
- A new vented cabinet was built to house the equipment.

CHAPTER 5

EXPERIMENTAL PROCEDURE

The acquisition of accurate VLE data requires intricate experimental procedures to suit the equipment being used and extensive time can be spent on developing and fine tuning procedures on new pieces of equipment. Experimental procedures employed in this study were derived from those used in the study by Moodley [2002] with minor deviations and changes to the procedure, as presented in this section. The experimental procedure undertaken depended on whether vapour pressure measurements or VLE measurements were being undertaken and also on the physical properties of the components under investigation.

Prior to any experimentation it was essential to commission the equipment to assure reliable operation of the equipment and the acquisition of accurate data during experimentation. Due to the equipment being re-assembled from individual pieces and with the new design of various components, this was a highly critical and lengthy process.

Commissioning of the equipment entailed the following:

- Leak testing at high pressure right down to vacuum. Leak testing was performed on the equilibrium cell, the vapour recirculation loop and the previously problematic and newly designed nitrogen recirculation cooling loop.
- Calibration of the Pt-100 temperature sensor in the equilibrium cell as described in Appendix A.1.
- Tuning of the Eurotherm and Shinka temperature controllers.
- Calibration of the new Sensotec pressure transducer used for pressure measurement in the equilibrium cell as described in Appendix A.2.
- Reliability test on modified pneumatic pump over extended periods under high pressures.
- Testing system capability of achieving low temperatures (down to -30°C).

5.1 Gas chromatograph calibration

Analysis of the samples to determine the equilibrium phase compositions was achieved with the use of a Shimadzu Model GC-17A chromatograph. The FID detector of the GC was used in this study.

The method of direct injection calibration was used to calibrate the GC. By injecting known volumes of each pure component into the GC, a linear relationship calibration curve of number of moles of material versus GC peak area (A) was generated. Calibration curves varied depending on the pure component under investigation as represented below in the linear equations derived via linear regression:

$$n = C_1 A \tag{5-1}$$

$$n = C_1 A^2 + C_2 A \tag{5-2}$$

where C_1 and C_2 are constants determined via linear regression.

The number of moles of pure component injected can be calculated from:

$$n = \frac{V_T}{V} \tag{5-3}$$

where V_T is the total volume of the pure component injected and V is the molar volume of the pure component. The molar volumes of gases were calculated by using the two-parameter virial equation of state, where the pure-component 2nd virial coefficients were calculated using correlations presented in the AIChE DIPPR compilation [Daubert & Danner, [1993]. For liquids the Rackett equation as modified by Spencer & Danner [1972] was used.

Calibration was carried out by using a 0 to 1.0 µl SGE liquid syringe to inject the liquid material directly into the GC, while a 0 to 100 µl. SGE GasTight syringe was used to inject the gases. The method of direct injection calibration required repeated injection of the same volume of material several times. When performing the calibration the same volume of material was injected more than 15 times and only those results that correlated to within 1.5% were used. This method of repeated injections improved the overall accuracy of the calibrations.

The method of direct injection calibration was employed by Mühlbauer [1990] and Ramjugernath [2000] who both observed drifts in the calibration factors with time. This however was not observed by Moodley [2002] who while also using the method of direct injection did not observe any drift in the calibration factor over a period of a year. During

this study calibration factors were not verified over time, as it was deemed unnecessary, due to the short time interval between the pure component calibrations and the binary VLE measurements.

5.2 Vapour pressure & phase equilibrium measurements

It was first necessary to verify that the pressure and temperature sensors in the equilibrium cell were calibrated accurately. This was accomplished by performing vapour pressure measurements for certain pure components. These vapour pressure measurements also displayed the pressure and temperature operating limits of the equipment. Thereafter HPVLE measurements were carried out on various binary systems. The following sections outline details of the various steps followed during pure component vapour pressure measurements and the HPVLE measurements carried out.

5.2.1 Start-up of an experimental run

Before the start of an experimental run, the equipment was leak tested at vacuum and under pressure to ensure measurements were to be carried out in a leak free environment, thus eliminating errors which would be introduced if leaks were present during experimentation. After leak testing the system was stabilised at surrounding atmospheric conditions. The liquid feed was replaced with a new one to eliminate possible contaminants on the old septum. Valves in the equipment were positioned as follows:

- Valves V05, V06 and V12 were opened. Remaining globe, needle and fine metering valves were closed.
- The six-port valve used for vapour-sampling and the GC six-port valve were switched to their sampling positions.
- The three-way valve V15 used for switching pressure measurements between the jet-mixers, was positioned such that pressure transducer PT2 was connected to the inlet of jet-mixer 1 of the liquid sampling system.

When measuring data at temperatures above 5 °C the low-temperature bath was charged with 35 litres of acetone and two Julabo FT 200 ‘cold-fingers’ were immersed in the bath and switched into operation. The low-temperature bath agitator was started to promote heat-transfer. Cooling from +20 to -20°C took around four hours. Thus this was performed

timeously such that it did not cause any delays once the rest of the system was ready for experimentation.

When measuring data at temperatures below 5°C, the low-temperature bath was charged with a dry ice + acetone slush mixture. The agitator was operated to promote heat transfer. Rapid cooling of the bath temperatures down to around -80°C was achieved by the addition of dry ice to the acetone in the bath.

The pre-cooler was operated when measuring data across the entire temperature range of the equipment, as it functioned primarily to eliminate the heat added to the system via the nitrogen recirculation pump, and thus reduce the load on the low-temperature bath enabling it to function far more efficiently. The pre-cooler bath was charged with a 50/50 ethylene glycol + water mixture. The refrigeration unit and the agitator were turned on. Cooling of the pre-cooler contents from +20 to -15 °C took around 5 hours. The pre-cooler was however kept in operation at all times and only stopped during long periods when maintenance was being done on the equipment.

The annular space in the thermostat wall was evacuated by opening valve V14 thus connecting the vacuum pump to the inlet of the annular space. The space was evacuated to -100 kPa(g) as indicated on PG2 and valve V14 was closed to isolate the evacuated space. The vacuum in the annular space was maintained constant at -100 kPa(g) as long as valve V14 was kept closed and it was only necessary to re-evacuate the space after maintenance was done on the thermostat and the vacuum was lost as indicated by PG2 which was monitored closely.

To eliminate air and moisture present in the nitrogen recirculation loop the section was evacuated to -100 kPa(g) as indicated by PG1 then pressurized with nitrogen gas to +240 kPa(g). The nitrogen gas was then re-circulated through the system for fifteen minutes after which it was evacuated to -100 kPa(g) again. Thereafter the loop was pressurized to +240 kPa(g), at which pressure it was maintained while re-circulating the nitrogen gas used to cool the equilibrium cell.

Power supply to the nichrome wire wound around the stainless-steel tubing of the external vapour re-circulation was turned on thus heating up the lines to prevent condensation of the re-circulating vapour during experimentation. The vapour re-circulation loop was thereafter evacuated by opening valve V13, for at least three hours to eliminate traces of air and other impurities that were present in the system with the heating of the lines aiding the elimination

of condensables. After evacuation the loop valve V13 was closed to isolate the loop from the vacuum pump.

5.2.2 Charging of the equilibrium cell

The method of charging the equilibrium cell was largely dependant on the systems under investigation and the type of measurements being done:

- When performing vapour pressure measurements on liquid components, the liquid was injected into the system via the liquid feed septum. Five minutes were allowed for the liquid to settle in the equilibrium cell as it had to flow downward through the heat exchanger coil before entering the equilibrium cell chamber. The volume of liquid injected for the particular component was determined by visually monitoring the level in the equilibrium cell. Generally the more volatile components required a bigger volume to be injected. It was important that during experimentation the temperature sensor was immersed in the liquid and there was sufficient vapour space above the liquid level in the equilibrium cell to minimize liquid entrainment. Ideally it was aimed to operate the equilibrium cell level at around 60 % during experimentation. Once the equilibrium cell was charged with the liquid, valve V13 was opened and the vacuum pump was used to degas the liquid to remove traces of dissolved residual gases. This in situ degassing was carried out for fifteen minutes after which valve V13 was closed. Degassing reduced the liquid-level in the equilibrium cell, thus when initially charging the cell with liquid this needed to be taken into account. Degassing could be extended to attain the desired liquid level if the cell was over full.
- When performing vapour pressure measurements on gases, in this case propane, the temperature of the equilibrium cell was initially dropped to 0 °C. The gas was slowly bled into the system such that there was a minimal rise in the equilibrium cell temperature. This was done by opening valve VO3 and adjusting the propane gas pressure regulator. The liquid level in the equilibrium cell was slowly built up by continuously stopping the gas feeding into the cylinder and dropping the temperature in the equilibrium cell to 0 °C. This was done repeatedly until the equilibrium cell was totally filled with liquid. The supply of gas was the set at a low rate and the equilibrium cell was partially opened to the vacuum pump by partially opening valve V13. The contents of the equilibrium cell were then degassed at 0 °C for ten minutes which saw a slight drop in the liquid level. The propane supply was thereafter stopped. The temperature in the equilibrium cell was then set at the upper end of the vapour pressure measurements and the contents of the

equilibrium cell were allowed to reach this temperature. This temperature rise saw a drop in the liquid level, however the equilibrium cell was still over charged with liquid. Valve V13 was once again opened and the contents of the equilibrium cell were degassed for a minimum of ten minutes until the desired liquid level in the equilibrium cell was attained.

- During HPVLE measurements the liquid was initially charged into the equilibrium cell as discussed in the procedure of charging liquids, for the vapour pressure measurements of liquids. The degassing step of the process was however omitted. The gas in the system to be investigated was then bubbled through the liquid in the equilibrium cell while simultaneously venting the gas from the top of the cell which was partially opened to the vacuum pump. This process was performed to saturate the liquid with the gas component and also assist in the removal of traces of residual dissolved gases. After fifteen minutes the gas supply was stopped and the top of the equilibrium cell was completely opened to the vacuum pump to degas the liquid in the cell to remove any remaining dissolved gases. This in situ degassing was carried out for fifteen minutes after which the system was isolated from the vacuum pump. The gas was then fed into the vapour recirculation loop to provide the desired operating pressure. The vapour recirculation pump was started thus forcing the gas through the liquid in the equilibrium cell, and thus resulting in the gas slowly dissolving in the liquid and a subsequent rise in the liquid level in the equilibrium cell. Stabilization of the liquid level while the gas supply was still open indicated a complete saturation of the gas in the liquid. Incomplete saturation of the liquid with the gas could be detected by a significant pressure drop in the equilibrium cell upon termination of the supply of fresh gas.

5.2.3 Attainment of equilibrium

The method employed to achieve equilibrium was similar when performing vapour pressure and HPVLE measurements with the time required to reach equilibrium the noted difference. The desired temperature, at which the measurement was to be carried out, was entered as the set-point on the Eurotherm temperature controller. Once the temperature in the equilibrium cell was within 2 °C of the set-point the vapour recirculation pump was started with an initial flow of around 5cm^3/s. This flow rate produced good agitation of the equilibrium cell contents thus once thermal equilibrium was attained, chemical equilibrium followed shortly due to the good agitation of the cell contents. Once the temperature and the pressure in the equilibrium cell had stabilized, the vapour recirculation rate was reduced to minimize liquid entrainment. After operating the system under these conditions for thirty minutes, with no changes to temperature, pressure and liquid level, the system was assumed to be at

thermodynamic equilibrium. The following steps were then followed depending on whether vapour pressure measurements or HPVLE measurements were being carried out:

- When performing pure-component vapour pressure measurements, the vapour re-circulation was stopped and the pressure in the equilibrium cell was noted as the vapour pressure at the system operating temperature. Subsequent measurements at different temperatures were measured by inputting a new set-point on the Eurotherm temperature controller and allowing the system to re-equilibrate. The same material was used. Vapour pressure measurements were undertaken starting at the maximum temperature to be investigated with lower temperatures following. This resulted in a gradual increase in the equilibrium cell level with subsequent measurements. Any excess liquid was removed via the liquid sampling system which was temporarily opened to drain liquid from the cell to attain the desired liquid level.
- When performing HPVLE measurements, samples of the liquid and vapour phases were drawn and analyzed as described in the following section.

5.2.4 Sample withdrawal and analysis

The following procedure was employed for the critical task of removing vapour and liquid samples from the system. All pressure measurements referenced were carried out with pressure transducer PT2.

1) The Shinka temperature controllers connected to the jet-mixers were given an input set-point of a temperature at which the partial pressure of the less volatile component in the system was only 10 % of its saturation pressure. This temperature was considered high enough to prevent the condensation of the material during sample homogenisation in the jet-mixers.
2) Stainless-steel lines in the sampling systems were heated to a similar temperature to that of the jet-mixers using the Nichrome wire wound around the tubing.
3) All jet-mixers and lines of the sampling systems were evacuated to less then 0.1 kPa(a) using the vacuum pump to remove air and other contaminants present. This was done while performing other steps in the experimentation to minimize preparation times. Evacuation was carried out for a minimum period of one hour. After evacuation all valves in the sampling sections were closed to isolate the sampling systems from the vacuum pump and into separate sections of the sampling systems.

4) Following evacuation flushing of the system with helium was carried out to ensure no contaminants were present. Valves V08, V10, V16, V17 and V19 were opened and the lines between valves V08 and V21 in the liquid-sampling system pressurized with helium to 200 kPa(a).Valve V21 was then opened and the line was continuously flushed through. After ten minutes the venting helium was sent to the GC for analysis to detect the presence of any impurities. If impurities were detected the cleaning process involving evacuation and flushing was repeated until no impurities could be detected. After successful cleansing valves V08 and V21 were closed.
5) Valve V20 was opened and the liquid sampling system was evacuated to less than 0.1 kPa(a). Valves V19 and V20 were then closed.
6) Valve V08 was opened and the liquid-sampling system was filled with helium to 100 kPa(a). Valves V08 and V10 were then closed. To prevent condensation of material in the lines during subsequent flushing of the liquid sample into Jet-mixer 1 the helium trapped between valves V08 and V10 was given time to heat up to the line temperature.
7) Valve V20 was opened and Jet-mixers 1 and 2 together with the tubing between valves V10 and V19 were evacuated to less than 0.1 kPa(a). Valve V16 was then closed.
8) Once thermodynamic equilibrium was achieved the vapour recirculation pump was stopped. After 10 minutes the liquid sampling valve was partially opened to permit the flow of liquid from the equilibrium cell into Jet-mixer 1. The pressure rise in the Jet-mixer was representative of the quantity of material drawn from the equilibrium cell. This initial step was performed to remove non-equilibrium material initially trapped in the capillary machined in the bottom end-plate of the equilibrium cell. A pressure increase of 15 kPa in Jet-mixer 1 was considered sufficient to ensure removal of this material. The liquid sampling valve was thereafter closed.
9) The vapour recirculation pump was restarted and valve V16 was opened. Jet-mixers 1 and 2 and the tubing between valves V10 and V19 were evacuated to less than 0.1 kPa(a). Valves V16, V17 and V20 were then closed.
10) Thermodynamic equilibrium was re-established in the equilibrium cell. Once thermodynamic was established the vapour re-circulation was stopped and the system was left for 30 minutes to allow the vapour and liquid phases in the equilibrium cell to disengage.
11) System pressure and temperature were noted. Valves V05 and V06 were then closed, isolating a sample of the equilibrium vapour phase in the vapour re-circulation loop. A liquid phase sample was thereafter drawn from the equilibrium cell as described in

step (8) above. The pressure rise in Jet-mixer 1 was however only restricted to 5 kPa ensuring complete vaporization of the sample in the jet-mixer, and a large enough sample to ensure accurate analysis via gas chromatography.

12) Valve V10 was opened. Material trapped in the line between V10 and Jet-mixer 1 was flushed into the jet-mixer using previously heated helium from step (6) above. Valve V08 was opened and helium was then bled into Jet-mixer 1 at a flow rate of around 4 kPa/s until a pressure of 200 kPa(a) was attained in the jet-mixer. This rapid in feed of helium to the jet-mixer promoted sample homogenization and ensured the liquid sample remained trapped in the jet-mixer.
13) Valve V08 was closed and the jet-mixer pressure was monitored for 5 minutes. Any pressure drop indicated condensation of the sample in the jet-mixer or the line leading to it.
14) If no condensation was observed, valve V16 was opened and the diluted liquid sample flowed to Jet-mixer 2 for further homogenisation prior to GC analysis.
15) Valve V08 was again opened and the pressure in the jet-mixers were built up to 200 kPa(a) using helium. Valves V08 and V10 were then closed and the jet-mixers pressure was monitored for condensation as done previously. No condensation indicated a totally vaporized, homogenous sample ready for GC analysis.
16) Valve V17 at the outlet of Jet-mixer 2 was opened, followed by valve V19, thereby filling the evacuated line between valves V19 and V21. Valve V21 was then opened to allow the homogenised liquid sample from the jet-mixers to slowly flow through the sample loop of the GC six-port valve at a flow rate of around 0.5 kPa/s. Once the pressure in the jet-mixers dropped to 190 kPa(a) valve V21 was closed to stop the flow of homogenised sample. This pressure drop was assumed sufficient to ensure complete filling of the sample loop. Once the jet-mixer pressure stabilized valve V19 was closed. The GC six-port valve was switched to its flushing position and the sample was conveyed to the GC for analysis. Results from the GC were noted after elution time elapsed.
17) After results were obtained the GC six-port valve was returned to its sampling position in preparation for the acquisition of another set of results. Valves V21 and V19 were opened successively and the sample loop of the GC valve was flushed with a homogenised sample from the jet-mixers. The jet-mixers pressure was dropped by another 10 kPa as before at the same rate. Valve V21 was then closed. Once the jet-mixer pressure stabilized valve V19 was closed and the sample was conveyed to the GC for analysis by switching the six-port valve. Results were once again noted after elution time.

18) The liquid sample analysis was performed several times according to the procedure described in step (17) above. The minimum permissible pressure to which the jet-mixers could be dropped was 110 kPa(a).

19) Following liquid sample analysis, valve V17 was closed, the GC six-port valve was returned to its sampling position and the three-way valve V15 was switched to connect the pressure transducer PT2 to Jet-mixer 3 of the vapour sampling system. Valves V18, V19 and V20 were opened and the lines were evacuated to less than 0.1 kPa(a) in preparation for equilibrium vapour sample analysis. Valve V20 was thereafter closed.
20) The vapour sample isolated in the vapour-sampling valve during step (11) was analysed as described below.
21) Valves V08 and V07 were opened. The line between valves V08 and V21 were pressurized with helium to 200 kPa(a). Valve V21 was then opened and the line continuously flushed through. After 10 minutes, the venting helium was injected into the GC to detect if any contaminants were present. This procedure was repeated until the system was free of contaminants. Valves V08 and V21 were then closed.
22) Valve V20 was then opened and the vapour sampling system was evacuated to less than 0.1 kPa(a). Valves V19 and V20 were then closed.
23) Valve V08 was opened and the section between valves V08 and V19 in the vapour-sampling system was filled with helium to 100 kPa(a). Valves V07 and V08 were then closed and the helium trapped in the tubing between these valves was allowed to heat up to the line temperature.
24) Valve V20 was opened and Jet-mixer 3 together with the tubing between valves V07 and V19 in the vapour-sampling system were evacuated to less than 0.1 kPa(a). Valves V18 and V20 were then closed.
25) The six-port vapour-sampling valve was switched from its sampling position to its flushing position and valve V07 was then opened. The vapour sample was thereafter flushed from the sample loop of the six-port valve into Jet-mixer 3.
26) Metering valve V08 was opened and helium was bled into the jet-mixer at a rate of 4 kPa/s until a pressure of 250 kPa was reached in the jet-mixer. This assisted in improving sample homogenization in the jet-mixer. Valves V07 and V08 were then closed.
27) The jet-mixer pressure was monitored to detect condensation over a period of 5 minutes. If no condensation was detected the homogenised sample was thereafter analysed in the same way in which the liquid sample was previously analysed with a

pressure drop 15 kPa in Jet-mixer 3 employed during sample flushing to the GC six-port valve.

5.2.5 Measuring a new HPVLE data point

Before commencing the measurement of new HPVLE data points, the vapour sample loop of the six-port vapour-sampling valve was cleaned out while maintaining the valve in its flushing position. The loop was evacuated to less than 0.1 kPa(a) where it was maintained for over an hour. Valves V05 and V06 were then opened and the vapour-sampling valve was switched to its sampling position to reconnect the vapour sample loop with the vapour re-circulation loop. This resulted in a slight drop in the equilibrium cell pressure.

Binary HPVLE measurements at each isotherm were all conducted from the lowest to the highest pressure. A new data point was measured after establishing a new operating pressure by feeding the volatile gaseous component into the system as described in Section 5.2.2. The procedures to reach equilibrium and so forth were thereafter followed.

CHAPTER 6

SYSTEMS CHOSEN FOR EXPERIMENTATION

This study formed a continuation of the work of Moodley [2002] also performed at the School of Chemical Engineering at the University of KwaZulu Natal (Durban). Moodley [2002] aimed to develop a piece of equipment capable of measuring HPVLE data in the temperature range -80 to +30 °C and pressures up to 10 bar in the first phase of the project. The ultimate aim was to use the new equipment in the measurement of low-temperature HPVLE data of systems containing fluorinated hydrocarbons. Moodley [2002] developed a vapour recirculation apparatus, however owing to problems associated with the design of the equipment the equipment was only able to reach temperatures down to -5°C and pressures up to 6.7 bar. Successful VLE measurements were performed on the equipment however not within the desired operating range. This meant that the desired fluorinated hydrocarbon systems could not be studied on the equipment of Moodley [2002].

This study thus aimed to modify and rebuild the equipment of Moodley [2002] to enable it to reach a wider range of operating conditions and thus enable the future measurement of data of the fluorinated hydrocarbon systems of interest.

Following modifications and the reconstruction of parts of the equipment pure component vapour pressure measurements were performed on isopentane and propane to display the operating limits that could be achieved by the modified equipment. Thereafter HPVLE measurements were performed on similar systems as those studied by Moodley [2002] to ensure reliable operation of the vapour and liquid sampling systems. Similar systems were chosen due to their suitability to the temperature and pressure range at which the study was to be carried out and the on-site availability of the chemicals at the School of Chemical Engineering at the University of Natal (Durban) thus eliminating the cost of procuring new chemicals for testing.

6.1 Pure-component vapour-pressure measurements

Pure-component vapour pressure measurements were conducted to display the range of operating conditions which could be achieved using the equipment, in particular the low temperatures. Vapour pressure measurements were performed on propane and isopentane. These components were chosen due to their availability and also to demonstrate that the apparatus can be used to measure vapour-pressures of liquids and gases at room temperature.

Vapour pressures of a liquid at room temperature, isopentane were conducted between -14 and 27.9 °C and compared against literature values given by the correlations of Reid *et al.* [1988]. Vapour-pressures of propane, the gas at room temperature, were measured between -30.1 and 26.0 °C. Vapour-pressure data obtained for propane were compared against the data obtained in the correlations of Reid *et al.* [1988] and the AIChE DIPPR compilation [Daubert & Danner, 1993].

6.2 Binary system HPVLE measurements

6.2.1 Propane + 1-propanol

The binary propane + 1-propanol system at 19.9 °C was used as the initial test system to assess reliability of the general operation of the system and fine-tune the sampling techniques employed. Table 6-1presents a list of previous studies performed on the binary propane + 1-propanol system.

Table 6-1: Literature HPVLE studies for the binary system propane + 1-propanol

Author(s)	Temperature [°C]	Pressure range [bar]
Nagahama *et al.* [1971]	19.9	1.43 – 7.99
Mühlbauer & Raal [1993]	81.6	4.53 – 22.39
	105.2	4.58 – 35.49
	120.1	4.46 – 40.45
Ramjugernath [2000]	105.1	5.81 – 31.81
	120	5.23 – 40.31
Naidoo [2002]	50	3.47 – 14.52
	105	2.96 – 34.89
Moodley [2002]	0	0.717 – 4.523
	19.9	1.780 – 6.011

6.2.2 Propane + isopentane

To gain more confidence in the reliability of the modified apparatus further tests were done with the binary propane + isopentane system at 25.0 and 0 °C. This test system would also be used to demonstrate the control capabilities of the equipment at low temperatures. New HPVLE data were measured for the binary propane + isopentane system at -10°C. Table 6-2 displays some of the reported HPVLE literature data for the propane + isopentane system.

Table 6-2 :Literature HPVLE studies for the binary propane + isopentane system

Author(s)	Temperature [°C]	Pressure range [bar]
Vaughan & Collins [1942]	0	0.507 – 4.053
	25	1.520 – 7.093
	50	3.040 – 15.199
Moodley [2002]	0	0.343 – 4.518

CHAPTER 7

EXPERIMENTAL RESULTS

The experimental results presented in this chapter display the reliability of the equipment in obtaining accurate data across the desired operating limits of the equipment. Vapour pressures measured for isopentane and propane displayed that data could be measured at temperatures as low as -30.1°C and pressures just under 10 bar(a) using the newly modified equipment, showing an improvement in the original equipment design. Following GC calibrations for the components under investigation, binary HPVLE data was measured for the propane + 1-propanol system at one isotherm and at three isotherms for the system propane + isopentane with binary data obtained at a lowest isotherm of -10°C. Uncertainty in measured system variables and purity of chemicals used are also discussed to assist in verifying the accuracy of experimental data measured.

7.1 Purity of chemicals

Propane

Pure component vapour pressure measurements, as well as binary VLE measurements were performed with propane. The instrument grade propane with a specified purity of 99.5 % was supplied by the Special Gases Division of Air Products South Africa (Pty) Ltd.

Nitrogen

Nitrogen was used as the cooling medium in the nitrogen recirculation loop to cool the equilibrium cell contained in the thermostat. Nitrogen was also used for leak testing during the commissioning of the equipment as well as to test for leaks during routine maintenance of the equipment. Industrial grade nitrogen gas supplied by Afrox Ltd was used as a high-purity product was not required for the above applications.

Helium

Helium was used as the primary carrier gas in gas chromatography. Instrument grade helium with a minimum purity of 99.999 % supplied by Afrox Ltd.

Hydrogen

Instrument grade hydrogen was used during the operation of the FID of the Shimadzu GC. This gas had a minimum purity of 99.999 % and was supplied by Afrox Ltd.

Air

Instrument grade air was used during the operation of the Shimadzu GC. The air contained 20.0-22.0 % oxygen and 78.0-80.0 % nitrogen and was supplied by Afrox Ltd.

1-Propanol

The 1-propanol used in the binary VLE measurements had a minimum purity of 99.9 % with the main impurities reported to be 0.05 % water and the 0.0015 free acid (as CH_3CH_2COOH). The 1-propanol was supplied by Riedel-de Haën.

n-Pentane

The n-pentane used for pressure calibration through pure component vapour pressure measurements had a minimum purity of 99.0 % with the main impurities reported to be 0.01 % water, 0.005 % sulphur, and 0.001 % non-volatile matter. The n-pentane was supplied by Riedel-de Haën.

Isopentane

The isopentane used in pure component vapour pressure measurements and binary VLE measurements had a minimum claimed purity of 99.5 % with the main impurity being water at 0.05 % The isopentane was supplied by FLUKA Chemika.

Acetone

The acetone used in the low temperature bath had a minimum purity of 98.0 %. Purity of acetone was not a critical factor for its use in the low temperature bath.

Ethylene Glycol

Ethylene glycol was used together with water in the pre-cooler bath to prevent freezing at low temperatures. Industrial grade ethylene glycol of 91.1 % purity was used.

7.2 Accuracy of measurements

7.2.1 Temperature

As only the accuracy of the temperature measurement in the equilibrium cell was of major importance in the measured data during experimentation it was decided to only do a full calibration on the Pt-100 sensor used for this measurement. The Pt-100 sensor in the equilibrium cell was calibrated against an Agilent 34401a 6.5 digit multi-meter coupled with

a Pt-100 standard as detailed in Appendix A.1. The temperature measurement in the equilibrium cell could be read to only 0.1°C on the Eurotherm 2204 controller used and temperature measurements were considered to be accurate to within ± 0.1 °C. A temperature reading to 0.01 °C with a higher accuracy would be more ideal for this study but it was not possible with the equipment available. All other temperature measurements were used as an indication and obtaining exact temperatures were not entirely necessary during experimentation. A comparison was however made between the readings on all the Pt-100 sensors and the Agilent 34401a 6.5 digit multi-meter coupled to the Pt-100 standard to determine that they were functioning within an acceptable error to give a good indication of temperature where they were located in the equipment. Upon comparison with the standard it was found that all measurements were accurate to within ± 1.5 °C which was considered to be sufficient for their applications.

7.2.2 Pressure

Pressure measurements were carried out on a Sensotec Model Super TJE transducer coupled to a Sensotec model GM display unit indicating pressure in units of pounds per square inch absolute (psia) with a reading to 0.1 psia (0.69 kPa). As no standard was available for calibration at high pressures calibration of the pressure transducer was achieved by doing pure component vapour pressure measurements on n-Pentane with an accurate temperature indication. Pressure readings obtained were then adjusted to literature values by applying a correction factor to measured values. A linear calibration chart was thus obtained for the Sensotec Pressure transducer used in this study. Pressure calibration details are fully discussed in Appendix A.2. This method of calibration did not provide an ideal approach as it did not take into account errors in experimentation during the vapour pressure measurements for the calibration. Taking into account all factors pressure measurements were considered to be accurate to within ± 0.2 psia (± 1.38 kPa). This relatively low degree of accuracy in the pressure measurement introduced a high degree of uncertainty in measured data, particularly in the low pressure region.

7.2.3 Composition

During GC calibrations peak areas agreeing within ± 1.25 % were used to obtain data points for the calibration curves. Mole fractions in the binary VLE systems investigated were calculated as follows

$$x_{volatile-component} = \frac{n_{volatile-component}}{n_{volatile-component} + n_{non-volatile-component}} \quad (7\text{-}1)$$

where *n* is the number of moles of material present. Based on the above mole fraction data was considered to be accurate to ± 2.5 %.

7.3 Vapour pressure measurements

Pure component vapour pressure measurements were undertaken for isopentane and propane according to the procedures described in Section 5.2.

This choice of components investigated displayed the capability in measuring data for liquids at room temperature with the data for isopentane and that of gases at room temperature with the data obtained for propane. The temperature ranges investigated for the pure component measurements clearly demonstrated the capabilities of the equipment in attaining and measuring data at temperatures down to -30.1 °C and pressures up to 10 bar(a). Vapour pressures measured were also used to indicate the accuracy of the calibrations performed on the equilibrium cell pressure and temperature measuring devices, by comparing measured data with literature data and thus indicating the percentage error in measured data relative to the quoted literature data.

$$\Delta P\%Error = \frac{100(P_{Experimental} - P_{Literature})}{P_{Literature}} \quad (7\text{-}2)$$

7.3.1 Isopentane vapour pressure measurements

The results of experimental vapour pressure measurements for isopentane are presented in Table 7-1 and graphically represented in Figure 7-1. The vapour pressures were measured at temperatures between -14.0 °C and 27.9 °C and compared against vapour pressures given by correlations in Reid et al. [1988] by calculating the ΔP % error for each data point as displayed in Table 7-1 and Figure 7-2. The average ΔP % error in the isopentane vapour pressure measurements across the temperature range measured was found to be ± 0.49 %.

Table 7-1: Vapour-pressure measurements for isopentane

Temperature [°C]	Temperature [K]	$P_{Experimental}$ [kPa]	$P_{Literature*}$ [kPa]	ΔP% Error*
-14.0	259.15	18.48	18.17	1.67
-10.3	262.85	21.92	21.71	0.98
-6.0	267.15	26.74	26.50	0.91
-3.4	269.75	29.50	29.79	-0.99
0.0	273.15	34.32	34.58	-0.76
2.0	275.15	37.76	37.67	0.24
4.0	277.15	41.21	40.99	0.54
6.0	279.15	44.65	44.53	0.28
8.0	281.15	48.10	48.31	-0.44
10.0	283.15	52.23	52.34	-0.20
12.0	285.15	56.36	56.63	-0.47
14.0	287.15	61.18	61.19	-0.02
16.0	289.15	66.00	66.05	-0.06
18.0	291.15	71.52	71.20	0.44
20.0	293.15	77.03	76.66	0.48
22.0	295.15	82.54	82.44	0.11
24.0	297.15	88.73	88.57	0.19
26.0	299.15	94.93	95.04	-0.11
27.9	301.05	101.13	101.52	-0.38

* Reid *et al.* [1988]

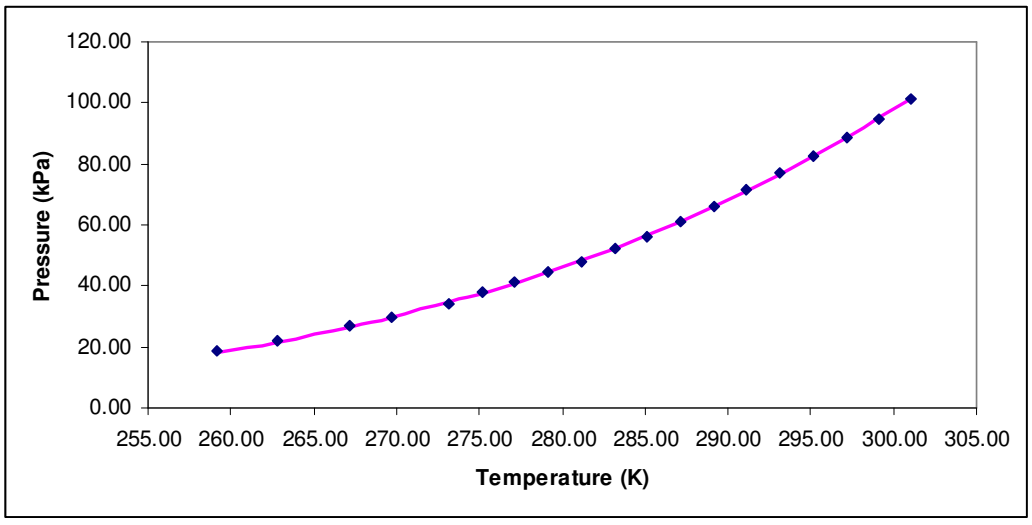

Figure 7-1: Comparison of experimental vapour-pressure data (♦) for isopentane with those predicted by the correlations of Reid et al. [1988] (–).

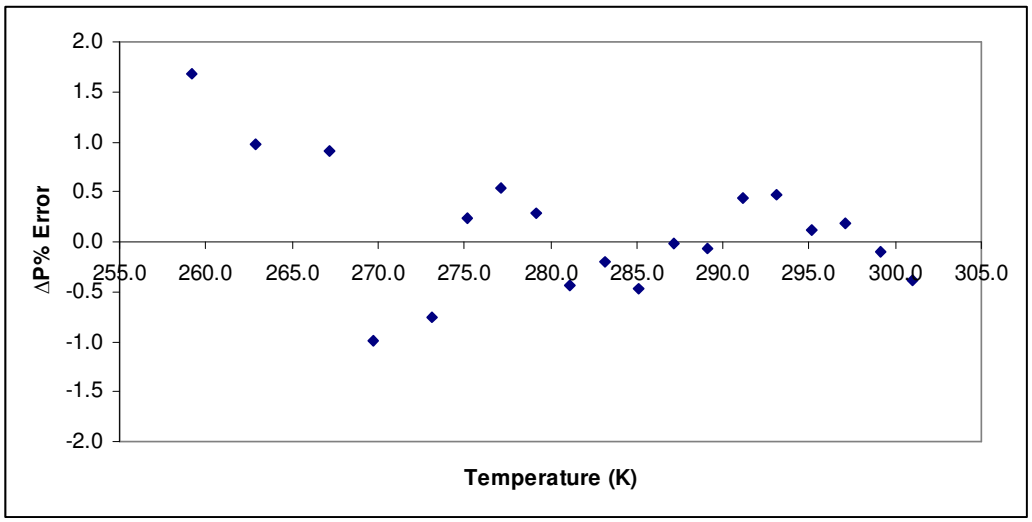

Figure 7-2: Deviations of experimental vapour-pressures for isopentane from the correlations of Reid et al. [1988].

7.3.2 Propane vapour pressure measurements

Vapour pressures were measured for pentane at temperatures ranging from -30.10 °C to 26.00 °C. Results obtained are tabulated in Table 7-2 and graphically represented in Figure 7-3 and Figure 7-4. The experimental data obtained were compared against data obtained from the correlations by Reid et al. [1988]1* and the AIChE DIPPR compilation [Daubert & Danner, 1993]2* at corresponding temperatures as represented in Table 7-2 and graphically displayed in Figure 7-5. The average ΔP % error in measured data across the temperature range studied was found to be ± 0.29 % when compared to data by Reid et al [1988] 1* and ± 0.35 % when compared to data by Daubert & Danner [1993] [2*].

Table 7-2: Vapour-pressure measurements for propane.

Temp. [°C]	Temp. [K]	$P_{Experimental}$ [kPa]	$P_{Literature}$ [1*] [kPa]	$P_{Literature}$ [2*] [kPa]	$\Delta P\%_{Literature}$ [1*] Error	$\Delta P\%_{Literature}$ [2*] Error
-30.10	243.05	167.26	167.45	167.16	-0.12	0.06
-28.10	245.05	180.34	181.06	180.79	-0.40	-0.25
-26.10	247.05	195.50	195.49	195.26	0.00	0.12
-24.10	249.05	210.65	210.79	210.59	-0.07	0.03
-22.10	251.05	226.49	226.98	226.82	-0.22	-0.14
-20.10	253.05	243.71	244.11	243.99	-0.16	-0.11
-17.60	255.55	266.44	266.87	266.81	-0.16	-0.14
-15.10	258.05	290.55	291.20	291.21	-0.22	-0.23
-12.50	260.65	317.41	318.24	318.33	-0.26	-0.29
-10.00	263.15	344.96	345.99	346.16	-0.30	-0.35
-7.00	266.15	380.09	381.63	381.91	-0.41	-0.48
-4.00	269.15	418.66	419.95	420.34	-0.31	-0.40
-1.00	272.15	459.99	461.08	461.58	-0.24	-0.35
2.00	275.15	503.38	505.12	505.74	-0.35	-0.47
5.00	278.15	550.91	552.21	552.96	-0.24	-0.37
8.00	281.15	600.50	602.48	603.33	-0.33	-0.47
11.00	284.15	654.23	656.05	657.01	-0.28	-0.42
14.00	287.15	710.71	713.05	714.09	-0.33	-0.48
17.00	290.15	768.57	773.61	774.72	-0.66	-0.80
20.00	293.15	832.62	837.87	839.01	-0.63	-0.77
23.00	296.15	901.50	905.95	907.09	-0.49	-0.62
26.00	299.15	975.20	978.01	979.09	-0.29	-0.40

[1*] Reid *et al.* [1988]
[2*] [Daubert & Danner, 1993]

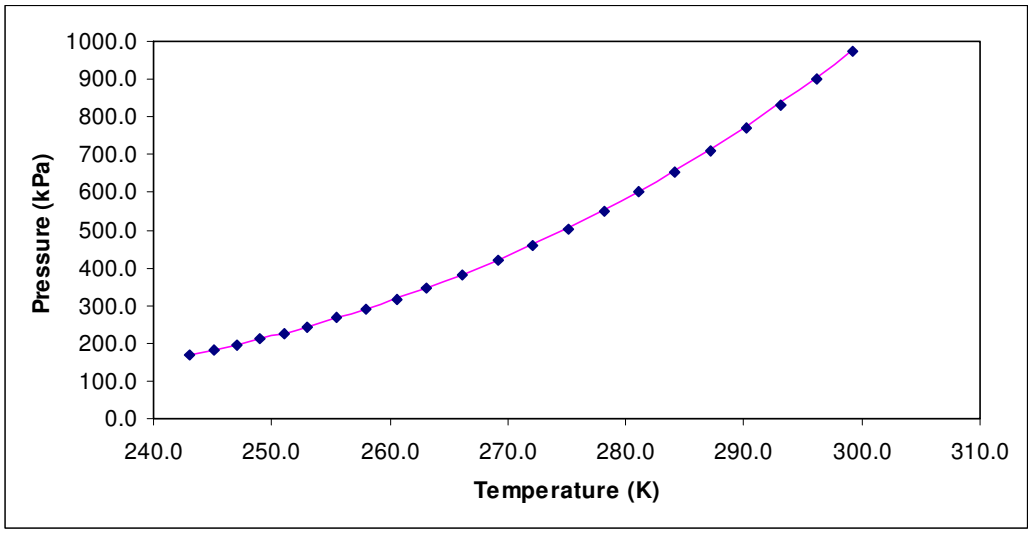

Figure 7-3: Comparison of experimental vapour-pressure data (♦) for propane with those predicted by the correlations of Reid et al. [1988] (–).

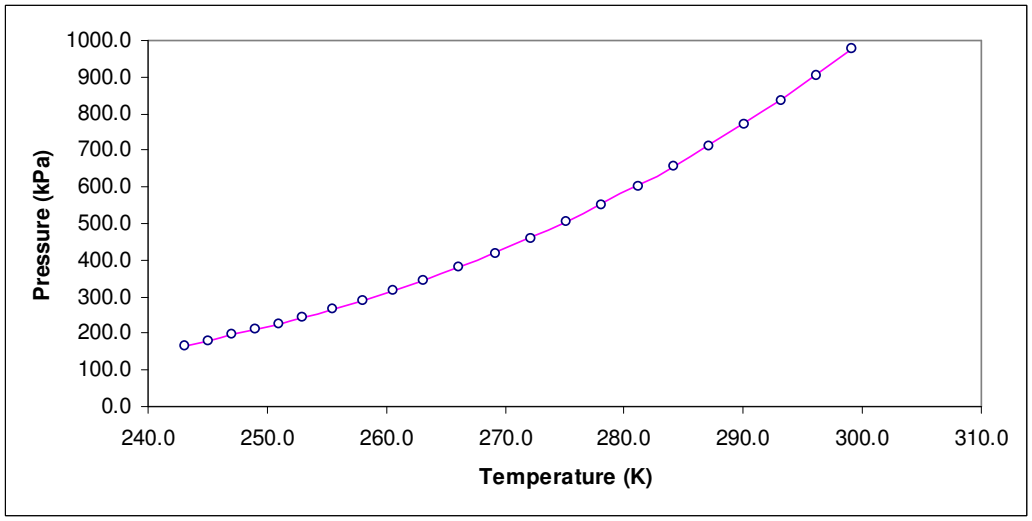

Figure 7-4: Comparison of experimental vapour-pressure data (o) for propane with those predicted by the correlations of Daubert & Danner [1993] (–).

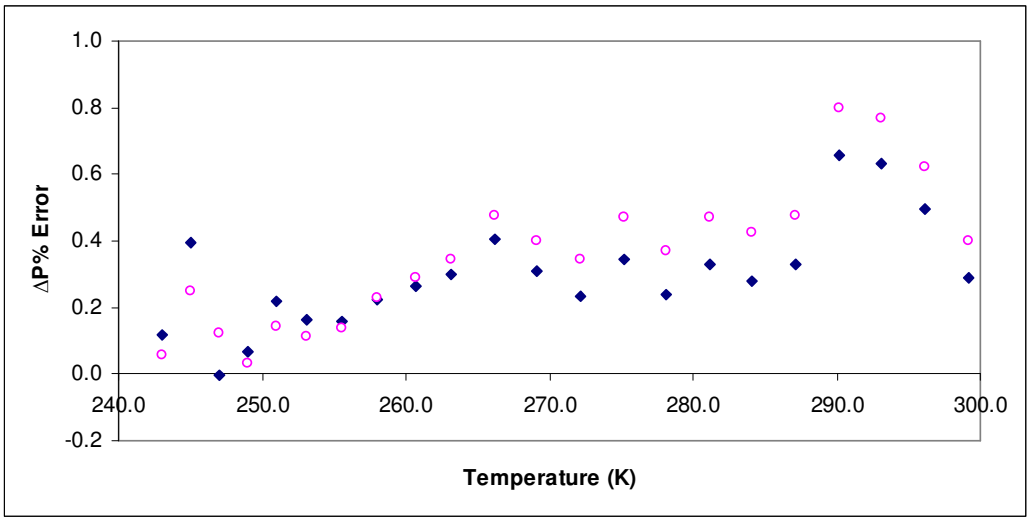

Figure 7-5: Deviations of experimental vapour-pressures for propane from the correlations of Reid et al. [1988] (♦) and Daubert and Danner [1993] (o).

7.4 Gas chromatograph calibrations

Calibrations of all three components investigated were carried out on the Shimadzu GC fitted with the J & W Scientific GS-Q column as described in Section 5.1. The FID on the GC was used for the analysis of the components. Settings of the GC were adjusted according to the binary system being investigated as indicated in Table 4-1 of Section 4.9.3 with the method of direct injection calibration being used. Figure 7-6, Figure 7-7 and Figure 7-8 displays the calibration curves for propane, 1-propanol and isopentane respectively, and their resulting calibration equations which were used during all subsequent compositional analyses carried out are displayed in Table 7-3.

Table 7-3: GC Calibration Equations

Component	Calibration Equation
Propane	$A = -0.0056n^2 + 0.2078n$
1-Propanol	$A = 0.3816n$
Isopentane	$A = -0.0141n^2 + 0.9993n$

Where:

A = GC Peak Area

n = Moles of Component

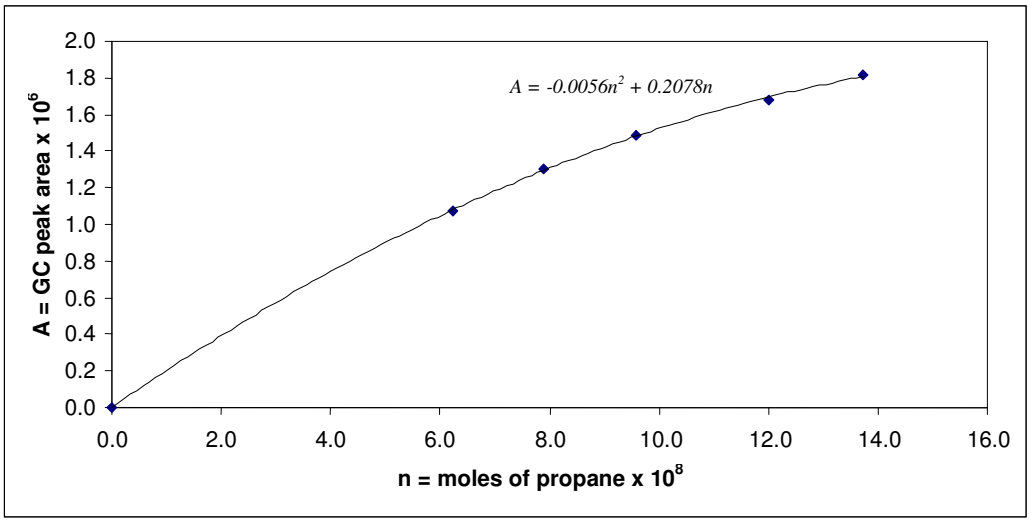

Figure 7-6: GC calibration with propane.

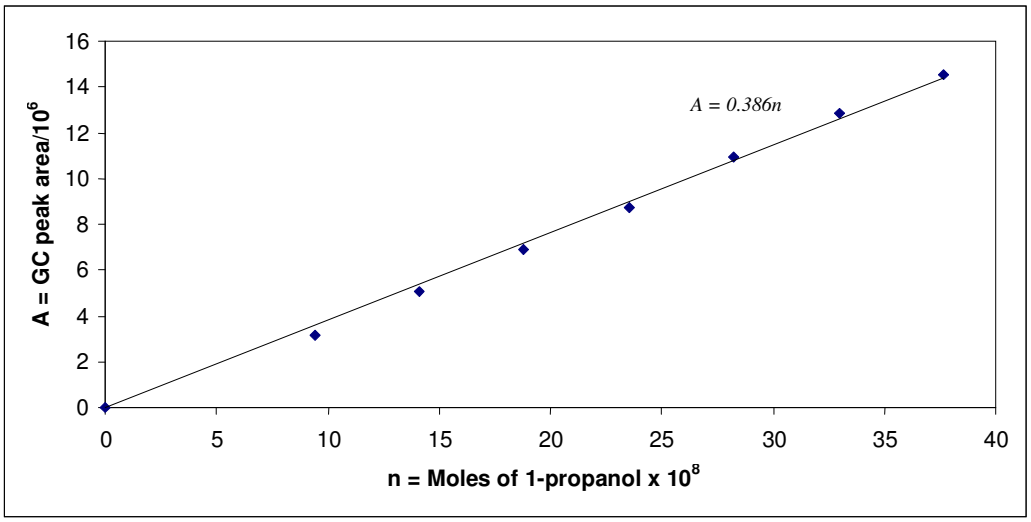

Figure 7-7: GC calibration with 1-propanol.

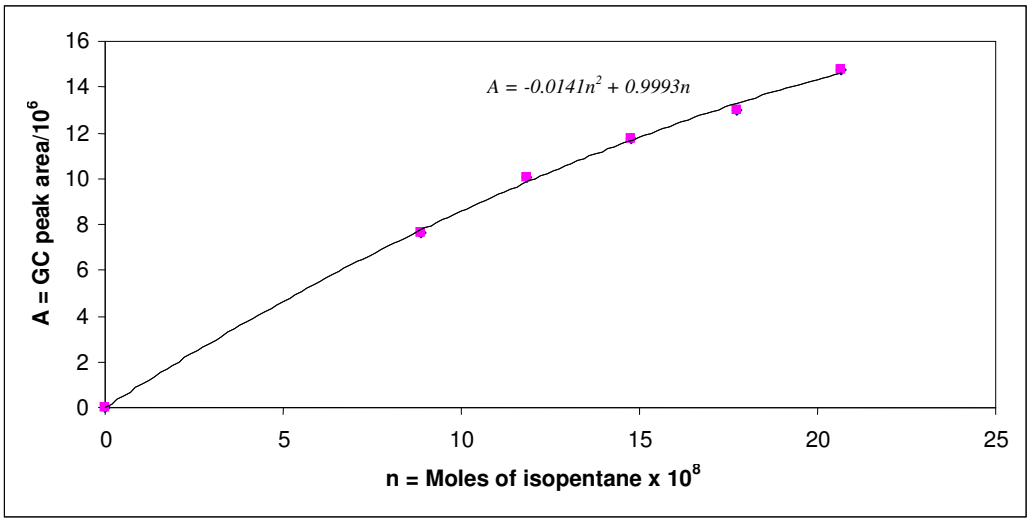

Figure 7-8: GC calibration with isopentane.

7.5 Binary system measurements

To validate the reliability of the equipment and the methods used in its operation to obtain VLE data it was necessary to first obtain VLE data and compare against previously measured data. Tests were done on the equipment using two different systems at a total of three different isotherms to verify accuracy of data for future studies. Tests were done on more than one system and at different isotherms as problems were encountered during initial tests with some inaccurate data being obtained. It was thus necessary to improve on experimental procedures to ensure consistency in accuracy of measured data. It was thus decided to test the system on different systems and at different isotherms until full confidence in the measured data obtained with the equipment was achieved before new binary data could be measured. New binary isothermal VLE data were obtained for the propane + isopentane system at -10°C.

7.5.1 Propane (1) + 1-propanol (2) system

The propane (1) + 1-propanol (2) system was chosen as one of the test systems where isothermal binary VLE data were measured. Isothermal VLE data were obtained at 19.9 °C and compared with literature data from previous studies by Nagahama et al. [1971] in Figure 7-9 and Moodley [2002] in Figure 7-10. Experimental data obtained are tabulated in Table 7-4. The data measured in this study did not extend over the entire composition range as in comparable literature data.

The experimental P-x data obtained show a fairly good agreement to both sets of literature data against which it is compared in the composition range studied. P-y experimental data showed a relatively good agreement with the experimental data obtained by Moodley [2002], as well as the computed P-y data obtained by Nagahama *et al.* [1971].

Table 7-4: Experimental vapour-liquid equilibrium data for the binary propane (1) + 1-propanol (2) system at 19.9°C

$P_{Experimental}$ [kPa]	x_1	y_1
422.80	0.1908	0.9953
490.30	0.2289	0.9958
577.77	0.3003	0.9969
652.85	0.3939	0.9972
702.44	0.4347	0.9976
803.01	0.7503	0.9982
807.83	0.9844	0.9983
830.06	1.0	1.0

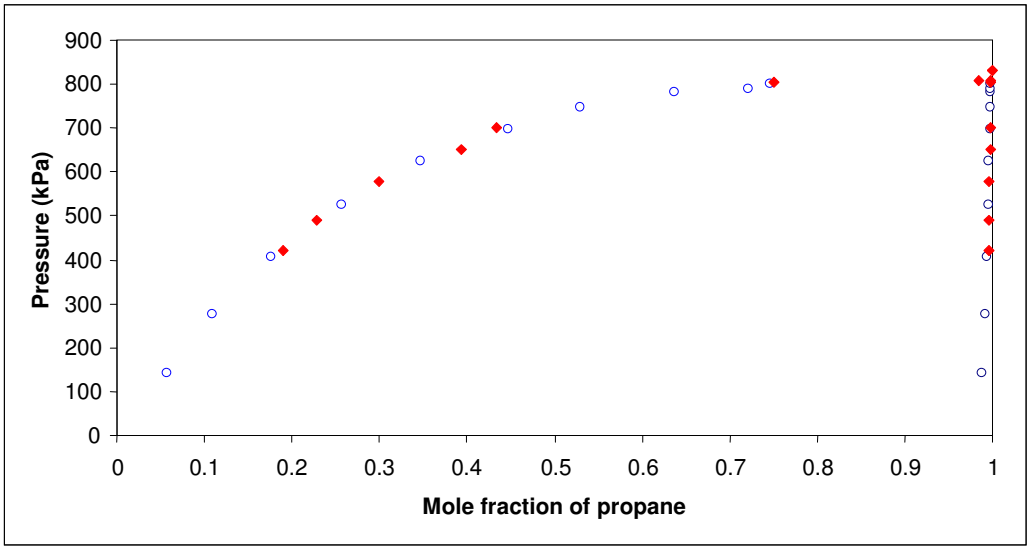

Figure 7-9: Comparison of experimental VLE data (♦) for the propane + 1-propanol system at 19.9 °C with those of Nagahama et al. [1971] (o).

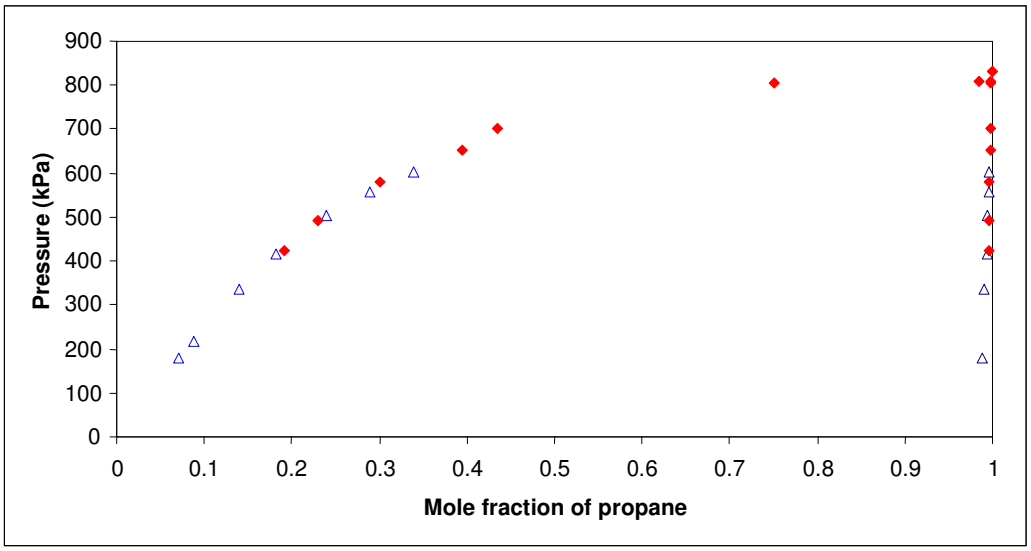

Figure 7-10: Comparison of experimental VLE data (♦) for the propane + 1-propanol system at 19.9 °C with those of Moodley [2002] (Δ).

7.5.2 Propane (1) + isopentane (2) system

Propane (1) + isopentane (2) was chosen as another test system to help validate the accuracy of the equipment with measurements being done at three different isotherms, 25 °C, 0 °C and new VLE data for the system at -10 °C. The fairly ideal phase behaviour of this system made it an excellent system to test the reliability of the equipment at low temperatures. Data obtained at 25 °C tabulated in Table 7-5 was compared with that of data obtained by Vaughan & Collins [1942] and show a good agreement with this data as seen in Figure 7-11. Data measured at 0 °C, tabulated in Table 7-5 was compared to data by Vaughan & Collins [1942] illustrated in Figure 7-12 and with data obtained by Moodley [2002] represented in Figure 7-13 with a good agreement being achieved in the comparison with both sets of data. Following the above mentioned binary measurements new HPVLE data was obtained for the propane (1) + isopentane (2) system at -10 °C with data tabulated in Table 7-5 and graphically represented in Figure 7-14.

Table 7-5: Experimental vapour-liquid equilibrium data for the binary propane (1) + isopentane (2) system at 25, 0 and -10°C.

25 °C Isotherm			0 °C Isotherm			-10 °C Isotherm		
$P_{Experimental}$ [kPa]	x_1	y_1	$P_{Experimental}$ [kPa]	x_1	y_1	$P_{Experimental}$ [kPa]	x_1	y_1
90.32	0.0000	0.0000	34.27	0.0000	0.0000	22.13	0.0000	0.0000
219.60	0.1734	0.6076	142.46	0.2597	0.8163	239.58	0.6163	0.9420
323.61	0.2957	0.7793	199.63	0.3868	0.8747	272.64	0.7079	0.9627
406.27	0.4045	0.8358	290.55	0.5984	0.9241	302.95	0.8075	0.9794
482.03	0.4810	0.8731	353.23	0.7477	0.9692	324.99	0.9242	0.9922
606.70	0.6345	0.9186	431.06	0.8828	0.9846	344.94	1.0000	1.0000
763.06	0.8080	0.9664	476.00	1.0000	1.0000			
937.00	1.0000	1.0000						

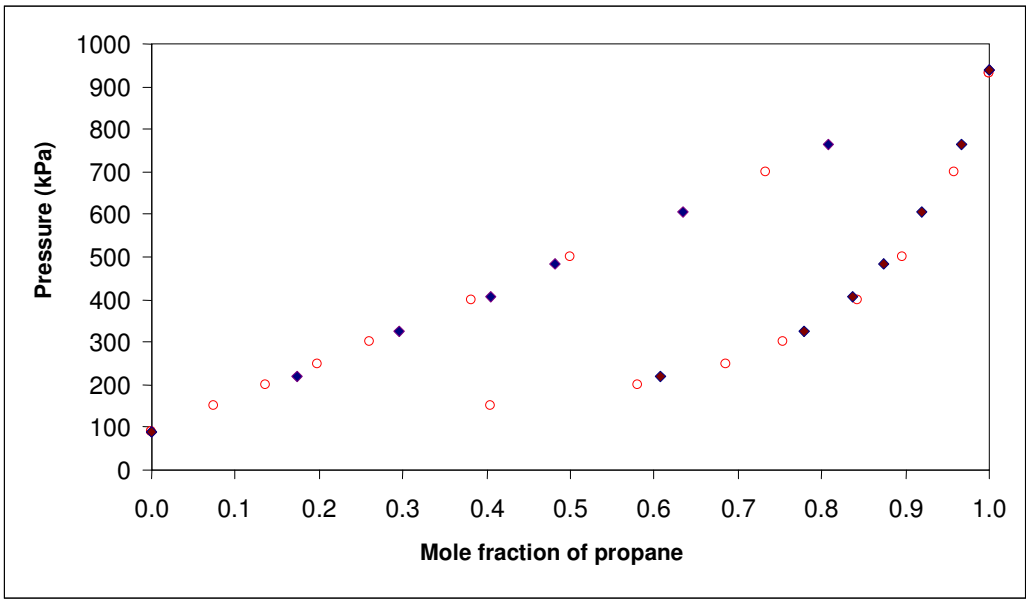

Figure 7-11: Comparison of experimental VLE data (♦) for the binary propane + isopentane system at 25 °C with those of Vaughan & Collins [1942] (o).

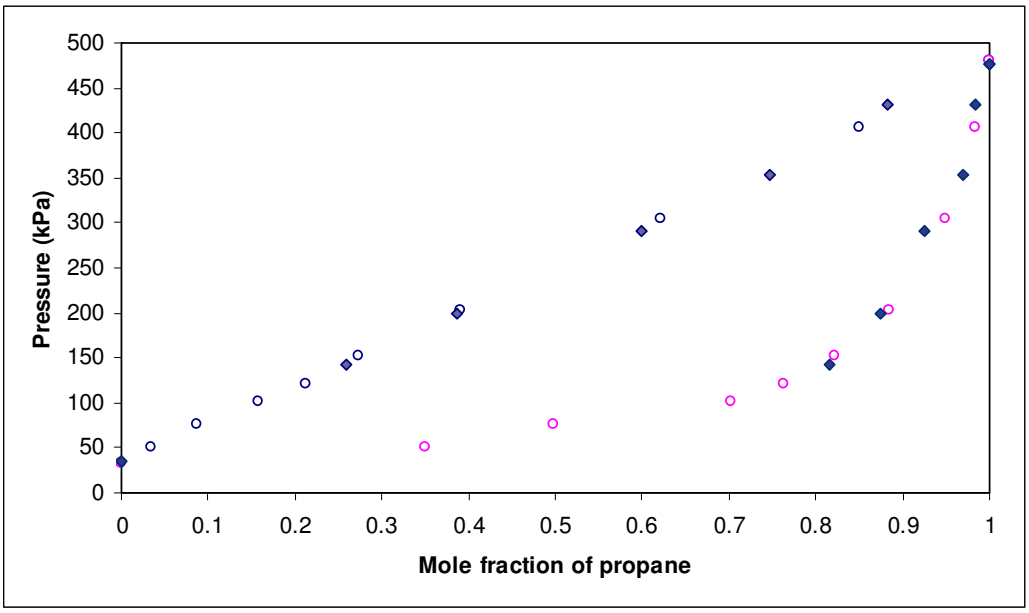

Figure 7-12: Comparison of experimental VLE data (♦) for the binary propane + isopentane system at 0 °C with those of Vaughan & Collins [1942] (o).

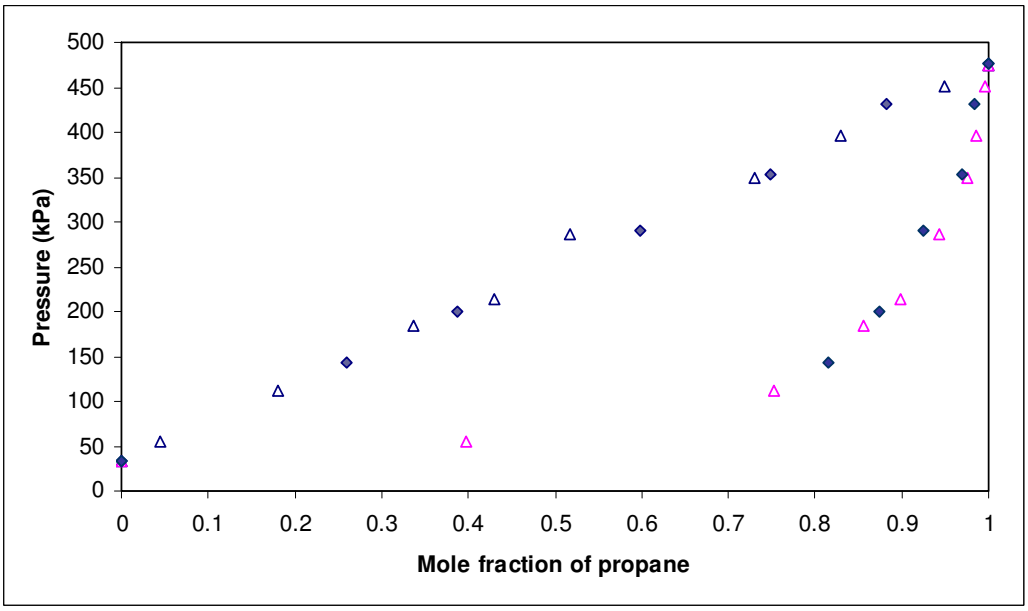

Figure 7-13: Comparison of experimental VLE data (♦) for the binary propane + isopentane system at 0 °C with those of Moodley [2002] (Δ).

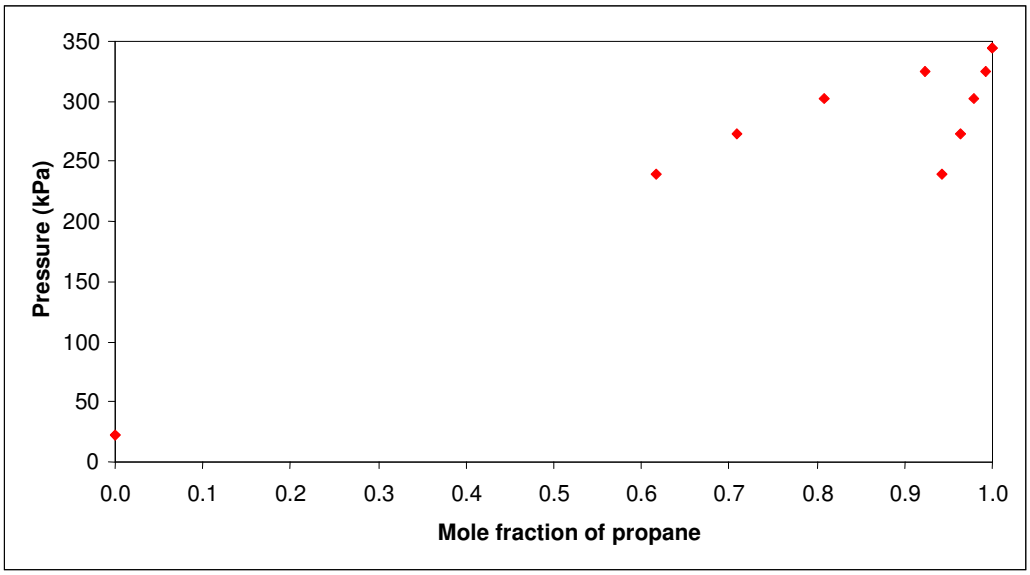

Figure 7-14: Experimental VLE data for the binary propane + isopentane system at -10 °C.

CHAPTER 8

DISCUSSION

The acquisition of VLE experimental data forms the basis from which theoretical techniques can be applied to the data to develop a mathematical model of a particular chemical system which can be applied over a wide range of temperatures and pressures. This chapter focuses on applying theoretical techniques, discussed in Chapter 3, to the experimental data obtained in this study. Correlation of the HPVLE data was carried out via the direct method which was considered to be sufficient for the isothermal data obtained during this study. Pure component vapour pressures were also correlated via the direct method.

All pure component physical properties used in the theoretical treatment are contained in Appendix B with relevant sources of data noted. All correlations of the experimental data was carried out using a software package called Thermopack Version 1.10, developed by C. Coquelet & A. Baba-Ahmed [2002] at Ecole des Mines de Paris, Laboratory of Thermodynamics and Phase Equilibria.

8.1 Theoretical treatment of the experimental data

8.1.1 Application of the direct method

The direct method entails the use of a single EOS to describe both the liquid and vapour phases. This study made use of the Peng-Robinson (PR) Eq. (3-34) and the Soave-Redlich-Kwong (SRK) Eq. (3-22) EOSs. As discussed in Chapter 3 modifications of these original equations of state to improve regression can be achieved by adjusting the temperature dependence through the choice of a specific $\alpha(T)$ function. In this study the Mathias-Copeman (MC) $\alpha(T)$ function Eq. (3-50) with three adjustable parameters κ_1, κ_2, κ_3 was applied to the PR & SRK EOS's. Binary HPVLE regression was achieved by extending the modified PR & SRK EOS's to mixtures through incorporation of the Wong-Sandler mixing rule Eq. (3-90) together with the NRTL local composition model Eq. (3-112) as the chosen activity coefficient model used to calculate the Gibbs energy.

8.1.2 Regression of vapour pressures

The Mathias-Copeman (MC) adjustable parameters κ1, κ2, κ3 were obtained via regression of the experimentally determined pure component vapour pressures of Propane and Isopentane. A set of adjustable parameter values for each of the components was determined through application of the PR-EOS and another set through application of the SRK-EOS. These parameters were evaluated using a modified Simplex algorithm with the following objective function:

$$S = \frac{100}{N}\sum_{j=1}^{N}\left(\frac{P^{\exp} - P^{cal}}{P^{\exp}}\right)_j^2 \tag{8-1}$$

The percentage standard deviation (s_r) provides a measure of the percentage deviation of the experimental data from the predicted data and is determined as follows (Ruzicka *et al*., 1998):

$$s_r = 100\sqrt{\left(\sum_{j=1}^{N}\left[\frac{\left(P^{\exp} - P^{cal}\right)}{P^{\exp}}\right]_j^2\right)\left(\frac{1}{N-m}\right)} \tag{8-2}$$

Where $P^{\exp}$ is the experimental vapour pressure value, P^{cal} is the value that is calculated by the model, N is the number of experimental values in the data set and m is the number of adjustable parameters in the correlating model. As no pure-component vapour pressures were measured for 1-Propanol, the Mathias-Copeman adjustable parameters required for the binary system regression, were obtained from the database software program Component Plus Version 3.4.0.15 which derives physical properties and data from the AIChE DIPPR compilation.

Table 8-1: Pure-component Mathias-Copeman coefficients together with percentage deviations for the PR-MC EOS

	κ1	κ2	κ3	Sr
Isopentane	0.5485	1.4674	-3.2694	0.53
Propane	0.6296	-0.3924	1.2930	0.12
1-Propanol	1.08141	1.33438	-2.09376	-

Table 8-2: Pure-component Mathias-Copeman coefficients together with percentage deviations for the SRK-MC EOS

	κ1	κ2	κ3	Sr
Isopentane	0.6995	1.2422	-3.0886	0.53
Propane	0.7838	-0.7162	1.7461	0.12
1-Propanol	1.27789	0.963748	0.963748	-

Table 8-1 contains the Mathias-Copeman adjustable parameters obtained for the pure components via the PR- EOS while Table 8-2 contains the parameters obtained via the SRK-EOS. The tables also depict the percentage standard deviation for the experimentally measured pure-component vapour-pressure data against the respective regressed data. These percentage deviations show an acceptable error for both the pure component vapour-pressure measurements when compared to regressed data using both the PR and the SRK EOS's thus verifying that the equipment is capable of performing accurate pure-component vapour-pressure measurements over the temperature and pressure ranges investigated in this study.

8.1.3 Regression of binary system VLE data

Binary HPVLE for the systems under investigation were regressed using the thermodynamic models described earlier in this section. Optimised adjustable interaction parameters, τ_{12}, τ_{21} and k_{12}, were determined and the deviations of the calculated equilibrium pressures and vapour compositions from the experimentally determined values defined in Equations (8-4) to (8-7) also calculated and presented along with tabulated and graphical bubble point calculation data. The adjustable parameters were adjusted directly to the VLE data through a modified Simplex algorithm with the following objective function:

$$S = \frac{100}{N}\left[\sum_{j=1}^{N}\left(\frac{x_{\exp} - x_{cal}}{x_{\exp}}\right)_j^2 + \sum_{j=1}^{N}\left(\frac{y_{\exp} - y_{cal}}{y_{\exp}}\right)_j^2\right] \tag{8-3}$$

This particular objective function was selected due to the availability of a full set of isothermal *P-x-y* experimental data for the binary systems investigated.

$$AAD(\Delta P\%) = \frac{100}{N_P}.\sum_{j=1}^{N_p}\left(\frac{\left|P^{calc} - P^{\exp}\right|}{P^{\exp}}\right)_j \quad (8\text{-}4)$$

$$Bias(\Delta P\%) = \frac{100}{N_p}.\sum_{j=1}^{N_p}\left(\frac{P^{calc} - P^{\exp}}{P^{\exp}}\right)_j \quad (8\text{-}5)$$

$$AAD(\Delta y) = \frac{1}{N_p}.\sum_{j=1}^{N_p}\left|y_1^{calc} - y_1^{\exp}\right|_j \quad (8\text{-}6)$$

$$Bias(\Delta y) = \frac{1}{N_p}.\sum_{j=1}^{N_p}\left(y_1^{calc} - y_1^{\exp}\right)_j \quad (8\text{-}7)$$

8.1.3.1 Propane (1) + 1-propanol (2) system

The PR-EOS coupled with the Mathias-Copeman (MC) alpha function together with the WSMR and the NRTL equation (PR-MC-WSMR(NRTL)) and the SRK-EOS coupled with the Mathias-Copeman alpha function together with the WSMR and the NRTL equation (SRK-MC-WSMR(NRTL)) were both used to regress the HPVLE data of the propane (1) + 1-propanol system at 19.9 ºC. Results of bubble point calculations for the respective models are contained in Table 8-3 and Table 8-4 while Figure 8-1 and Figure 8-2 provide graphical comparisons of the experimental data against the calculated data.

Table 8-3: Experimental VLE data for the propane (1) + 1-propanol (2) system at 19.9 ºC compared to regressed data obtained via the PR-MC-WSMR(NRTL) model

x_1	$P^{\exp}$ (kPa)	P^{calc} (kPa)	$y_1^{\exp}$	y_1^{calc}
0.1908	422.8	415.40	0.9953	0.9955
0.2289	490.3	481.87	0.9958	0.9962
0.3003	577.77	579.11	0.9969	0.9969
0.3939	652.85	668.54	0.9972	0.9973
0.4347	702.44	696.16	0.9976	0.9975
0.7503	803.01	747.27	0.9982	0.9978
0.9844	807.83	813.82	0.9983	0.9994
1.0000	830.06	832.00	1.0000	1.0000

Table 8-4: Experimental VLE data for the propane (1) + 1-propanol (2) system at 19.9 ºC compared to regressed data obtained via the SRK-MC-WSMR(NRTL) model

x_1	P^{exp} (kPa)	P^{calc} (kPa)	y_1^{exp}	y_1^{calc}
0.1908	422.8	415.84344	0.9953	0.9955
0.2289	490.3	482.1557	0.9958	0.9962
0.3003	577.77	579.09987	0.9969	0.9969
0.3939	652.85	668.32275	0.9972	0.9974
0.4347	702.44	695.93761	0.9976	0.9975
0.7503	803.01	748.03939	0.9982	0.9978
0.9844	807.83	814.03036	0.9983	0.9994
1.0000	830.06	832.10477	1	1.0000

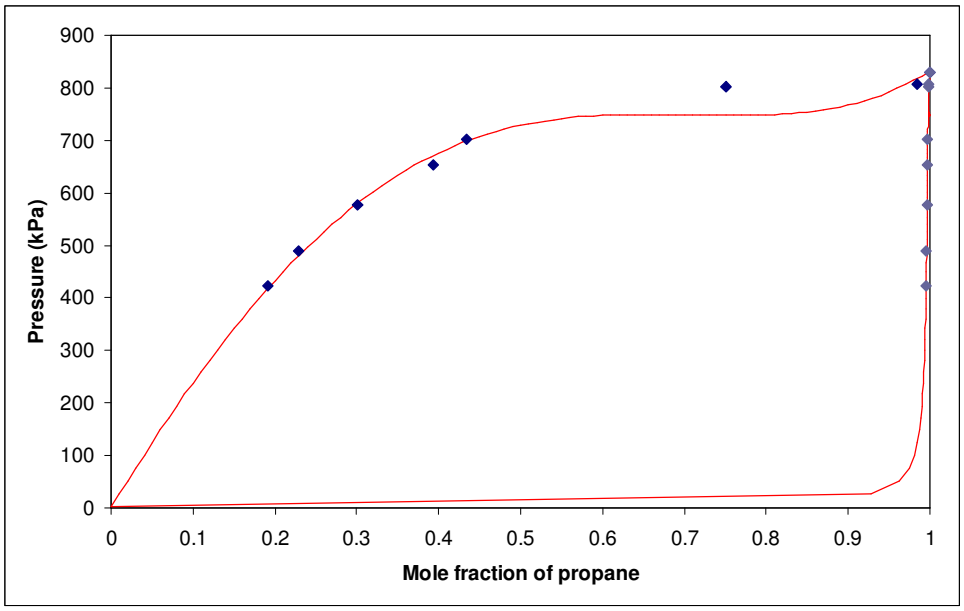

Figure 8-1: Comparison of experimental data (♦) for the propane (1) + 1-propanol (2) system at 19.9 ºC to the P-x-y diagram generated via the PR-MC-WSMR(NRTL) model (–).

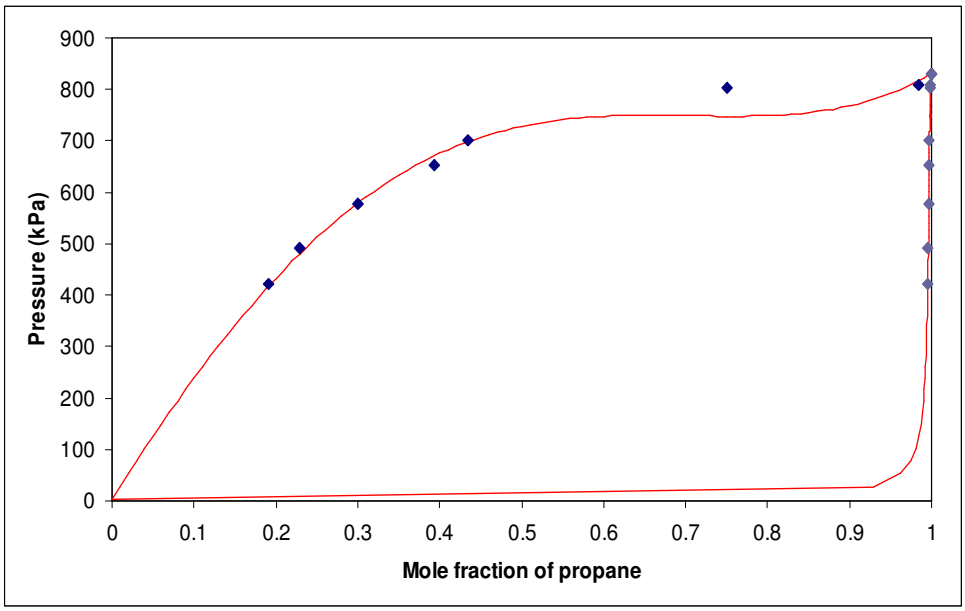

Figure 8-2: Comparison of experimental data (•) for the propane (1) + 1-propanol (2) system at 19.9 °C to the P-x-y diagram generated via the SRK-MC-WSMR(NRTL) model (–).

Table 8-5 contains the calculated optimized adjustable interaction parameters together with the respective calculated deviations for the two different models when comparing the regressed data to the experimental VLE data.

Table 8-5: Model parameters regressed for propane (1) + 1-propanol (2) system at 19.9 °C through application of the PR-MC-WSMR(NRTL) model and the SRK-MC-WSMR(NRTL) model together with calculated deviations for the bubble point pressure and the propane vapour composition when comparing the calculated data to the experimental VLE data

Thermodynamic Model	**PR-MC-WSMR(NRTL)**	**SRK-MC-WSMR(NRTL)**
τ_{12} (J/mol)	4320	4398.5
τ_{21} (J/mol)	-759.41	-746.56
k_{12}	0.31417	0.3150
$AAD(\Delta P\%)$	1.8645	1.865
$Bias(\Delta P\%)$	0.9620	0.9330
$AAD(\Delta y)$	0.0003	0.0003
$Bias(\Delta y)$	0.0001	0.0002

From the observed graphical and calculated deviation results it can be concluded that both models performed relatively well in the correlation of the propane + 1-propanol system at

19.9 ºC. The differences of the calculated deviations obtained for this data set, when comparing the two models used, can be regarded as negligible. Significant deviations of certain experimentally measured values from the calculated data are observed and these can be attributed to errors that occurred during experimentation.

8.1.3.2 Propane (1) + isopentane (2) system

The propane + isopentane system was studied at three different isotherms, 25 ºC, 0 ºC and -10 ºC. The system was regressed at each of the three mentioned isotherms through application of the PR-MC-WSMR(NRTL) model and the SRK-MC-WSMR(NRTL) model. Due to the narrow temperature range investigated it was deemed sufficient to combine the experimental data and generate a single set of optimized adjustable parameters over all isotherms for each of the two thermodynamic models applied in the correlations for this binary system. Table 8-6 displays the respective calculated adjustable parameters for the propane + isopentane system.

Table 8-6: Model parameters regressed for the propane (1) + isopentane (2) system through application of the PR-MC-WSMR(NRTL) model and the SRK-MC-WSMR(NRTL) model

Thermodynamic Model	**PR-MC-WSMR(NRTL)**	**SRK-MC-WSMR(NRTL)**
τ_{12} (J/mol)	9919.1	10332
τ_{21} (J/mol)	-423.71	-303.73
k_{12}	-0.52171	-0.52044

Table 8-7 to Table 8-12 contains a comparison between the experimentally measured data at each of the three isotherms investigated for the propane + isopentane system against the regressed bubble point data obtained through applications of PR-MC-WSMR(NRTL) model and the SRK-MC-WSMR(NRTL) model. Graphical comparisons are represented in Figure 8-3 to Figure 8-8, while Table 8-13 to Table 8-15 contains the calculated deviations for the models when applied at each of the isotherms and compared to the experimental data. Analysis of the results shows a good agreement between the experimental data and the calculated data at the 25 ºC and the 0 ºC isotherms. The experimental data agreement applies to the data generated through the PR-EOS as well as the SRK-EOS at these isotherms. The calculated deviations signify a slightly better representation of the system pressure by the SRK-EOS for both mentioned isotherms while both EOS's provide a similar representation of the vapour compositions. The PR-EOS slightly more accurate representation of the vapour compositions than the SRK-EOS at the -10 ºC isotherm with the system pressure

comparisons showing quite significant deviations for both the PR and SRK EOS's. The magnitude of the deviations can be attributed to a poor set of experimental data obtained at this isotherm. The graphical comparison of the experimental data to both the PR-EOS and the SRK-EOS regressions clearly show deviation increasing at lower propane compositions in both the vapour and liquid phases that can be attributed to experimental inaccuracies.

Table 8-7: Experimental VLE data for the propane (1) + isopentane (2) system at 25 ºC compared to regressed data obtained via the PR-MC-WSMR(NRTL) model

x_1	$P^{\exp}$ (kPa)	P^{calc} (kPa)	$y_1^{\exp}$	y_1^{calc}
0.0000	90.32	91.87	0	0.0000
0.1734	219.6	214.68	0.6076	0.6180
0.2957	323.61	320.20	0.7793	0.7677
0.4045	406.27	404.42	0.8358	0.8320
0.4810	482.03	472.71	0.8731	0.8682
0.6345	606.7	602.80	0.9186	0.9174
0.8080	763.06	766.94	0.9664	0.9612
1.0000	937	949.30	1	1.0000

Table 8-8: Experimental VLE data for the propane (1) + isopentane (2) system at 25 ºC compared to regressed data obtained via the SRK-MC-WSMR(NRTL) model

x_1	$P^{\exp}$ (kPa)	P^{calc} (kPa)	$y_1^{\exp}$	y_1^{calc}
0.0000	90.32	91.87	0	0.0000
0.1734	219.6	216.50	0.6076	0.6212
0.2957	323.61	322.05	0.7793	0.7691
0.4045	406.27	405.80	0.8358	0.8326
0.4810	482.03	473.57	0.8731	0.8686
0.6345	606.7	602.95	0.9186	0.9176
0.8080	763.06	767.46	0.9664	0.9615
1.0000	937	949.48	1	1.0000

Table 8-9: Experimental VLE data for the propane (1) + isopentane (2) system at 0 ºC compared to regressed data obtained via the PR-MC-WSMR(NRTL) model

x_1	P^{exp} (kPa)	P^{calc} (kPa)	y_1^{exp}	y_1^{calc}
0.0000	34.27	34.60	0	0.0000
0.2597	142.46	142.26	0.8163	0.8060
0.3868	199.63	203.30	0.8747	0.8827
0.5984	290.55	302.76	0.9241	0.9432
0.7477	353.23	370.94	0.9692	0.9680
0.8828	431.06	425.77	0.9846	0.9844
1.0000	476	473.89	1	1.0000

Table 8-10: Experimental VLE data for the propane (1) + isopentane (2) system at 0 ºC compared to regressed data obtained via the SRK-MC-WSMR(NRTL) model

x_1	P^{exp} (kPa)	P^{calc} (kPa)	y_1^{exp}	y_1^{calc}
0.0000	34.27	34.61	0	0.0000
0.2597	142.46	143.47	0.8163	0.8075
0.3868	199.63	204.41	0.8747	0.8832
0.5984	290.55	303.64	0.9241	0.9433
0.7477	353.23	372.05	0.9692	0.9681
0.8828	431.06	426.88	0.9846	0.9844
1.0000	476	473.88	1	1.0000

Table 8-11: Experimental VLE data for the propane (1) + isopentane (2) system at -10 ºC compared to regressed data obtained via the PR-MC-WSMR(NRTL) model

x_1	P^{exp} (kPa)	P^{calc} (kPa)	y_1^{exp}	y_1^{calc}
0.0000	22.132	22.21	0	0.0000
0.6163	239.58	207.27	0.941982	0.9444
0.7079	272.64	262.15	0.9627	0.9693
0.8075	302.95	293.30	0.9794	0.9803
0.9242	324.99	323.43	0.9922	0.9905
1.0000	344.94	345.16	1	1.0000

Table 8-12: Experimental VLE data for the propane (1) + isopentane (2) system at -10 ºC compared to regressed data obtained via the SRK-MC-WSMR(NRTL) model

x_1	P^{exp} (kPa)	P^{calc} (kPa)	y_1^{exp}	y_1^{calc}
0.0000	21.92	22.21	0	0.0000
0.6163	239.58	208.07	0.934	0.9445
0.7079	272.64	263.14	0.9627	0.9694
0.8075	302.95	294.44	0.9794	0.9804
0.9242	324.99	324.18	0.9922	0.9905
1.0000	344.94	345.15	1	1.0000

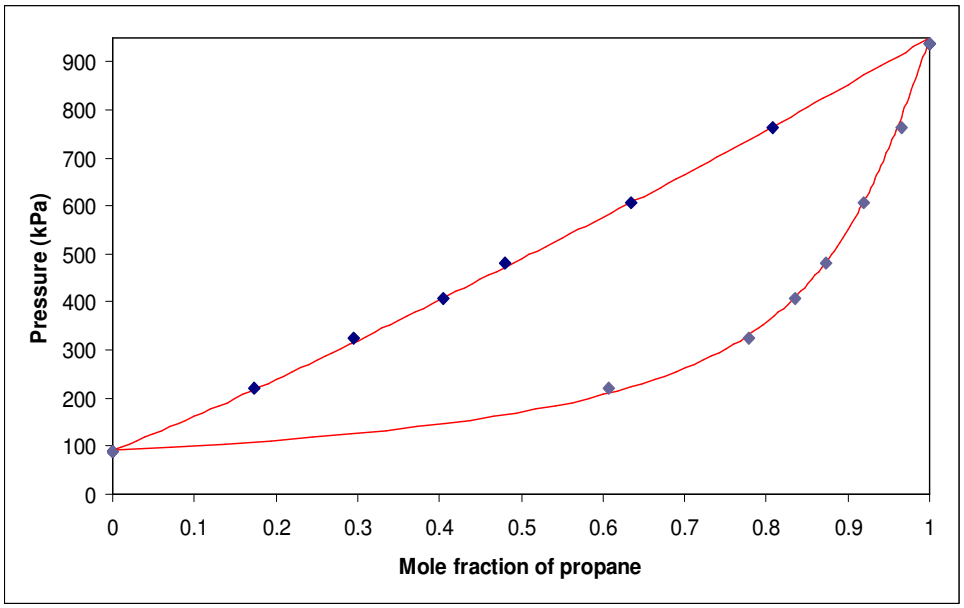

Figure 8-3: Comparison of experimental data (•) for the propane (1) + isopentane (2) system at 25 ºC to the P-x-y diagram generated via the PR-MC-WSMR(NRTL) model (–).

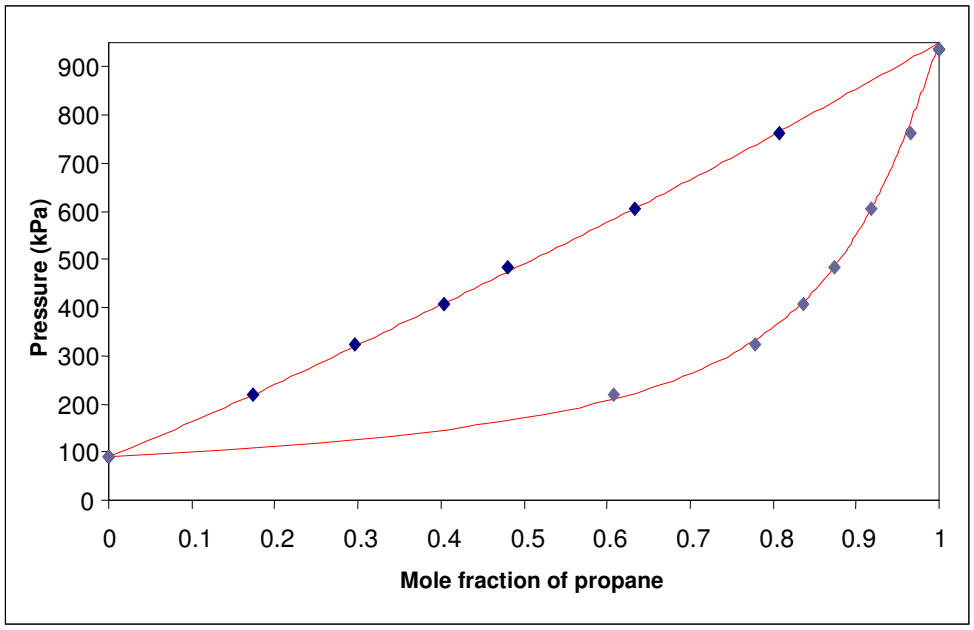

Figure 8-4: Comparison of experimental data (•) for the propane (1) + isopentane (2) system at 25 °C to the P-x-y diagram generated via the SRK-MC-WSMR(NRTL) model (–).

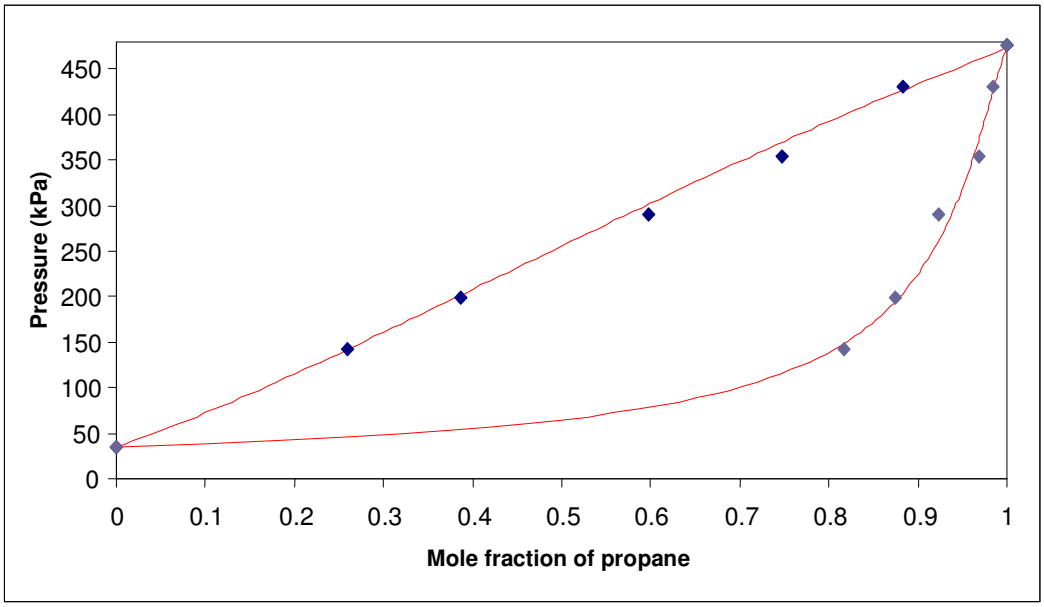

Figure 8-5: Comparison of experimental data (•) for the propane (1) + isopentane (2) system at 0 °C to the P-x-y diagram generated via the PR-MC-WSMR(NRTL) model (–).

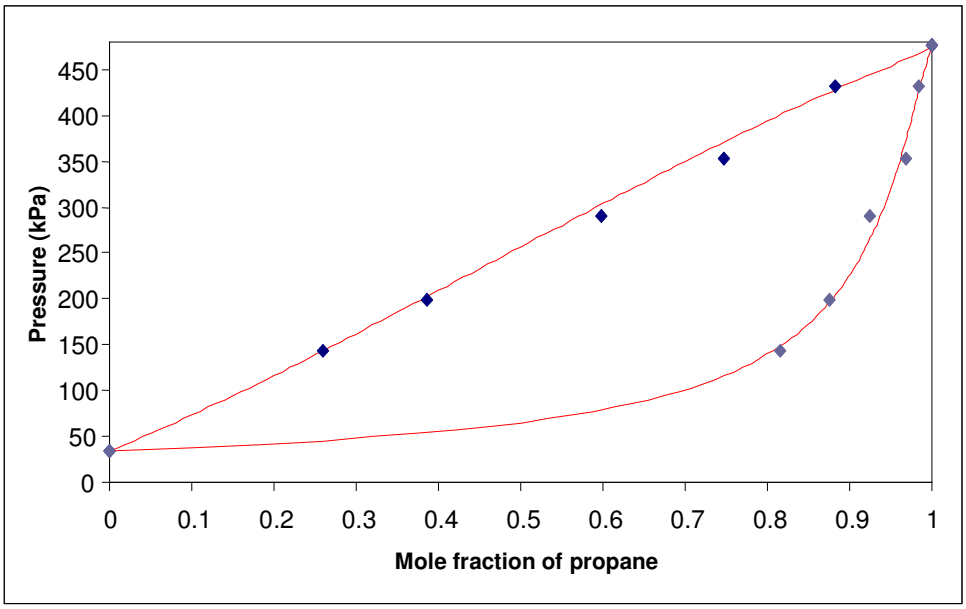

Figure 8-6: Comparison of experimental data (•) for the propane (1) + isopentane (2) system at 0 ºC to the P-x-y diagram generated via the SRK-MC-WSMR(NRTL) model (–).

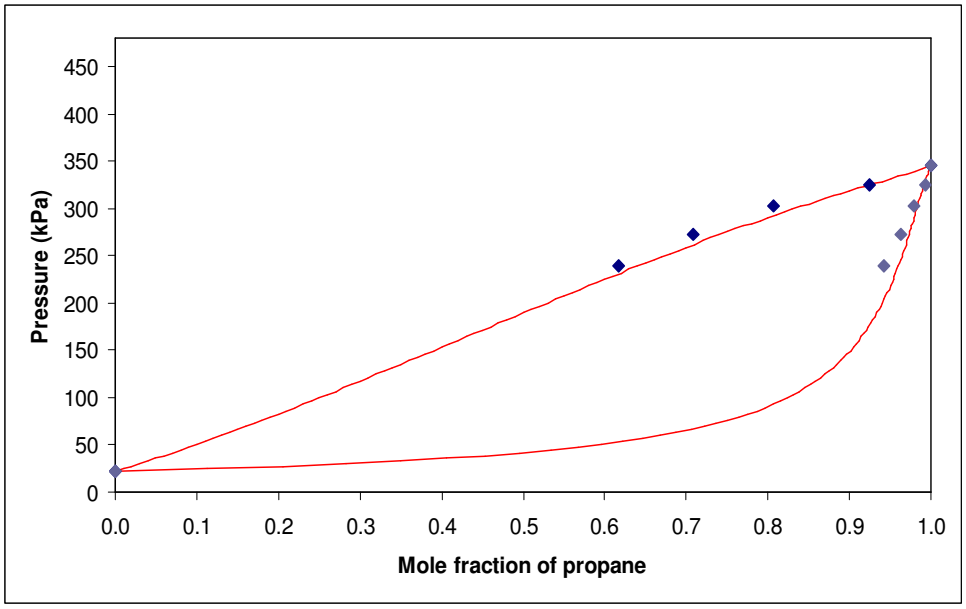

Figure 8-7: Comparison of experimental data (•) for the propane (1) + isopentane (2) system at -10 ºC to the P-x-y diagram generated via the PR-MC-WSMR(NRTL) model (–).

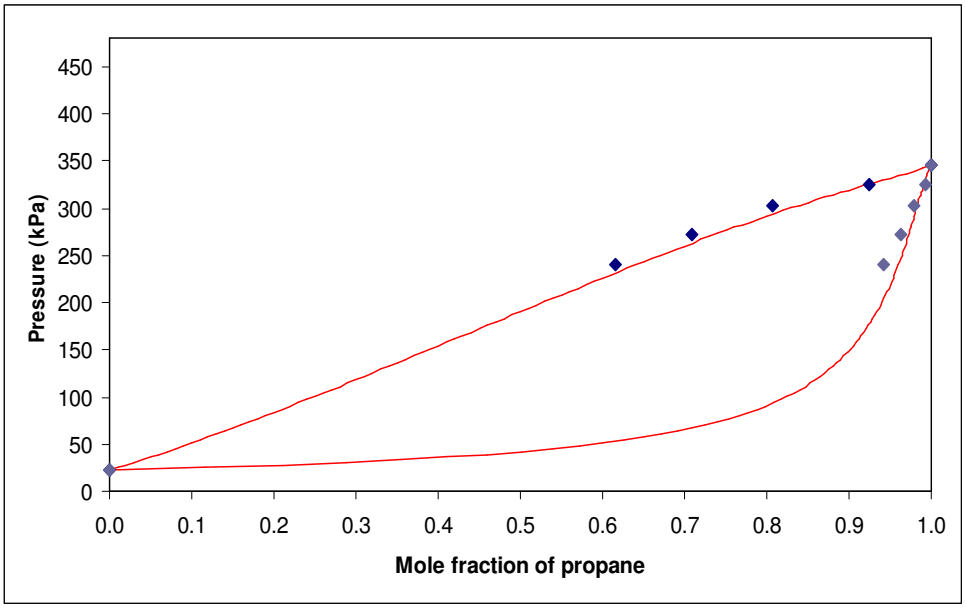

Figure 8-8: Comparison of experimental data (•) for the propane (1) + isopentane (2) system at -10 °C to the P-x-y diagram generated via the SRK-MC-WSMR(NRTL) model (–).

Table 8-13: Calculated deviations for the bubble point pressure and the propane vapour composition when comparing the calculated data derived via the PR-MC-WSMR(NRTL) and the SRK-MC-WSMR(NRTL) to the experimental VLE data for the propane (1) + isopentane (2) system at 25 °C.

Thermodynamic Model	**PR-MC-WSMR(NRTL)**	**SRK-MC-WSMR(NRTL)**
$AAD(\Delta P\%)$	1.2327	1.0008
$Bias(\Delta P\%)$	0.3488	-0.0956
$AAD(\Delta y)$	0.0046	0.0047
$Bias(\Delta y)$	-0.0020	-0.0013

Table 8-14: Calculated deviations for the bubble point pressure and the propane vapour composition when comparing the calculated data derived via the PR-MC-WSMR(NRTL) and the SRK-MC-WSMR(NRTL) to the experimental VLE data for the propane (1) + isopentane (2) system at 0 ºC

Thermodynamic Model	**PR-MC-WSMR(NRTL)**	**SRK-MC-WSMR(NRTL)**
$AAD(\Delta P\%)$	1.9775	2.1904
$Bias(\Delta P\%)$	1.460	1.7863
$AAD(\Delta y)$	0.0056	0.0054
$Bias(\Delta y)$	0.0022	0.0025

Table 8-15: Calculated deviations for the bubble point pressure and the propane vapour composition when comparing the calculated data derived via the PR-MC-WSMR(NRTL) and the SRK-MC-WSMR(NRTL) to the experimental VLE data for the propane (1) + isopentane (2) system at -10 ºC

Thermodynamic Model	**PR-MC-WSMR(NRTL)**	**SRK-MC-WSMR(NRTL)**
$AAD(\Delta P\%)$	3.5681	3.5111
$Bias(\Delta P\%)$	3.4319	3.0533
$AAD(\Delta y)$	0.0019	0.0033
$Bias(\Delta y)$	0.0014	0.0027

8.2 Difficulties encountered during experimentation

Inherent problems in the vapour recirculation apparatus of Moodley [2002] used in this study warranted a redesign of certain components of the original equipment to enable achievement of desired operating conditions. Some of the difficulties encountered during the equipment re-development and experimental stages are discussed in the subsequent chapter.

8.2.1 Obtaining low temperatures and isothermal conditions in the equilibrium cell

Major barriers were encountered in achieving the desired low temperatures in the equipment of Moodley [2002]. It was for this reason that the cooling circuit was redesigned to enable the attainment of stable isothermal conditions at low temperatures. Major problems

accounting for the inability of the equipment of Moodley [2002] to achieve low stable temperatures included the poor sealing of the equipment cooling circuit thus resulting in the loss of cooling gas (nitrogen) and consequently resulting in lower operating pressure limit at which the cooling circuit could be operated, hence a reduced heat transfer rate. The thermostat was redesigned with stainless steel chosen as the preferred material of construction as opposed to the original Pyrex borosilicate thermostat. This redesign totally eliminated leaks in the system thus eliminating the loss of cooling medium from the system and enabling operation of the cooling circuit at a higher pressure resulting in an improvement of heat transfer. The annular space of the thermostat which upon evacuation provided insulation of the thermostat contents was increased in volume by increasing the distance between the inner and outer thermostat walls thus improving thermal insulation. Improved vacuum fittings with valves on the new stainless steel setup increased the magnitude of the vacuum that could be pulled in the annular space improving insulation and also provided a leak tight annular space preventing the decline in insulation with time experienced on the Pyrex thermostat due to loss of vacuum with time due to leaks. Attaining of a stable low temperature environment over extended periods was another problem experienced. This was due to the high heat generated by the nitrogen recirculation pump resulting in heating of the cooling nitrogen gas medium and thus accelerated consumption of the dry-ice in the cooling bath resulting in a relatively rapid overall decline in cooling efficiency with time. The rapid consumption of dry-ice was significantly reduced through the introduction of a pre-cooler in the cooling circuit. A refrigeration unit immersed in a low-temperature bath used to cool the re-circulating nitrogen gas after passing through the heat generating nitrogen recirculation pump and just prior to passing through the dry-ice containing low-temperature bath. This unit greatly reduced the effects of the heat generating nitrogen recirculation pump and thus reduced consumption of dry-ice enabling a more stable operation at low-temperatures over extended periods.

8.2.2 Reliability of the vapour recirculation pump

The vapour recirculation pump of Moodley [2002] was used in the initial stages of the study, however when experimentation was carried out at pressures above 6 bar(a) over extended periods of more than 5-6 hours it was found that the pump sealing failed resulting in leaks and loss of vapour from the vapour recirculation loop. A leak tight environment was essential in order to ensure accurate experimentation. To eliminate this problem the pump of Moodley [2002] was modified with a major focus placed on changes to the sealing arrangement along the pump head where the leaking problem was evident. The piston in the

pump head was modified with the neoprene seals and Teflon guide rods being replaced by new pistons each made up of a cylindrical solid steel billet with three lubricated Viton o-rings spaced evenly along the length of the piston. These modifications of the pump enabled a reliable operation over extended periods at pressures tested up to 11 bar(a).

8.2.3 Leaks in the vapour recirculation loop

Due to the re-use of many old spare fittings and the nature of the design of numerous components, leaks in the vapour recirculation loop were a common problem encountered. As a leak free system was essential for accurate experimentation the system was tested for leaks on a regular basis. Leaks were generally repaired through retightening of the fittings and application of Loctite with the system under vacuum. In situations where leaks could not be eliminated fittings were replaced. Leaks occurring during experimentation could be detected by monitoring for any abnormal fluctuations in the system pressure. Upon detection of any leaks experimentation would be ceased and the leak fixing process would be followed. The high frequency of leaks developing accounted for a large portion of time lost during experimentation.

8.2.4 Setting the vapour recirculation rate

Modifications to the vapour recirculation pump resulted in the need to re-set the vapour recirculation flow rate to optimise contact between the liquid and vapour phases in the equilibrium cell and aid the attainment of chemical equilibrium. Too low a flow rate would not provide sufficient agitation of the equilibrium cell contents to promote the attainment of chemical equilibrium while a high flow rate would result in liquid entrainment in the re-circulating vapour phase. A too high flow would also result in insufficient time for the heat exchange system to cool the re-circulating vapour exiting the heated external vapour re-circulation loop down to the equilibrium cell temperature thus preventing thermodynamic equilibrium from being achieved. Time was spent setting the vapour recirculation rate through monitoring of the vapour as it passed through the equilibrium cell to detect insufficient bubbling and agitation or excessive bubbling and thus liquid entrainment. The flow was set at what was deemed to be an acceptable balance between the two extremes. Further checks were done to determine if sufficient cooling of the returning vapour was being achieved. Checks were done by re-circulating the vapour at a controlled temperature set-point over a period then terminating the vapour flow rate. If there was insufficient

cooling of the re-circulating vapour phase a temperature drop would take place in the equilibrium cell after stopping the flow. The flow rate was thereafter reduced, while still maintaining sufficient agitation, to minimise the temperature drop upon termination of flow and thus indicate sufficient cooling of the re-circulating vapour phase. A maximum temperature drop of around 0.2 °C was considered to be acceptable with the temperature returning to the equilibrium temperature a short while after termination of the vapour re-circulation.

8.2.5 Sampling and analysis

Sampling, as reported in literature, often provides a major challenge during HPVLE measurements. In this study producing consistent and reproducible results was a major challenge and significant time was spent perfecting the sampling to produce consistent results. Often during test system data acquisition experiments had to be repeated to produce results which agreed with the reported literature data. The main errors in the data were determined to be a result of the sampling techniques employed. It was found that the sampling procedure had to be followed in the exact sequence as described in Section 5.2.4 and any deviation from this resulted in error and the need to clean out the system totally and start the data point measurement from initial stage of charging of the equilibrium cell. Error was also introduced if the equilibrium cell contents were left to stand for some time and experimentation resumed after this. These errors were possibly attributed to the collection of non-equilibrium material in the stagnant sample region of the equilibrium cell, but the problem cannot be fully explained as it is presumed that the equilibrium should be re-attainable and the sample corrected if the system was allowed to re-equilibrate but this however was not the case in this study. To ensure reproducible results, as mentioned earlier the data point measurement was started from scratch. These were the main uncertainties experienced during the experimentation and are possibly the main reason for the relatively poor agreement of the regressed data with the experimental data of the Propane + Isopentane system at -10°C and owing to time constraints and limited availability of chemicals these errors were evident and not corrected in the reported data.

CHAPTER 9

CONCLUSION

The vapour recirculation apparatus of Moodley [2002] was modified, reconstructed and commissioned in order for it to achieve a wider range of operating conditions for isothermal high-pressure vapour-liquid equilibrium (HPVLE) measurements at low temperatures. The modified equipment saw an improvement in the operating limits with the minimum attainable temperature improving from -5°C to -30°C, while the maximum attainable pressure improved from 6.9 bar(a) to 10.0 bar(a) in the modified equipment. The equipment was thereafter used in the acquisition of pure-component vapour pressures and binary HPVLE data. Experimental data obtained was thereafter regressed via the direct method to obtain mathematical models to describe the binary systems investigated.

9.1 Equipment modifications

Major modifications were carried out on the equipment cooling circuit to enable lower temperatures to be achieved. The Pyrex thermostat was discarded and replaced by a newly designed stainless steel thermostat. The new thermostat was a major improvement from the old thermostat, as it eliminated leaks, a major problem with the old thermostat and it provided better insulation due to a wider annular space which could have a stronger more consistent vacuum applied to it due to better sealing. Other improvements in the cooling circuit involved the addition of a pre-cooler, a piece of line immersed in a low temperature ethylene/glycol mixture bath cooled by a refrigeration unit. The pre-cooler acted as a heat sink removing the heat generated by the nitrogen recirculation pump from the cooling circuit and thus minimizing the consumption of dry-ice during operation. These modifications of the cooling circuit enabled the equipment to achieve temperatures down to -30°C. Lower temperatures were not attempted due to temperature limits of sealing equipment used in the equilibrium cell.

Limiting factors in achieving high pressures included the maximum pressure rating on the pressure transducer and the pressure limits of the vapour recirculation pump which failed due to leaks when operated at high pressures over extended periods. The pressure transducer was replaced with a new transducer with a higher pressure rating and the vapour recirculation pump was modified. Modifications to the pump focused on re-designing the problematic sealing arrangement on the pump heads. These modifications enabled the equipment to be

operated at pressures up to 10 bar(a) over extended periods thus improving the overall operating limits of the equipment.

9.2 Experimental measurements

To display the operating limit capabilities of the equipment vapour pressure measurements were performed on isopentane at temperatures between -14 and +27.9 °C and pressures up to 10.1 bar and on propane at temperatures between -30.1 and +26.0 °C and pressures up to 9.7 bar. The isopentane vapour-pressure measurements had an average deviation of ± 0.49 % when compared to literature data while the propane vapour-measurements had a maximum average deviation of ± 0.35 % when compared to literature data indicating the good reliability of the equipment in attaining accurate pure-component vapour-pressures in the temperature and pressure range investigated in this study.

Binary HPVLE measurements were thereafter performed on the Propane + 1-Propanol system at 19.9 °C. Problems were experienced during the acquisition of this data due to experimental procedure and other inherent problems in the system, but a full set of binary HPVLE data for the system that compared relatively well with literature data was eventually measured. To improve the experimental techniques and procedure and gain more confidence, measurements were performed on an additional test system, propane + isopentane. Measurements were performed at the 25°C and 0°C isotherms and data acquired compared well with literature data. There was however some inherent problems in the equipment which often affected results obtained thus preventing full confidence in the equipments ability to measure binary HPVLE data to be achieved. The main problem was the consistency of results obtained. The equipment was however thereafter used to measure a new set of HPVLE data for the propane + isopentane system at -10°C. A full understanding of the problems experienced in the binary system measurements was not gained owing to time constraints and chemical availability. More time is required to fully understand the problems experienced and thus implement corrective measures to eliminate these problems.

9.3 Data regression

The experimental data obtained was thereafter modeled via the direct method. Models investigated included modified forms of the Peng-Robinson and Soave-Redlich Kwong equations of state as modified through incorporation of the Mathias-Copeman alpha function. The modified EOS's provided a good representation of the pure-component vapour-pressure data measured. These modified equations of state were thereafter extended

to mixtures through incorporation of the Wong-Sandler mixing rule together with the NRTL local composition model as the chosen activity coefficient model used to calculate the Gibbs energy. Both models investigated gave a fairly good representation of the binary systems investigated at all isotherms except for new data of the propane + isopentane system at the -10°C isotherm where the relatively poor representation is possibly due to the small number of data points measured for the system and predominantly due to the experimental error experienced during the HPVLE measurements on the equipment.

CHAPTER 10

RECOMMENDATIONS

The performance of the equipment showed a number of inconsistencies in the acquisition of the binary HPVLE data. This was noted as a number of repeat binary measurements had to be performed to improve accuracy of results on test systems. These inconsistencies are identified as a result of both the experimental techniques as well as inherent problems in the equipment. Owing to time constraints and availability of chemicals these problems could not be entirely studied and fully understood. A number of issues which need to be further investigated are listed as follows:

- Calibration of the pressure transducer needs to be carried out against a standard for any future measurements. As no pressure standard was available pressure calibration was carried out via a correction applied to vapour pressure measurements on a pure component. This increases the degree of uncertainty in the pressure measurements.
- The Eurotherm 2204 controller which provided a 3-digit display of the equilibrium cell temperature measurement needs to be replaced with a temperature controller providing a minimum of a 4-digit display. This should be implemented to improve the accuracy of temperature measurements.
- Methods and the sequence of charging the equilibrium cell during binary HPVLE measurements needs to be further investigated as this provided a possible source of inconsistencies during the binary HPVLE measurements. The conditions of charging during experimentation at temperatures below 10ºC can be challenging due to the reaction of the chemicals when introduced into the equilibrium cell. The temperature rise associated with the introduction of a gas into the system often leads to flashing of vapour which can result in overcharging of the equilibrium cell. At the same time if charging the equilibrium cell is terminated before saturation of the liquid phase this results in insufficient addition of the gas. Alternate methods of charging the equilibrium cell may provide some improvement over the method employed during this study.
- Methods of accurately controlling the vapour recirculation rate to ensure that it is sufficiently cooled via the heat exchange system before re-introduction into the equilibrium cell needs to be investigated. At lower temperatures this is critical to eliminate temperature disturbances to the equilibrium cell.
- Liquid sampling perhaps provided the biggest source of uncertainty during experimentation. The inherent dead volume in the liquid sampling section of the equilibrium cell and the disturbance to equilibrium during liquid sampling need some

attention. Alternate methods of liquid sampling need to be investigated to improve accuracy and repeatability of results.

BIBLIOGRAPHY

Abdel-Ghani, R.M.& Heidemann, R.A., (1996). Comparison of ΔG excess mixing rules for multi-phase equilibria in some ternary systems. *Fluid Phase Equilibria*, 116: 495-502.

Abildskov, J., Gani, R., Rasmussen, P. & O'Connell, J.P., (1999). Beyond basic UNIFAC. *Fluid Phase Equilibria*, 158-160: 349-356.

Abovsky, V. & Watanasiri, S., (1999). Equation of state mixing rule based on activity coefficient model: explicit solution for 'finite pressure approach'. *Fluid Phase Equilibria*, 158-160: 259-269.

Abrams, D. S. & Prausnitz, J.M. (1975). "Statistical Thermodynamics of Liquid Mixtures: A New Expression for the Excess Gibbs Energy of Partly or Completely Miscible Systems," *AIChE J.,* 21: 116-128.

Adachi, Y., Lu, B.C.-Y. & Sugie, H., (1983). A four-parameter equation of state. *Fluid Phase Equilibria*, 11: 29-48.

Adachi, Y., Sugie, H. & Lu, B.C.-Y., (1983). Development of a five-parameter cubic equation of state. *Fluid Phase Equilibria*, 28: 119-136.

Adachi, Y., Lu, B.C.-Y. & Sugie, H., (1983). Three-parameter equations of state. *Fluid Phase Equilibria*, 13: 133-142.

Adachi, Y. & Sugie, H., (1985). A new mixing rule–modified conventional mixing rule. *Fluid Phase Equilibria*, 28: 103-118.

Adachi, Y. & Sugie, H., (1985). Effects of mixing rules on phase equilibrium calculations. *Fluid Phase Equilibria*, 24: 353-362.

Aroyan, H. J. & Katz, D.L. (1951). "Low-Temperature Vapour-Liquid Equilibria in Hydrogen-n-Butane System," *Ind. Eng. Chem.,* 43: 185-189.

Ashcroft, S., Shean, R. & Williams, C. (1983). "A Visual Equilibrium Cell for Multiphase Systems at Pressures up to 690 bar," *Chem. Eng. Res. Des.,* 61: 51-55.

Battino, R., Banzhof, M. Bogan, M. & Wilhelm, E. (1971). "Apparatus for Rapid Degassing of Liquids, Part III," *Analytical Chemistry,* 43: 806-807.

Behrens, P.K. & Sandler, S.I. (1983). "Vapour-Liquid Equilibria for the Carbon Dioxide-1-Butene System at 37.7 and 45.0˚C," *J. Chem. Eng. Data,* 28: 52-56.

Benmekki, E.H. & Mansoori, G.A., (1987). Phase equilibrium calculations of highly polar systems. *Fluid Phase Equilibria*, 32: 139-149.

Besserer, G. & Robinson, D.B. (1971). "A High Pressure Autocollimating Refractometer for Determining Coexisting Liquid and Vapour Phase Densities," *Can. J. Chem. Eng.,* 49: 651-656.

Bobbo, S., Stryjek, R., Elvassore, N. & Bertucco, A., (1998). A recirculation apparatus for vapor-liquid equilibrium measurements of refrigerants. Binary mixtures of R600a, R134a and R236fa. *Fluid Phase Equilibria*, 150-151: 343-352.

Bobbo, S., Camporese, R. & Stryjek, R., (1999). High-pressure vapor-liquid equilibrium of binary systems with R236fa. Fluid Phase Equilibria, 161: 305-313.

Boublik, T. (1981). "Statistical Thermodynamics of Nonspherical Molecule Fluids," *Ber. Bunsenges. Phys. Chem.,* 85: 1038-1041

Boukouvalas, C., Spiliotis, N., Coutsikos, P., Tzouvaras, N. & Tassios, D., (1994). Prediction of vapor-liquid equilibrium with LCVM model: a linear combination of the Vidal and Michelsen mixing rules coupled with the original UNIFAC and the t-mPR equation of state. *Fluid Phase Equilibria*, 92: 75-106.

Bradshaw, S. M. (1985). MscEng Thesis: *A Static Equilibrium Cell for High Pressure and Temperature Vapour-Liquid Equilibrium Measurement,* Department of Chemical Engineering, University of Natal, Durban, South Africa.

Brunner, G., Steffen, A. & Dohrn, R. (1993). "High Pressure Liquid-Liquid Equilibria in Ternary Systems Containing Water, Benzene, Toluene, n-Hexane and n-Hexadecane," *Fluid Phase Equilibria,* 82: 165-172.

Cabezas, J.L., Beltran, S. & Coca, J., (1991). Isobaric vapor-liquid equilibrium data for furfural with chlorinated hydrocarbons. *Fluid Phase Equilibria*, 62: 163-172.

Calado. J. C. G., Dieters, U. Street, W.B. (1981). "liquid-Vapour Equilibrium in the Krypton + Methane System," *J. Chem. Soc. Faraday Trans. I,* 77: 2503-2513.

Carnahan, N. F. and Starling, K. E. (1969), "Equation of State for Nonattracting Rigid Spheres", *J. Chem. Phys.* 51, 635-636.

Cebola, M.J., Saville, G. & Wakeham, W.A., (1998). Vapor—liquid equilibrium in the ternary system methane-n-hexane-n-tetradecane. Fluid Phase Equilibria, 150-151: 703-711.

Chang, E., Calado, J.C.G. & Streett, W.B., (1982). vapor-liquid equilibrium in the system dimethyl ether/methanol from 0 to 180˚C and at pressures to 6.7 MPa. *J. Chem. Eng. Data,* 27: 293-298.

Chang, H. L., Hurt, L. J. & Kobayashi, R. (1966). "Vapour-Liquid Equilibria of Light Hydrocarbons at Low temperatures and High Pressures: The Methane-n-Heptane System," *AIChE J.,* 12: 1212-1216.

Chang, S.-D. & Lu, B.C.-Y. (1967). "vapour-Liquid Equilibria in the Nitrogen-Methane-Ethane System," *Chem. Eng. Progr. Symp. Ser.,* 63: 18-27.

Charoensombut-amon, T., Martin, R.J. & Kobayashi, R., (1986). Application of a generalized multiproperty apparatus to measure phase equilibrium and vapor phase densities of supercritical carbon dioxide in n-hexadecane systems up to 26 Mpa. *Fluid Phase Equilibria*, 31: 89-104.

Chen, A.-Q., Urbanus, G.J. & Chao, K.-C., (1994). A new vapor-liquid equilibrium cell and VLE data for mixtures of 1-propanol + p-xylene. *Fluid Phase Equilibria,* 94: 281-288.

Chou, G.F., Forbert, R.R. & Prausnitz, J.M., (1990). High pressure vapor-liquid equilibria for CO_2/n-decane, CO_2/tetralin, and CO_2/n-decane/tetralin at 71.1 and 104.4˚C. *J. Chem. Eng. Data,* 35: 26-29.

Collie, N. (1889). "Note on Fluoride of Methyl," *Journ. Chem. Soc.,* 55: 110-113.

Coquelet, C., Chareton, A., Valtz, A., Baba-Ahmed, A. & Richon, D., (2003). " Vapour-Liquid Equilibrium Data for thr Azeotropic Difluoromethane + Propane System at Temperatures from 294.83 to 343.26 K and Pressures up to 5.4 MPa. *J. Chem. Eng. Data,* 48: 317-323.

Coutsikos, P., Kalospiros, N.S. & Tassios, D.P. (1995). "Capabilities and Limitations of the Wong-Sandler Mixing Rules," *Fluid Phase Equilibria,* 108: 59-78.

Currier, R.P. & O'Connell, J.P., (1987). An analysis of the solution of groups method for component activity coefficients. *Fluid Phase Equilibria*, 33: 245-265.

Danesh, A. & Todd, C. (1990). "a Novel Sampling Method For Compositional Analysis of High Pressure Fluids," *Fluid Phase Equilibria,* 57: 161-171.

Daubert, T.E. & Danner, R.P. (1993). *Physical and Thermodynamic Properties of Pure Compounds: Data Compilation,* Design Institute for Physical Property Data, AIChE, Taylor & Francis, Washington.

Deiters, U.K., (1987). Density-dependent mixing rules for the calculation of fluid phase equilibria at high pressures. *Fluid Phase Equilibria*, 33: 267-293.

Deiters, U.K. & Schneider, G.M. (1986). "High Pressure Phase Equilibria: Experimental Methods," *Fluid Phase Equilibria,* 29: 145-160.

Dimitrelis, D. & Prausnitz, J.M., (1986). Comparison of two hard-sphere reference systems of perturbation theories for mixtures. *Fluid Phase Equilibria*, 31: 1-21.

Dohnal, V. & Fenclova, D., (1985). A new procedure for consistency testing of binary vapor-liquid equilibrium data. *Fluid Phase Equilibria*, 21: 211-235.

Dorau, W., Kremer, H.W. & Knapp, H., (1983). An apparatus for the investigation of low-temperature, high-pressure, vapor-liquid and vapor-liquid-liquid equilibria. *Fluid Phase Equilibria*, 11: 83-89.

D'Souza, R. & Teja, A.S. (1988). "High-Pressure Phase Equilibria in the System Glucose + Fructose + Water + Ethanol + Carbon Dioxide." *Fluid Phase Equilibria,* 39: 211-224.

D'Souza, R., Patrick, J.R. & Teja, A.S. (1988). "High Pressure Phase Equilibria in the Carbon Dioxide-n-Hexadecane and Cabon Dioxide-Water Systems," *Can. J. Chem. Eng.,* 66: 319-323.

Eckert, C.A. & Prausnitz, J.M. (1965). "Phase Equilibria for Strongly Nonideal Liquid Mixtures at Low Temperatures," *AIChE J.,* 11: 886-890.

Elliot, D.G., Chen, R.J.J., Chappelaar, P.S. & Kobayashi, R. (1974). "Vapour-Liquid Equilibrium of Methane-n-Butane System at Low Temperatures and High Pressures," *J. Chem. Eng. Data,* 19: 71-77.

Figuiere, P., Horn, J., Laugier, S., Renon, H., Richon, D. & Szwarc, H. (1980). "Vapour-Liquid Equilibria up to 40000 kPa and 400˚C: A New Static Method," *AIChE J.,* 26: 872-875.

Fink, S.D. & Hershey, H.C., (1990). Modeling the Vapour-Liquid Equilibria of 1,1,1-Trichloroethane + Carbon Dioxide and Toluene + Carbon Dioxide at 308, 323, and 353 K. *Ind. Eng. Chem. Res.* 29: 295-306.

Fredenslund, A., Mollerup, J. & Christiansen, L.J., (1973). An apparatus for accurate determination of vapour-liquid equilibrium properties and gas PVT properties. *Cryogenics,* 414-419.

Fredenslund, A. & Sather, G.A., (1970).Gas-liquid equilibrium of the oxygen-carbon dioxide system. *J. Chem. Eng. Data,* 15: 17-22

Freitag, N.P. & Robinson, D.B., (1986). Equilibrium phase properties of the hydrogen-methane-carbon dioxide, hydrogen-carbon dioxide-n-pentane and hydrogen-n-pentane systems. *Fluid Phase Equilibria*, 31: 183-201.

Fuller, G. G. (1976), "A modifed Redlich-Kwong-Soave equation of state capable of representing the liquid phase", *Ind. Eng. Chem. Fund*. 15, 254-257.

Grauso, L., Fredenslund, A. & Mollerup, J., (1977). Vapour-liquid equilibrium data for the systems $C_2H_6 + N_2$, $C_2H_4 + N_2$, $C_3H_8 + N_2$, and $C_3H_6 + N_2$. *Fluid Phase Equilibria,* 1: 13-26.

Griswold, J., Andres, D. & Klein, V.A., (1943). Determination of High-Pressure Vapour-Liquid Equilibrium. *Petr. Refiner,* 22: 99-106.

Guggenheim, E.A. (1965). "Variations on van der Waals' Equation of State for High Densities," *Mol. Phys.,* 9: 199.

Gupte, P.A. & Daubert, T.E., (1986). Extension of UNIFAC to high pressure VLE using Vidal mixing rules. *Fluid Phase Equilibria*, 28: 155-170.

Harmens, A. & Knapp, H. (1980). "Three-Parameter Cubic Equation of State for Normal Substances," *Ind. Eng. Chem. Fundam.,* 19: 291-294.

Heintz, A. & Streett, W.B. (1983). "Phase Equilibria in the H_2/C_2H_4 System at Temperatures from 114.1 to 247.1 K and Pressures to 600 MPa," *Ber. Bunsenges. Phys. Chem.,* 87: 298-303.

Herring, R.N. & Barrick, P.L. (1965). "Gas-Liquid Equilibrium Solubilities for the Helium-Oxygen System," *Adv. Cryog. Eng.,* 10: 151-159.

Huang, S.S.S., Leu, A.D., Ng, H.J. & Robinson, D.D. (1985). "The Phase Behaviour of Two Mixtures of Merhane, Carbon Dioxide, Hydrogen Sulphide, and Water," *Fluid Phase Equilibria,* 19: 21-32.

Houzelle, C., Legret, D., Richon, D. & Renon, H., (1983). Vapour-liquid equilibria of corrosive components using a dynamic method: a new flow apparatus. *Fluid Phase Equilibria*, 11: 179-185.

Hsu, J.J.-C., Nagarajan, N. & Robinson, R.L., Jr., (1985). Equilibrium Phase Compositions, Phase Densities, and Interfacial Tensions for CO_2 + Hydrocarbon Systems. 1. CO_2 + n-Butane. *J. Chem. Eng. Data,* 30: 485-491.

Inglis, J.K.H. (1906). "The Isothermal Distillation of Nitrogen and Oxygen and of Argon and Oxygen," *Philos. Mag.,* 11: 640-658.

Inomata, H., Tuchiya, K., Arai, K. & Saito, S (1988). "Vapour-Liquid Equilibria for the Ammonia-Methanol-Water System," *J. Chem. Eng. Data,* 33: 26-29.

Jennings, D.W. &Teja, A.S. (1989). "Vapour-Liquid Equilibria in the Carbon Dioxide-1-Hexene and Carbon Dioxide-1-Hexyne Systems," *J. Chem. Eng. Data,* 34: 304-309.

Jin, Z.-L., Liu, K.-Y. & Sheng, W.-W. (1993). "Vapour-Liquid Equilibrium in Binary and Ternary Mixtures of Ntrogen, Argon, and Methane," *J. Chem. Eng. Data,* 38: 353-355.

Jou, F.-Y., Deshmukh, R.D., Otto, F.D. & Mather, A.E., (1987). Vapor-liquid equilibria for acid gases and lower alkanes in triethylene glycol. *Fluid Phase Equilibria*, 36: 121-140.

Kalra, H. & Robinson, D.B. (1975). "An Apparatus for the Simultaneous Measurement of Equilibrium Phase Compositions and Refractive Index Data at Low temperatures and High Pressures," *Cryogenics,* 15: 409-412.

Kaminishi, G., Takano, S., Yokoyama, C. & Takahashi, S., (1989). Concentration of triethylene glycol, diethylene glycol and ethylene glycol in supercritical carbon dioxide up to 16 Mpa at 313.15 and 333.15K. *Fluid Phase Equilibria*, 52: 365-372.

Kalra, H., Kubota, H., Robinson, D. & Ng, H. (1978). "Equilibrium Phase Properties of the Carbon Dioxide-n-Heptane System," *J.Chem. Eng. Data*, 23: 317-321.

Katayama , T., Ohgaki, K., Maekawa, G., Goto, M. & Nagano, T., (1975). Isothermal vapor-liquid equilibria of acetone-carbon dioxide and methanol-carbon dioxide systems at high pressures. *J. Chem. Eng. Of Japan,* 8: 89-92.

Kim, C.-H., Vimalchand, P. & Donohue, M.D., (1986). Vapor-liquid equilibria for binary mixtures of carbon dioxide with benzene, toluene and p-xylene. *Fluid Phase Equilibria*, 31: 299-311.

Klink, A., Cheh, H. & Amich, E., Jr. (1975). "The Vapour-Liquid Equilibrium of the Hydrogen-n-Butane System at Elevated Pressures," *AIChE J.,* 21: 1142-1148.

Kubic, W.L., Jr. & Stein, F.P., (1981). An experimental and correlative study of the vapor-liquid equilibria of the tetrafluoromethane-chlorotrifluoromethane system. *Fluid Phase Equilibria*, 5: 289-304.

Kubota, H., Inatome, H., Tanaka, Y., & Makita, T., (1983). Vapour-Liquid Equilibria of the Ethylene-Propylene System Under High Pressure. *J. Chem. Eng. Of Japan,* 16: 99-103.

Kobayashi, R. & Katz, D. (1953). "Vapour-Liquid Equilibria for Binary Hydrocarbon-Water Systems," *Ind. Eng. Chem.,* 45: 440-451.

Konrad, R., Swaid, I. & Schneider, G.M., (1983). High-pressure phase studies on fluid mixtures of low-volatile organic substances with supercritical carbon dioxide. *Fluid Phase Equilibria*, 10: 307-314.

Legret, D., Richon, D. & Renon, H. (1980). "Static Still for Measuring Vapour-Liquid Equilibria up to 50 bar," *Ind. Eng. Chem. Fundam.,* 19: 122-126.

Legret, D., Richon, D. & Renon, H. (1981). "vapour-Liquid Equilibria up to 100 MPa: A New Apparatus," *AIChE J.,* 27: 203-207.

Li, J., Chen, C. & Wang, J., (2000). Vapor-liquid equilibrium data and their correlation for binary systems consisting of ethanol, 2-propanol, 1,2-ethanediol and methyl benzoate. *Fluid Phase Equilibria*, 169: 75-84.

Malanowski, S. & Anderko, A. (1992). *Modelling Phase Equilibria: Thermodynamic Backround and Practical Tools,* John Wiley & Sons, New York.

Mathias, P.M. & Copeman, T.W., (1983). Extension of the Peng-Robinson equation of state to complex mixtures: Evaluation of the various forms of the local composition concept. *Fluid Phase Equilibria*, 13: 91-108.

Mathias, P.M., Naheiri, T., & Oh, E.M. (1989). "A density correction for the Peng-Robinson equation of state," *Fluid Phase Equilibria,* 47: 77-87.

Matos, H.A., Azevedo, E.J.S.G., Simoes, P.C., Carrondo, M.T. & Nunes da Ponte, M. (1989). "Phase Equilibria of Natural Flavours and Supercritical Solvents," *Fluid Phase Equilibria,* 52: 357-364.

Melhem, G., Saini, R. & Goodwin, B. (1989). "A Modified Peng-Robinson Equation of State," *Fluid Phase Equilib*ria, 47: 189-237.

Miller, R.C., Kidnay, A.J. & Hiza, M.J. (1977). "Liquid + Vapour Equilibria in Methane + Ethene and in Methane + Ethane from 150.00 to 190.00 K," *J. Chem. Thermodynamics,* 9: 167-178.

Mohamed, R.S. & Holder, G.D., (1987). High pressure phase behaviour in systems containing CO_2 and heavier compounds with similar vapor pressures. *Fluid Phase Equilibria*, 32: 295-317.

Morris, W.O. & Donohue, M.D. (1985). "Vapour-Liquid Equilibria in Mixtures Containing Carbon Dioxide, Toluene, and 1-Methylnaphthalene," *J. Chem. Eng. Data,* 30: 259-263.

Moodley, K. (2002). PhD Thesis: *High-Pressure Vapour-Liquid Equilibrium Studies at Low Temperatures*, School of Chemical Engineering, University of Natal, Durban, South Africa.

Mraw, S.C., Hwang, S.-C. & Kobayashi, R. (1978). "Vapour-Liquid Equilibrium of the CH_4-CO_2 System at Low Temperatures," *J. Chem. Eng. Data,* 23: 135-139.

Mühlbauer, A.L.(1990). PhD Thesis: *Measurement and Thermodynamic Interpretation of High Pressure Vapour-Liquid Equilibrium Data,* Department of Chemical Engineering, University of Natal, Durban, South Africa.

Mühlbauer, A.L. & Raal, J.D. (1991). "Measurement and Thermodynamic Interpretation of High Pressure Vapour-Liquid Equilibria in the Toluene-CO_2 System," *Fluid Phase Equilibria,* 64: 213-236.

Mühlbauer, A.L. & Raal, J.D. (1995). "Computation and Thermodynamic Interpretation of High-Pressure Vapour-Liquid Equilibrium – A Review," *Chem. Eng. J.,* 60: 1-29.

Muirbrook, N.K. & Prausnitz, J.M. (1965). Multicomponent Vapour-Liquid Equilibria at High Pressures: Part 1. Experimental Study of the Nitrogen-Oxygen-Carbon Dioxide System at 0°C. *AIChE J.,* 11: 1092-1096.

Nagahama, K. (1996). "VLE Measurements at Elevated Pressures for Process Development," *Fluid Phase Equilibria,* 116: 361-372.

Nagahama, K., Suda, S., Hakuta, T. & Hirata, M. (1971). "Determination of Vapour-Liquid Equilibria from Total Pressure Measurement: C_3-Hydrocarbon-Solvent," *Sekuja Gakkai Shi,* 14: 252-256.

Nagahama, K., Konishi, H., Hoshino, D. & Hirata, M. (1974). "Binary Vapour-Liquid Equilibria of Carbon Dioxide-Light Hydrocarbons at Low Temperatures," *J. Chem. Eng. Japan,* 7: 323-328.

Nagata, I., (1985). Vapor-liquid equilibrium in ternary mixtures formed by ethanol, acetonitrile and benzene. *Fluid Phase Equilibria*, 19: 13-20.

Naidoo, P. (2004), *High-Pressure Vapour-Liquid Equilibrium Studies*, PhD thesis, Chemical Engineering University Of Kwa-Zulu Natal, Durban, South Africa

Nakayama, T., Sagara, H., Arai, K. & Saito, S. (1987). "High-Pressure Liquid-Liquid Equilibria for the system of Water, Ethanol, and 1,1-Difluoroethane at 323.2 K," *Fluid Phase Equilibria,* 38: 109-127.

Nasir, P., Martin, R.J. & Kobayashi, R. (1980/1981). "A Novel Apparatus for the Measurement of the Phase and Volumetric Behaviour at High Temperatures and Pressures and its Application to Study VLE in the Hydrogen-Tetralin System," *Fluid Phase Equilibria,* 5: 279-288.

Niesen, V., Palavra, A., Kidnay, A.J. & Yesavage, V.F., (1986). An apparatus for vapor-liquid equilibrium at elevated temperatures and pressures and selected results for the water-ethanol and methanol-ethanol systems. *Fluid Phase Equilibria*, 31: 283-298.

Orbey, H. & Sandler, S.I. (1995a). "Reformulation of Wong-Sandler Mixing Rule for Cubic Equations of State," *AIChE J.,* 41: 683-689.

Orbey, H. & Sandler, S.I. (1996a). "Analysis of Excess Free Energy Based Equation of State Models," *AIChE J.,* 42: 2327-2334.

Orbey, H. & Sandler, S.I. (1996b). "A Comparison of various cubic equation of state mixing rules for the simultaneous description of excess enthalpies and vapour-liquid equilibria," *Fluid Phase Equilibria,* 121: 67-83.

Orbey, H. & Sandler, S.I. (1997). "A Comparison of Huron-Vidal Type Mixing Rules of Mixtures of Compounds with Large Size Differences, and a New Mixing Rule," *Fluid Phase Equilibria,* 132: 1-14.

Orbey, H. & Vera, J.H. (1983). "Correlation for the Third Virial Coefficient Using T_c, P_c and ω as Parameters," *AIChE J.*, 29: 107-113.

Orbey, H. & Sandler, S.I. & Wong, D.S.H. (1993). "Accurate Equation of State Predictions at High Temperatures and Pressures Using the Existing UNIFAC Model," *Fluid Phase Equilibria,* 85: 41-54.

Peng, D. and Robinson, D. B. (1976), `A new two constant equation of state', *Ind. Eng. Chem. Fund.* 15, 59{64.

Pozo, M.E.& Streett, W.B., (1984). Fluid phase equilibria for the system dimethyl ether/water from 50 to 220˚C and pressures to 50.9 MPa . *J. Chem. Eng. Data,* 29: 324-329.

Prausnitz, J.M., (1985). Equations of state from Van der waals theory: The legacy of Otto Redlich. *Fluid Phase Equilibria*, 24: 63-76.

Price A.R. & Kobayashi, R., (1959). Low temperature vapor-liquid equilibrium in light hydrocarbon mixtures: Methane-ethane-propane system. *J. Chem. Eng. Data,* 4: 40-52.

Raal, J.D. (1992). "A New Volumetric Device for the Calibration of GC Detectors for Gas Mixtures," Pittsburgh Conference, New Orleans.

Raal, J.D. & Mühlbauer, A.L., (1994). "The Measurement of High Pressure Vapour-Liquid Equilibria," *Dev. Chem. Eng. Mineral Process.,* 2: 69-105.

Raal, J.D. & Mühlbauer, A.L., (1998). *Phase Equilibria: Measurement and Computation,* Taylor & Francis, Washington, D.C.

Ramjugernath, D. (2000). PhD Thesis: *High Pressure Phase Equilibrium Studies*, School of Chemical Engineering, University of Natal, Durban, South Africa.

Ramjugernath, D. & Raal, J.D. (1999). "Modelling, Prediction and Extrapolation of High Pressure Vapour-Liquid Equilibrium Data: Direct versus Combined Methods," *Proceedings of the International Conference Progress in Computing of Physicochemical Properties,* Warszawa, Poland, 308-322.

Ramjugernath, D., Valtz, A., Coquelet, C. & Richon, D. (2009). "Isothermal Vapour-Liquid Equilibrium Data for the Hexafluoroethane (R116) + Propane System at Temperatures from (263 to 323) K." *J. Chem. Eng. Data,* 54: 1292-1296.

Radosz, M., (1986). Vapour-Liquid Equilibrium for 2-Propanol and Carbon Dioxide. "*J. Chem. Eng. Data,* 31: 43-45.

Radosz, M., (1984). Variable-Volume Circulation Apparatus for Measuring High-Pressure Fluid-Phase Equilibria." *Ber. Bunsenges. Phys. Chem.,* 88: 859-862.

Redlich, O. & Kwong, J.N.S. (1949). "On the Thermodynamics of Solutions: V: An Equation of State. Fugacities of Gaseous Solutions," *Chem. Review,* 44: 233-244.

Reid, R.C., Prausnitz, J.M. & Poling, B.E. (1988). *The Properties of Gases & Liquids,* 4th ed., McGraw-Hill, New York.

Reiff, W., Peters-Gerth, P & Lucas, K., (1987). "A Static Equilibrium Apparatus for (Vapour + Liquid) Equilibrium Measurements at High Temperatures and Pressures. Results for (Methane + n-Pentane)," *J. Chem. Thermodynamics,* 19: 467-477.

Reiss, N. R., Frisch, H. L. and Lebowitz, J. L. L. (1959), "Statistical Mechanics of Rigid Spheres", *J. Chem. Phys*. 31: 369-380.

Renon, H. & Prausnitz, J.M. (1968). "Local Compositions in Thermodynamic Excess Functions for Liquid Mixtures," *AIChE J.,* 14: 135-144.

Rigas, T., Mason, D. & Thodos, G. (1958). "Vapour-Liquid Equilibria: Micro-sampling Technique Applied to a New Variable-Volume Cell," *Ind. Eng. Chem.,* 50: 1297-1300.

Rogers, B. & Prausnitz, J.M. (1970). "Sample-Extrusion Apparatus for High-Pressure Vapour-Liquid Equilibria," *Ind. Eng. Chem. Fundam.,* 9: 174-177.

Rousseaux, P., Richon, D. & Renon, H., (1983). A static method for determination of vapour-liquid equilibria and saturated liquid molar volumes at high pressures and temperatures using a new variable-volume cell. *Fluid Phase Equilibria*, 11: 153-168.

Rousseaux, P., Richon, D. & Renon, H., (1983). Volumetric properties of n-dodecane up to 423.1 K and 30.58 Mpa. *Fluid Phase Equilibria*, 11: 169-177.

Sadus, R. J. (1992), *High Pressure Phase Behaviour Of Multicomponent Fluid Mixtures,* Elsevier Science.

Sagara, H., Arai, Y. & Saito, S. (1972). "Vapour-Liquid Equilibria of Binary and Ternary Systems Containing Hydrogen and Light Hydrocarbons," *J. Chem. Eng. Jpn.,* 5: 339-348.

Sancho, N.K. (1998). MscEng Thesis: *Gas Chromatograph Calibration – A New Static Volumetric Device,* Department of Chemical Engineering, University of Natal, Durban, South Africa.

Schotte, W. (1980). "Collection of Phase Equilibrium Data for Separation Technology," *Ind. Eng. Chem. Process Des. Dev.,* 19: 432-439.

Schmidt, G. and Wenzel, H. (1980), "A modified Van der Waals equation of State", *Chem. Eng. Sci*. 35, 10503-1512.

Shah, N.N., Pozo de Fernandez, M.E., Zollweg, J.A. & Street, W.B., (1990). Vapor-liquid equilibrium in the system carbon dioxide + 2,2-dimethylpropane from 262 to 424 K at pressures to 8.4 MPa . *J. Chem. Eng. Data,* 35: 278-283.

Shibata, S.K. & Sandler, I.S. (1989). "High-Pressure Vapour-Liquid Equilibria Involving Mixtures of Nitrogen, Carbon Dioxide, and n-Butane," *J. Chem. Eng. Data,* 34: 291-298.

Smith, J.M., Van Ness, H.C. & Abbott, M.M. (1996). *Introduction to Chemical Engineering Thermodynamics,* 5th ed., McGraw-Hill, Singapore.

Soave, G. (1972). "Equilibrium Constants from a Modified Redlich-Kwong Equation of State," *Chem. Eng. Sci.,* 27: 1197-1203.

Soave, G. (1984). "Improvement of the van der Waals Equation of State," *Chem. Eng. Sci.,* 39: 357-369.

Soave, G., Bertucco, A. & Vecchiato, L. (1994). "Equation-of-State Group Contributions from Infinite-Dilution Activity Coefficients," *Ind. Eng. Chem. Res.,* 33: 975-980.

Soave, G., (1986). Direct calculation of pure-compound vapour pressures through cubic equations of state. *Fluid Phase Equilibria*, 31: 203-207.

Somait, F.A. & Kidnay, A.J., (1978). Liquid-vapor equilibria at 270K for systems containing nitrogen, methane, and carbon dioxide. *J. Chem. Eng. Data,* 23: 301-305.

Spencer, C.F. & Danner, R.P. (1972). "Improved Equation for Prediction of Saturated Liquid Density," *J. Chem. Eng. Data,* 17: 236-241.

Staby, A. & Mollerup, J. (1993). "Measurement of Mutual Solubilities of 1-Pentanol and Supercritical Carbon Dioxide," *J. Supercritical Fluids,* 6: 15-19.

Stead, K. & Williams, J.M., (1980). apparatus for studying phase equilibria. Phase equilibria of (carbon dioxide + 2,2-dimethylpropane) in the temperature range 220 to 300 K and at pressures up to 6.7 MPa. *J. Chem. Thermodynamics,* 12: 265-275.

Stein, F.P., Claitor, L.C. & Geist, J.M. (1962a). "A Study of the Phase Equilibria of the Hydrogen-Carbon Monoxide-Propane System at Low Temperatures," *Adv. Crog. Eng.,* 7: 106-113.

Stein, F.P. & Proust, P.C. (1971). "Vapour-Liquid Equilibria of the Trifluoromethane-Trifluorochloromethane System," *J. Chem. Eng. Data,* 16: 389-393.

Stein, F.P., Sterner, C.J. Geist, J.M. (1962b). "Vapour-Liquid Equilibrium Apparatus for Cryogenic Systems," *Chem. Eng. Progr.,* 58: 70-73.

Sterner, C.J. (1960). "Elecromagnetic Pump for Circulating Gases at Low Flow Rates," *Rev. Sci. Instrum.,* 31: 1159-1160.

Sterner, C.J. (1961). "Phase Equilibria in CO_2-Methane Systems," *Adv. Crog. Eng.,* 6: 467-474.

Streett, W.B. & Calado, J.C.G., (1978). Liquid-vapour equilibrium for hydrogen + nitrogen at temperatures from 63 to 110 K and pressures to 57 MPa. *J. Chem. Eng. Data,* 10: 1089-1100.

Streett, W.B., Sonntag, R.E. & Van Wylen, G.J. (1964). "Liquid-Vapour Equilibrium in the System Normal Hydrogen-Helium," *J. Chem. Phys*., 40: 1390-1395.

Stryjek, R. and Vera, J. H. (1986a), `PRSV: An improved Peng-Robinson equation of state for pure compounds and mixtures', *Can. J. Chem.Eng.* 64, 323-333.

Stryjek, R. and Vera, J. H. (1986b), `PRSV: An improved Peng-Robinson equation of state with New Mixing Rules for Strongly Non-ideal Mixtures," *Can. J. Chem. Eng.,* 64: 334-340.

Stryjek, R. and Vera, J. H. (1986c), `PRSV2: A cubic equation of state for accurate vapour-liquid equilibrium calculations', *Can. J. Chem. Eng.*
64, 820-826.

Stryjek, R. and Vera, J. H. (1986d), `PRSV: An improved Peng-Robinson equation of state for pure compounds and mixtures', *Can. J. Of Chem.* Eng. 64, 323-333.

Suzuki, K. & Sue, H., (1990). Isothermal Vapour-Liquid Equilibrium Data for Binary Systems at High Pressures: Carbon Dioxide-Methanol, Carbon Dioxide-Ethanon, Carbon Dioxide-1-Propanol, Methane-Ethanol, Methane-1-Propanol, Ethane-Ethanol, and Ethane-1-Propanol Systems.

Suzuki, T., Tsuge, N. & Nagahama, K., (1991). Solubilities of ethanol, 1-propanol, 2-propanol and 1-butanol in supercritical carbon dioxide at 313K and 333K. *Fluid Phase Equilibria*, 67: 213-226.

Takishima, S., Saiki, K., Arai, K. & Saito, S. (1986). "Phase Equilibria for CO_2-C_2H_5OH-H_2O System," *J.Chem. Eng. Jpn.,* 19: 48-56.

Thiele, E. (1963), "Equation of State for Hard Spheres", *J. Chem. Phys.* 39: 474-479.

Toyama, A., Chappelear, P.S., Leland, T.W.& Kobayashi, R., (1962). Vapor-liquid equilibria at low temperatures: The carbon monoxide-methane system. *Advances in Cryogenic Engineering,* 7: 125-136.

Trebble, M. A. and Bishnoi, P. R. (1987), "Development of a new four-parameter cubic equation of state", *Fluid Phase Equilib.* 35(1), 1-18.

Tsang, C.Y. & Streett, W.B., (1981). Vapor-liquid equilibrium in the system carbon dioxide/dimethyl ether. *J. Chem. Eng. Data,* 26: 155-159.

Tsonopoulos, C. & Heidman, J.L., (1985). From Redlich-Kwong to the present. *Fluid Phase Equilibria*, 24: 1-23.

Twu, C. H., Bluck, D., Cunningham, J. R. and Coon, J. E. (1991), "A cubic equation of state with a new alpha function and a new mixing rule", *Fluid Phase Equilibria*. 69, 33-50.

Twu, C. H., Bluck, D., Cunningham, J. R. and Coon, J. E. (1992a), "A cubic equation of state: Correlation between binary interaction parametersand inifinite dilution acitvity coefficients", *Fluid Phase Equilibria.* 72, 25-39.

Twu, C. H. and Coon, J. E. (1995), "Accurately estimate binary interaction Parameters", *Chem.Eng.Prog.* 46-53 pp. 46-53.

Twu, C. H., Coon, J. E. and Cunnigham, J. R. (1995b), "A new generalized alpha function for a cubic equation fo state part 1. Peng-Robinson Equation", *Fluid Phase Equilibria*. 105: 49-59.

Twu, C. H., Coon, J. E. and Cunningham, J. R. (1992b), "A new cubic equation of state" *Fluid Phase Equilibria.* 75, 65-79.

Twu, C.H. & Coon, J.E. (1996). "CEOS/A^E Mixing Rules Constrained by vdW Mixing Rule and Second Virial Coefficient," *AIChE J.,* 42: 3212-3222.

Twu, C. H., Sim, W. D. and Tassone, V. (2000), An extension of ceos/a^E zero pressure mixing rule for an optimum two-parameter cubic equation-of-state, in "In Proceedings of the 3rd China/USA Chemical Engineering Conference", Beijing China.

Van Ness, H.C. (1995). "Thermodynamics in the Treatment of (Vapour + Liquid) Equilibria," *J. Chem. Thermodynamics,* 27: 113-134.

Van Ness, H.C. & Abbott, M.M. (1978). "A Rapid Procedure for Degassing of Liquids," *Ind. Eng. Chem. Fundam.,* 17: 66-67.

Van Ness, H.C. & Abbott, M.M. (1982). *Classical Thermodynamics of Nonelectrolyte Solutions with Applications to Phase Equilibria,* McGraw-Hill, New York.

Van Ness, H.C., Byer, S.M. & Gibbs, R.E. (1973). "Vapour-Liquid Equilibrium: Part 1. An Appraisal of Data Reduction Methods," *AIChE J.,* 19: 238-244.

Vaughan, W.E. & Collins, F.C. (1942). "P-V-T-x Relations of the System Propane-Isopentane," *Ind. Eng. Chem.,* 34:885-890.

Vidal, J., (1983). Equations of state – Reworking the old forms. *Fluid Phase Equilibria*, 13: 15-33.

Wagner, Z. & Wichterle, I., (1987). High-pressure vapour-liquid equilibrium in systems containing carbon dioxide, 1-hexane, and n-hexane. *Fluid Phase Equilibria*, 33: 109-123.

Walas, S.M. (1985). *Phase Equilibria in Chemical Engineering,* Butterworth Publishers, Boston.

Wang, X., Wang, Y. & Shi, J. (1991). "Isothermal Vapour-Liquid Equilibria at Elevated Pressures for the Systems Containing Nitrogen, Carbon Dioxide, and Chlorodifluoromethane," *J. Chem. Eng. Data,* 36: 436-439.

Wang, W., Qu, Y., Twu, C.H. & Coon, J.E. (1996). "Comprehensive Comparison and Evaluation of the Mixing Rules of WS, MHV2, and Twu et al.," *Fluid Phase Eequilibria,* 116: 488-494.

Weber, W., Zeck, S. & Knapp, H., (1984). Gas solubilities in liquid solvents at high pressures: apparatus and results for binary and ternary systems of N_2, CO_2 and CH_3OH. *Fluid Phase Equilibria*, 18: 253-278.

Wei, Y. S. & Sadus, R.J. (2000). "Equations of State for the Calculation of Fluid-Phase Equilibria," *AIChE J.,* 46: 169-196.

Wichterle, I. & Kobayashi, R. (1972). "Vapour-Liquid Equilibrium of Methane-Propane System at Low Temperatures and High Pressures," *J. Chem. Eng. Data,* 17: 4-9.

Wilson, G.M. (1964). "Vapour-Liquid Equilibrium. XI. A New Expression fro the Excess Free Energy of Mixing," *J. Am. Chem. Soc.,* 86: 127-130.

Wilson, G.M. & Deal, C.H. (1962). "Activity Coefficients and Molecular Structure: Activity Coefficients in Changing Environments – Solutions of Groups," *Ind. Eng. Chem. Fundam.,* 1: 20-23.

Wiśniewska, B., Gregorowicz, J. & Malanowski, S., (1993). Development of a Vapour-Liquid Equilibrium Apparatus to Work at Pressures up to 3 MPa. *Fluid Phase Equilibria,* 86: 173-186.

Wong, D.S.H. 7 Sandler, S.I. (1992). "A Theoretically Correct Mixing Rule for Cubic Equations of State," *AIChE J.,* 38: 671-680.

Wong, D.S.H., Orbey, H. & Sandler, S.I. (1992b). "Equation of State Mixing Rule for Nonideal Mixtures Using Available Activity Coefficient Model Parameters and That Allows Extrapolation Over Large Ranges of Temperature and Pressure," *Ind. Eng. Chem. Res.,* 31: 2033-2039.

Yonker, C.R., Wright, B.W., Udseth, H.R. & Smith, R.D. (1984). "New Methods for Characterization of Supercritical Fluid Solutions," *Ber. Bunsenges. Phys. Chem,* 88: 908-911.

Yu, J. & Lu, B. (1987). "A Three-Parameter Cubic Equation of State for Asymmetric Mixture Density Calculations," *Fluid Phase Equilibria,* 34: 1-19.

Zabaloy, M.S. & Vera, J.H. (1998). "Special Algebraic Properties of Two-Parameter Equations of State: Homogeneous Azeotropy," *Ind. Eng. Chem. Res.,* 37: 1598-1612.

Zeck, S. & Knapp, H., (1986). Vapor-liquid and vapor-liquid liquid phase equilibria of binary and ternary systems of nitrogen, ethane and methanol: experiment and data evaluation. *Fluid Phase Equilibria*, 26: 37-58

APPENDICES

APPENDIX A
CALIBRATIONS

A.1 Calibration of temperature sensors

Accurate temperature sensor calibration was only carried out on the equilibrium cell temperature sensor. Other sensors were just checked to see if they were accurate to within ±1.5ºC.

The temperature calibration and accuracy checks were carried out against an Agilent 34401a 6.5 digit multimeter coupled with a PT-100 standard. During calibration and accuracy checks the sensors were immersed in an isothermal bath containing acetone. Cooling in the bath was achieved using two Julabo cold fingers. Dry-ice was also used to cool the bath during calibrations below 0ºC. Temperature in the bath was regulated using a temperature controller connected to an electrical heater. Agitation helped eliminate temperature gradients across the bath. Figure A-1 displays the Pt-100 standard calibration chart where *R* is the Resistance in Ohms as displayed on the multimeter and *T* is the true temperature.

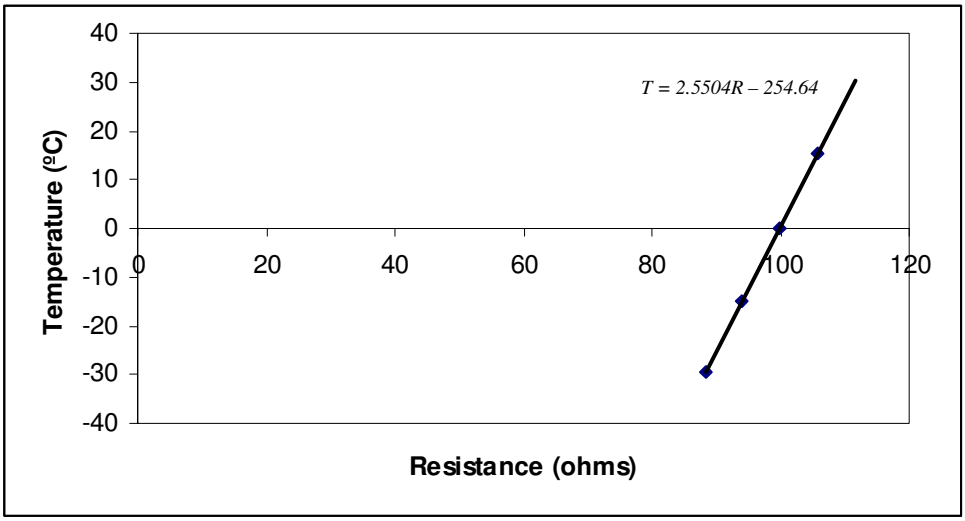

Figure A-1: Pt-100 standard calibration chart

The Pt-100 sensor used for equilibrium cell temperature measurement was calibrated while connected to the Eurotherm 2204 temperature controller. A straight line calibration was achieved by achieving steady conditions in the bath at a maximum and minimum temperature and entering the true temperature of the bath as obtained from the standard, into

the Eurotherm controller at the respective temperatures. A temperature range of -29.6ºC to 30.3ºC was used. This covered the temperature range at which this study was performed. Temperature measurements in the equilibrium cell were considered to be accurate to ±0.1ºC.

It was decided that accurate temperature measurement at other areas of the equipment was not critical to this study and it was only necessary for them to be close to the actual temperature and not exact. All other Pt-100 sensors in the equipment were thus connected to their respective display units and tested to see how closely they compared with the standard. It was found that all sensors were accurate to ±1.5ºC which was considered to be sufficient for their various applications.

A.2 Calibration of equilibrium cell pressure transducer

No high pressure standard was available at the School of Chemical Engineering at the time of this study thus it was decided to do a calibration on the equilibrium cell pressure transducer based on a correction applied to vapour pressure measurements over a temperature range on a particular component. This method required an accurate temperature measurement, thus temperature calibration was first carried out. Equilibrium cell pressure was measured using a Sensotec pressure transducer and display unit as described in Section 4.2.2.2.

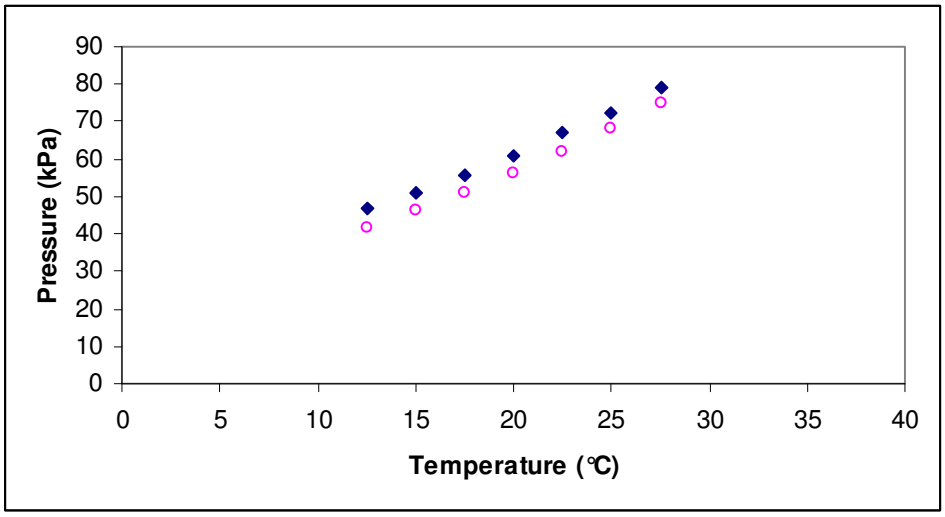

Figure A-2: Comparison of gauge vapour pressure measurements (♦) to values predicted by Reid *et al.* [1988] (○) for n-Pentane

Vapour-pressure measurements were thereafter performed on n-Pentane over the temperature range 12.5ºC to 27.5ºC. The measured data was then compared to data from the correlations

of Reid et al. [1988] as displayed in Figure A-2 and a linear calibration graph as displayed in Figure A-3 was thereafter obtained to allow correction of the pressure readings on the equilibrium cell pressure measurement.

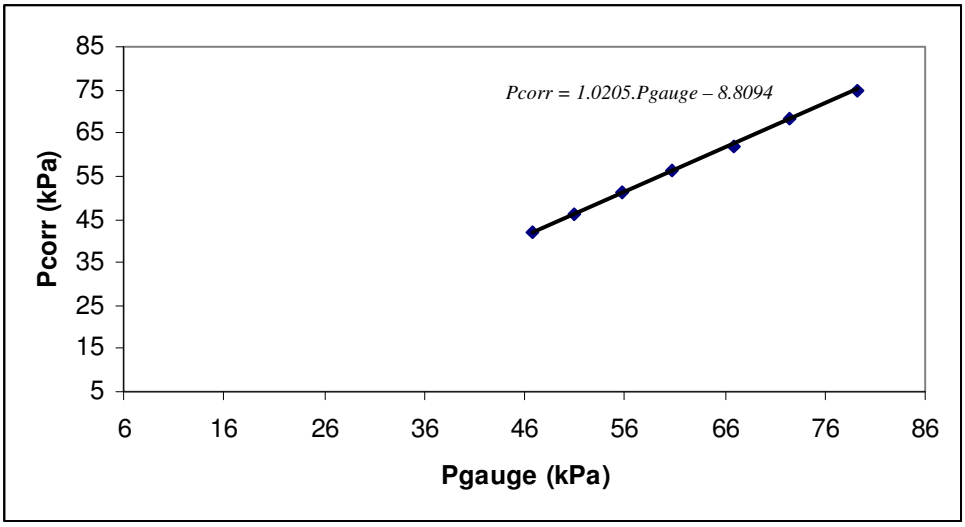

Figure A-3: Calibration graph for equilibrium cell pressure transducer

The following calibration equation was obtained,

$$P_{corr} = 1.0205 P_{gauge} - 8.8094 \quad \text{(A-1)}$$

Where:

P_{gauge} = Pressure reading on equilibrium cell pressure transducer display, (kPa)

P_{corr} = Corrected pressure, (kPa)

APPENDIX B
PHYSICAL PROPERTIES OF COMPONENTS INVESTIGATED

B.1 General pure component physical properties

Physical properties of components investigated in this study are contained in Table B-1. All physical properties were obtained from the AIChE DIPPR compilation [Daubert & Danner, 1993], with the exception of the dipole moments which were obtained from Prausnitz *et al.* [1980] where:

T_c = Critical temperature (K)
P_c = Critical pressure (bar)
ω = Accentric factor
V_c = Critical molar volume (m^3/kmol)
μ = Dipole moment, debye
R_D = Radius of gyration, A

Table B-1: Physical properties of components investigated in this study

Component	T_C (K)	P_C (bar)	ω	V_c (m^3/kmol)	μ (debye)	R_D (A)
n-Pentane	469.65	33.688	0.2486	0.31234	0	3.3370
Isopentane	460.43	33.812	0.2275	0.30583	0.13	3.3240
n-Propane	369.82	42.492	0.1518	0.20288	0	2.4310
1-Propanol	536.71	51.696	0.6279	0.21853	1.68	2.8250

B.2 Vapour pressures

The four-parameter equation or Wagner correlation from Reid *et al.* [1988] was used to calculate pure component vapour pressures P^s:

$$\ln\left(\frac{P^s}{P_c}\right) = \frac{1}{1-x}.\left[Ax + Bx^{1.5} + Cx^3 + Dx^6\right] \qquad \text{(B-1)}$$

Where:

$$x = 1 - \frac{T}{T_c} \tag{B-2}$$

Constants used to calculate the pure component vapour pressures for the respective components using the equation of Reid *et al.* [1988] are contained in Table B-2.

Table B-2: Vapour pressure constants used in the equation of Reid *et al.*

Component	A	B	C	D
n-Pentane	-7.28936	1.53679	-3.08367	-1.20456
Isopentane	-7.12721	1.38996	-2.54302	-2.45657
n-Propane	-6.72219	1.33236	-2.13868	-1.38551
1-Propanol	-8.05594	0.0425183	-7.51296	6.89004

Pure component vapour pressures were also computed using the five-parameter equation from Daubert & Danner [1993] with constants used in the equation for the various components investigated presented in Table B-3.

$$P^s = \exp\left[A + \frac{B}{T} + C.\ln T + D.T^E \right] \tag{B-3}$$

Table B-3: Vapour pressure constants used in the equation of Daubert & Danner [1993]

Component	A	B	C	D	E
n-Pentane	81.624	-5578.5	-9.2354	9.4522×10^{-6}	2.0000
Isopentane	72.350	-5010.9	-7.8830	8.9795×10^{-6}	2.0000
n-Propane	54.276	-3368.0	-5.2610	8.6000×10^{-6}	2.0000
1-Propanol	77.460	-7960.0	-7.5235	3.0000×10^{-6}	2.0000

APPENDIX C

Literature Data of Binary Systems Investigated

C.1 Propane + 1-propanol system

Two sets of HPVLE literature data for the propane (1) + 1-propanol (2) system at 19.9ºC are presented below. Table C-1 presents data measured by Nagahama *et al*. [1971] while data measured by Moodley [2002] is tabulated in Table C-2.

Table C-1: Vapour-liquid equilibrium data for the propane (1) + 1-propanol (2) system at 19.9ºC [Nagahama *et al.,* 1971]

Pressure [kPa]	x_1	y_1
143.0	0.0569	0.988
275.0	0.1098	0.9929
407.0	0.1764	0.995
525.0	0.2569	0.9962
623.0	0.3476	0.9969
697.0	0.4463	0.9975
746.0	0.5295	0.9977
780.0	0.6371	0.9978
790.0	0.7216	0.9979

Table C-2: Vapour-liquid equilibrium data for the propane (1) + 1-propanol (2) system at 19.9ºC [Moodley, 2002]

Pressure [kPa]	x_1	Y_1
178.0	0.0703	0.9889
218.0	0.0878	None
335.0	0.1399	0.9897
414.3	0.1811	0.9939
502.5	0.2396	0.9952
555.6	0.2897	0.9959
601.1	0.3386	0.9969

C.2 Propane + isopentane system

Binary HPVLE data for the propane (1) + isopentane (2) system is presented below. Vaughan & Collins [1942] measured data at 0ºC and 25ºC as displayed in Table C-3 and Table C-4 respectively. Table C-5 presents data measured by Moodley [2002] for the binary propane (1) + isopentane (2) system at 0ºC.

Table C-3: Vapour-liquid equilibrium data for the propane (1) + isopentane (2) system at 0ºC. [Vaughan & Collins, 1942]

Pressure [kPa]	x_1	Y_1
88.0	0	0
150.0	0.0740	0.4040
200.0	0.1370	0.5810
250.0	0.1980	0.6860
300.0	0.2610	0.7540
400.0	0.3820	0.8430
500.0	0.5010	0.8970
700.0	0.7340	0.9590
932.0	1.0000	1.0000

Table C-4: Vapour-liquid equilibrium data for the propane (1) + isopentane (2) system at 25ºC. [Vaughan & Collins, 1942]

Pressure [kPa]	x_1	y_1
33.4	0	0
50.7	0.0350	0.3510
76.0	0.0880	0.4980
101.3	0.1580	0.7030
121.6	0.2120	0.7640
152.0	0.2740	0.8210
202.7	0.3900	0.8840
304.0	0.6210	0.9496
405.3	0.8500	0.9845
481.3	1.0000	1.0000

Table C-5: Vapour-liquid equilibrium data for the propane (1) + isopentane (2) system at 0ºC. [Moodley, 2002]

Pressure [kPa]	x_1	y_1
34.3	0	0
55.2	0.0446	0.397
111.6	0.1805	0.7527
183.7	0.3376	0.855
213.9	0.4302	0.8986
285.4	0.518	0.9424
348.3	0.73	0.9757
396.1	0.8293	0.9849
451.8	0.9503	0.9952